Development of Analysis Methods to Detect the Use of Explosives and Chemical Warfare Agents

HEIDI LEES

TALLINN UNIVERSITY OF TECHNOLOGY
School of Science
Department of Chemistry and Biotechnology

The dissertation was accepted for the defense of the degree of Doctor of Philosophy in Chemistry on 21st of June, 2018.

Supervisors: Senior Researcher Merike Vaher
Department of Chemistry and Biotechnology
Tallinn University of Technology
Tallinn, Estonia

Emeritus Professor Mihkel Kaljurand
Department of Chemistry and Biotechnology
Tallinn University of Technology
Tallinn, Estonia

Opponents: Professor Bogusław Buszewski
Department of Environmental Chemistry and Bioanalytics
Nicolaus Copernicus University
Toruń, Poland

Professor Miguel de la Guardia
Department of Analytical Chemistry
University of Valencia
Valencia, Spain

Defense of the thesis: 24th of August, 2018, Tallinn

Declaration:

Hereby I declare that this doctoral thesis, my original investigation and achievement, submitted for the doctoral degree at Tallinn University of Technology has not been submitted for doctoral or equivalent academic degree before.

Heidi Lees

                                                            Signature

Analüüsimetoodikate arendamine keemiarelva- ja lõhkeainete kasutamise tuvastamiseks

HEIDI LEES

CONTENTS

LIST OF PUBLICATIONS

The thesis is based on the following publications, which are referred to by Roman numerals within the text:

I   P. Jõul, **H. Lees**, M. Vaher, E.-G. Kobrin, M. Kaljurand, M. Kuhtinskaja, Development of a capillary electrophoresis method with direct UV detection for the analysis of thiodiglycol and its oxidation products, Electrophoresis. 36 (2015) 1202–1207.

II **H. Lees**, M. Vaher, M. Kaljurand, Development and comparison of HPLC and MEKC methods for the analysis of cyclic sulfur mustard degradation products, Electrophoresis. 38 (2017) 1075–1082.

III E.-G. Kobrin, **H. Lees**, M. Fomitšenko, P. Kubáň, M. Kaljurand, Fingerprinting postblast explosive residues by portable capillary electrophoresis with contactless conductivity detection, Electrophoresis. 35 (2014) 1165–1172.

IV **H. Lees**, F. Zapata, M. Vaher, C. García-Ruiz, Simple multispectral imaging approach for determining the transfer of explosive residues in consecutive fingerprints, Talanta. 184 (2018) 437–445.

THE AUTHOR'S CONTRIBUTION

The contributions made by the author to the publications included are the following:

I.   The author was responsible for the analysis part of this article. She carried out the experiments for the optimization and validation of the capillary zone electrophoresis method with UV detection for the quantitative analysis of the acyclic degradation products of sulfur mustard in water samples. The author participated in the preparation of the manuscript.

II.   The author planned and carried out all the experiments for the development of the HPLC and MEKC methods with UV detection for the analysis of the cyclic degradation products of sulfur mustard. The author interpreted the obtained results, wrote the manuscript, and is the first and corresponding author.

III.   The author participated in the expedition to Hanko, Finland. The author performed a considerable part of the sample collection, preparation, and analysis using a portable CE instrument with conductivity detection.

IV.   The author was responsible for planning the experiments. She carried out all the experiments with the aim of studying the transfer of different explosives to different materials through successive fingerprints. She participated in setting up the purpose-built photo studio, and performed imaging of fingerprints on surfaces using a reflex camera and image analysis in MATLAB. The author wrote the manuscript and is the first author.

ABBREVIATIONS

ACN	Acetonitrile
ANOVA	Analysis of variance
BGE	Background electrolyte
C^4D	Capacitively coupled contactless conductivity detector
CE	Capillary electrophoresis
CMC	Critical micelle concentration
CTAB	Cetyltrimethylammonium bromide
CW	Chemical weapon
CWA	Chemical warfare agent
CWC	The Chemical Weapons Convention
CZE	Capillary zone electrophoresis
DAD	Diode array detector
DOEI	Dual opposite end injection
GC	Gas chromatography
HD	Sulfur mustard
HMTD	Hexamethylene triperoxide diamine
HPLC	High performance liquid chromatography
i.d.	Internal diameter
IC	Ion chromatography
IED	Improvised explosive device
IMS	Ion mobility spectrometry
IR	Infrared
IS	Internal standard
LD_{50}	Median lethal dose
LOD	Limit of detection
LOQ	Limit of quantification
MANOVA	Multivariate analysis of variance
MEKC	Micellar electrokinetic chromatography
MES	2-(N-morpholino)ethanesulfonic acid
MODUM	Towards the Monitoring of Dumped Munitions Threat (project)
MS	Mass spectrometry
MSI	Multispectral imaging
NIR	Near-infrared
NMR	Nuclear magnetic resonance
PC	Principal component
PCA	Principal component analysis
PETN	Pentaerythritol tetranitrate
R^2	Square of the correlation coefficient/Coefficient of determination
RDX	1,3,5-Trinitroperhydro-1,3,5-triazine
RGB	Red-green-blue

ROI	Region of interest
RSD	Relative standard deviation
S/N	Signal-to-noise ratio
SDS	Sodium dodecyl sulfate
SPE	Solid phase extraction
SSB	Sum of squares between groups
SST	Total sum of squares
SSW	Sum of squares within groups
TDG	Thiodiglycol
TDGO	Thiodiglycol sulfoxide
TDGOO	Thiodiglycol sulfone
TNT	2,4,6-Trinitrotoluene
VIS	Visible
WW	World War

INTRODUCTION

After World War (WW) II, large quantities of chemical weapons (CWs) were dumped into the sea, since at this time this was internationally accepted as a safe and efficient practice [1]. Approximately 50,000 tons of CWs, which contained 15,000 tons of toxic chemical warfare agents (CWAs), were dumped into the Baltic Sea [2]. Over time, the metal shells of the dumped munitions have started to corrode, causing leakage of the toxic chemicals into the sea environment, thus posing an environmental and security hazard. This has concerned many people, including scientists, who are making efforts to investigate the consequences of this dumping. In this regard, several projects have focused on the exploration of the dumpsites in the Baltic Sea, the identification of CWs, and the assessment of environmental risks. Our research group at Tallinn University of Technology has participated in one of these projects, named "Towards the Monitoring of Dumped Munitions Threat" (MODUM). Therefore, part of this work was carried out under the MODUM project, which involved nine countries in total. The aim of this project was to enhance the understanding of dumped munitions in the Baltic Sea. Our research group was responsible for developing capillary electrophoresis (CE) methodology for the identification and quantitative analysis of sulfur mustard (HD) degradation products. Detection of CWAs and their degradation products in water samples is important in identifying possible leakage locations. The topic of dumped CWs continues to be relevant, and studies carried out in this area have proven that these toxic chemicals are currently leaking and therefore pose a potential threat to the marine ecosystem.

As of today, 193 states (representing over 98% of the world's population) are party to the Chemical Weapons Convention (CWC), which outlaws the use of CWs and their precursors [3]. Unfortunately, recent incidents have shown that the use of CWs has not been abandoned. Although this thesis focuses on the detection of CWs dumped at sea, the detection principle remains the same. Usually, the degradation products of CWAs are detected and therefore, the developed methods could potentially be adapted to detect these compounds in different environments.

In addition to CWs, another concern is the use of explosives in terrorist attacks. The most recent incidents involved bombings in big cities such as Boston (2013), Brussels (2016), and Manchester (2017). Additional attacks could be prevented by developing trustworthy methods for the pre-blast detection of explosives at airports, as well as the post-blast detection of explosive residues at crime scenes. The latter could help to track down the origin of the chemicals and lead to possible suspects, which, in turn, prevents future attacks.

Considering the above, the development of new, rapid, simple and sensitive methods for the detection of CWAs and explosives is essential.

The present dissertation is divided into five chapters. Chapter 1 offers a literature overview of the explosives, and sea-dumped CWs investigated in this thesis. In addition, the degradation pathways of HD, the main dumped CWA, are discussed. Chapter 1 also gives an overview of previously used methods for the detection of CWAs and explosives. Moreover, a brief overview of the techniques used in this thesis for method development (capillary electrophoresis (CE), high performance liquid chromatography (HPLC), and multispectral imaging (MSI)) is provided. Chapter 2 outlines the main aims of the present work. The third chapter describes the reagents and samples used for method development. Procedures for sample preparation and experimental and instrumental details are also provided in this chapter. Chapter 4 discusses the results presented in

Publications I-IV. Methods for detecting the acyclic (**Publication I**) and cyclic (**Publication II**) degradation products of HD were developed by using CE and HPLC. The analysis of explosives was achieved in **Publications III** and **IV**. **Publication III** presents a method for the on-site detection of post-blast explosive residues, while **Publication IV** investigates the transfer of explosive residues in consecutive fingerprints. Chapter 5 summarizes the results obtained in this thesis. In addition to publications, the results of this thesis have been presented in international conferences in several countries: Estonia, Finland, Denmark, Italy, and the Czech Republic.

All four publications in this dissertation share a common goal of developing new methods to detect the use of CWAs and explosives, which is important in terms of counter-terrorism applications.

1 LITERATURE OVERVIEW

1.1 Sea-dumped chemical weapons

Chemical weapons (CWs) are defined as toxic chemicals contained in a bomb, shell, or any other delivery system [4]. The toxic chemicals that have been developed for use as CWs can be categorized to four main groups:

1) choking agents—chlorine, phosgene, and diphosgene
2) blister agents (or vesicants)—sulfur and nitrogen mustards, lewisite, and phosgene oxime
3) blood agents—hydrogen cyanide, cyanogen chloride, and arsine
4) nerve agents—sarin, tabun, soman, VX, and Novichok agents [4].

After World War (WW) I, the Geneva protocol, which prohibited the use of CWs in international armed conflicts, was signed by 36 countries in 1925 [5]. However, the treaty said nothing about the production, storage, or transfer of CWs, and therefore these toxic chemicals were still produced in mass quantities during WWII. Only in 1997 did the Chemical Weapons Convention (CWC) treaty enter into force, outlawing the development, production, stockpiling, and use of CWs and their precursors. To date, the convention has 193 parties [3,6].

After WWII, large quantities of produced CWs required disposal. Unfortunately, at that time dumping at sea was considered the most appropriate solution to this issue. Sea disposal of munitions was considered appropriate until the enactment of "the Convention on the Prevention of Marine Pollution by Dumping of Wastes and Other Matter" in 1972 [7]. Sea dumping was utilized for several reasons. Towards the end of the war, CWs were dumped to remove hazardous munitions from areas subject to attacks, while in later years it was considered an easier, cheaper, and safer method than land-based disassembly and decontamination procedures [8]. The intent was to dump these toxic chemicals as deep and far from land as possible. After the two world wars, more than 1 million tons of chemical munitions are estimated to have been dumped into seas and oceans [2]. Currently, 127 dumping areas have been documented, and many more dumpsites are suspected to exist. Dumpsites are located all over the world: in the Atlantic, Pacific, and Indian Oceans, along the Canadian and US coasts, in the Gulf of Mexico, along the coasts of Australia, New Zealand, India, Philippines, Japan, Great Britain, and Ireland, and in the Caribbean, Black, Red, Baltic, Mediterranean, and North Seas [2,9].

Dumped CWs present different types of threats to the environment. First, many of the dumped munitions contain explosives, which can self-detonate. Secondly, human activities such as fishing, dredging, and pipeline and sea cable construction may result in human exposure to toxic chemical warfare agents (CWAs). Thirdly, CWAs and their degradation products can cause direct and indirect harm to the marine environment. Unfortunately, despite many research efforts, information regarding the extent of environmental harm caused by CWAs is scarce [9]. What is certain is that CWA leakage causes chemical pollution of the sea and poses a threat to the marine ecosystem [2,8,10]. Unfortunately, the corrosion of CWs is an ongoing process, and in the future an increasing amount of toxic chemicals will leak into the sea environment.

Approximately 50,000 tons of chemical munitions were dumped in the Baltic Sea region, containing around 15,000 of CWAs [11]. Dumpsites in the Baltic Sea are located at depths of approximately 80–120 m, and the locations of the main dumping areas are

well known: south-east of Gotland, east of Bornholm, and south of Little Belt [2,8]. However, dumping is also known to have taken place outside these areas. Therefore, to date, the exact amounts and locations of dumped CW materials remain uncertain. The chemicals dumped in the Baltic Sea consisted mainly of sulfur and nitrogen mustards, arsenic compounds (arsine oil, Clark I and II, adamsite), α-chloroacetophenone, phosgene, and tabun [12]. Approximately 60% of all dumped munitions in the Baltic Sea contain sulfur mustard (HD), making this the most abundant dumped CWA [8]. These munitions have been lying on the seabed for many decades and thus, the dumped CWs at the bottom of the Baltic Sea are in different stages of decomposition [11]. An example of an object dumped at Bornholm Deep in the Baltic Sea is shown in Figure 1. The image was taken during the MODUM (Towards the Monitoring of Dumped Munitions Threat) project expedition in March 2016.

Figure 1. Image of a dumped object taken by the author of this thesis during the expedition in Bornholm Deep in March 2016 (project MODUM).

1.1.1 Sulfur mustard and its degradation products

Sulfur mustard (HD), also known as mustard gas or yperite, is a blistering agent that was first used in WWI [13]. HD is a colorless and odorless oily liquid in pure form; however, when mixed with other chemicals, it becomes brownish and can have a slight garlic smell. HD is not found naturally in the environment [14].

The harm that HD causes to an individual depends on the quantity of the chemical to which they were exposed, as well as the length of exposure [14]. The acute effect of HD exposure is severe blistering of the skin. Since mustard agents also cause severe damage to the eyes, respiratory system, and internal organs, they should be referred to as "blistering and tissue-injuring agents". The main active component of the mustard agent, bis-(2-chloroethyl)sulfide, reacts with a large number of biological molecules. The effect of HD is delayed, and the first symptoms might not occur until 2-24 hours after exposure [15]. HD has also mutagenic and carcinogenic properties [16,17]. Exposure can cause cancer of the airways, lungs, skin, and of other areas of the body later in life [14].

The median lethal dose (LD$_{50}$) of liquid HD for humans via skin contact is estimated to be 100 mg/kg [18,19].

In an aqueous environment, HD hydrolyzes to form many different degradation products [20]. Predominantly, HD hydrolyzes to thiodiglycol (TDG), which further oxidizes to thiodiglycol sulfoxide (TDGO), and more slowly to thiodiglycol sulfone (TDGOO) (Figure 2A) [21]. The degradation products are usually much less toxic than the original agents [22]. For example, in rats, the oral LD$_{50}$ values of TDG are usually higher than 5000 mg/kg [23,24], while the oral LD$_{50}$ for HD is claimed to be 17 mg/kg [19]. Thus, TDG is approximately 300 times less toxic than HD. In addition to open-chain compounds, HD degrades to form various cyclic compounds, such as 1,4-thioxane, 1,3-dithiolane, 1,4-dithiane, 1,2,5-trithiepane, and 1,4,5-oxadithiepane. The degradation pathways of HD to 1,4-thioxane or 1,4-dithiane are illustrated in Figure 2B [2].
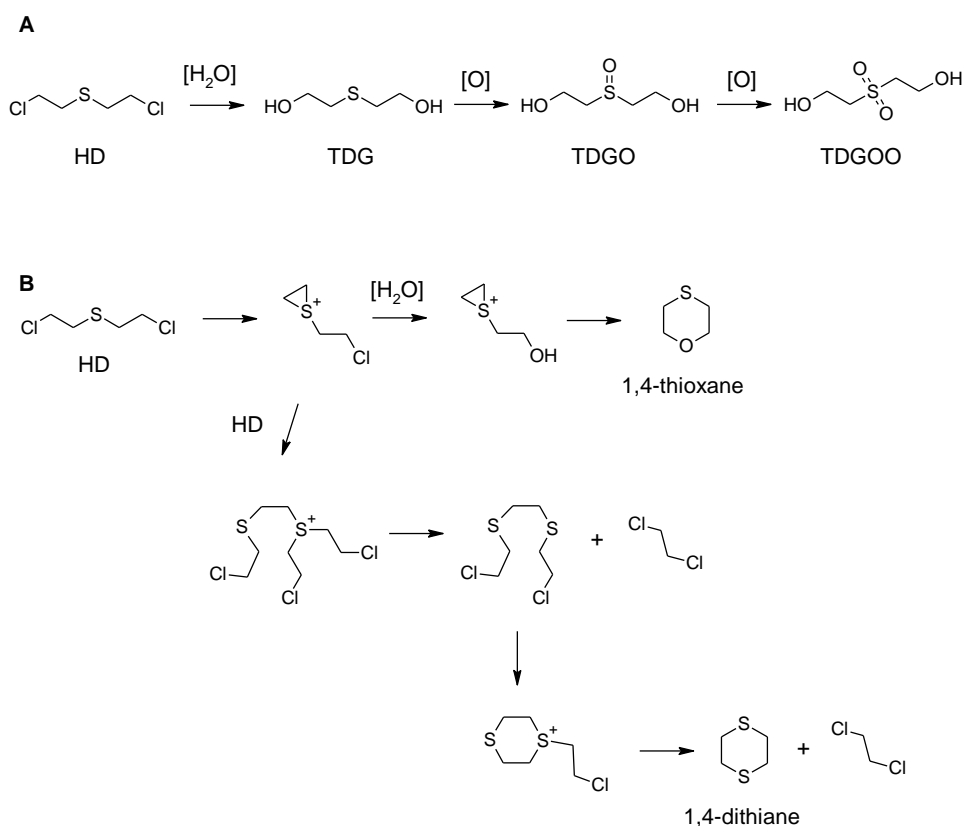
Figure 2. Degradation of HD to acyclic (A) or cyclic (B) degradation products. Adapted from ref. [2,21].

The degradation of HD is dependent on the temperature and environment. For example, the half-life of HD in seawater is 15 min at 25 °C, while it is 175 min at 5 °C [25]. The rate of HD hydrolysis in seawater is slower than the rate of hydrolysis in pure water [25]. HD tends to form solid or semi-solid lumps with a polymer coating of degradation products, which can remain on the sea floor for decades [10].

The parent HD is not very frequently detected in the marine environment close to the dumpsites, rather than its degradation products. Surprisingly, TDG and its oxidation products, which would be expected to be the main breakdown products, are rarely found in samples from dumping sites [22,26], whereas cyclic degradation products have been detected in a number of cases [22,27–29].

1.1.2 Analysis methods for sulfur mustard degradation products

The most commonly used methods for the analysis of HD degradation products are based on gas chromatography (GC) or liquid chromatography (LC) in combination with mass spectrometry (MS) [12,21,30–35]. However, other analytical techniques, such as NMR spectroscopy [36,37] or sulfur-selective flame photometric detection (S-FPD), have also been employed [38–41]. In addition to the above-mentioned separation techniques, ion mobility spectrometry (IMS) [42] and capillary electrophoresis (CE) [43–45] have also been employed.

Cyclic degradation products of HD have mainly been detected using GC-MS [12,27,28,46]. In this respect, Røen et al. [28,46] developed two methodologies for the trace determination of cyclic HD degradation products in soil and water samples using headspace-trap GC-MS. Magnusson et al. [27] presented an on-site analysis method based on dynamic headspace GC–MS for the analysis of five cyclic HD degradation products (1,4-thioxane, 1,3-dithiolane, 1,4-dithiane, 1,4,5-oxadithiepane, and 1,2,5-trithiepane). Their work enabled the successful identification of four cyclic HD degradation products at concentrations of 15–308 µg/kg in sediments. The analysis was carried out on board, which demonstrated the practical applicability of the method.

Acyclic degradation products of HD, such as TDG, TDGO, and TDGOO, are relatively polar and water-soluble compounds. Thus, LC is the first choice for their determination. In this regard, Read and Black [47] developed a rapid screening procedure for the hydrolysis products of CWAs, including TDG and it oxidation products, by LC-MS. GC-MS has also been applied, but in this case, derivatization of the analytes is essential [12,35].

Despite the considerable number of developed methods for the detection of CWA-related compounds, the development of new rapid analytical methods for the determination of HD and related compounds is still relevant and necessary due to the increasing environmental concerns related to dumped CWs. The positive detection of HD degradation products in environmental samples indicates the presence and leakage of HD from corroded shells, which, in turn, indicates the chemical pollution of that area. After confirming the leakage, precautionary measures can be taken into consideration.

To date, only a limited number of scientific articles about the analysis of HD and its degradation products by CE have been published, despite the many advantages of this method. These advantages include the simplicity of the instrumentation and the operation procedure, which makes it one of the best techniques for miniaturization and on-site detection. In terms of CE analysis, Cheicante et al. [44,45] separated uncharged sulfur-containing CW related compounds (TDG, 2,2'-sulfinyldiethanol, 1,4-dithiane, 1,4-thioxane, O-isobutyl methylphosphonothioic acid, and O-ethyl methylphosphonothioic acid) in aqueous samples by micellar electrokinetic chromatography (MEKC). Separation was achieved within 10 minutes using a background electrolyte (BGE) consisting of 10 mM borate and 100 mM SDS. The obtained LODs were 1-10 µg/mL.

In this dissertation, three new methodologies based on CE [43,48] and HPLC [48] with UV detection for the analysis of HD degradation products in aqueous samples were

developed. In the first article [43], an analysis method for the detection of acyclic HD degradation products (TDG, TDGO, and TDGOO) was developed, while in the second [48], MEKC and HPLC methods for the detection of cyclic HD degradation products (1,4-thioxane, 1,3-dithiolane, 1,4-dithiane, 1,4,5-oxadithiepane, and 1,2,5-trithiepane) were developed. The HPLC method with a sample concentration step provided lower detection limits, while the MEKC protocol was very simple and could be easily made portable and adapted to *in situ* analysis. These rapid and simple methods could offer a good alternative to the commonly used methods for detection of HD related compounds.

1.2 Explosives

An explosive is an energetically unstable chemical, which upon initiation by friction, impact, shock, spark, flame, heating, *etc.*, explodes with a sudden expansion of the compound. Explosion is typically accompanied by the production of heat and large changes in pressure [49].

Explosives have found usage for both constructive and destructive purposes for military and civil applications [50]. Many different ways to classify explosives exist. Several approaches to categorize explosives, as well as some examples of each class, are presented in Figure 3. Explosives can be classified as high or low (energy) explosives according to their decomposition rate. Low explosives undergo fast burning or deflagration (300-3000 ms^{-1}), whereas high explosives undergo detonation (5000-10000 ms^{-1}). Detonation produces higher pressures and is more destructive than deflagration. High explosives are subdivided according to their sensitivity into primary, secondary, and tertiary explosives, where primary explosives are the most sensitive and tertiary the least. The main difference between primary and secondary explosives is that the detonation of primary explosives is initiated by burning, while secondary high explosives require the use of a detonator and often a booster for initiation [50].
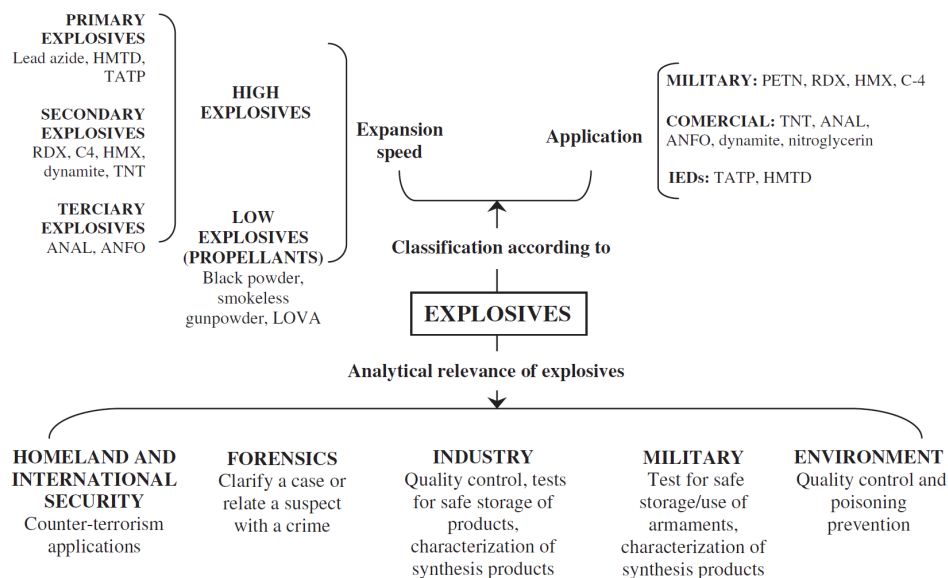

Figure 3. Classification of explosives, and fields in which the analysis of explosives is important. Reprinted from ref. [51] with permission from Elsevier.

1.2.1 Terrorism and the need for trace explosive detectors

The detection of explosives is an issue of major importance in homeland security and counter-terrorism applications, as shown in Figure 3. In recent years, numerous terrorist attacks have taken place, representing a constant threat to citizens. Unfortunately, a number of these attacks have resulted in deaths of many innocent people, for instance, the bombings in Madrid (2004), London (2005), Oslo (2011), Boston (2013), Brussels (2016), and Manchester (2017). Very often, improvised explosive devices (IEDs) are used in these criminal attacks, since the constituents are relatively easily accessible.

One way to prevent additional terrorist attacks is to analyze post-blast explosive residues in order to trace the origin of the chemical compounds used in the explosive devices. This can lead to quicker identification of possible suspects and thus, help to prevent further attacks. Inorganic explosives are known to produce ionic post-blast residues; however, little is known about the traces left by organic high explosives. This question was also of interest in this thesis.

When a terrorist handles an explosive, it is likely that a certain amount of explosive will remain on his or her hands and clothing. Therefore, the detection of explosive traces in samples from the hands of suspects has been the subject of many studies [52–54]. Explosive residues, in turn, may be transferred from contaminated hands and clothes to other items, such as laptops, luggage, *etc.* The detection of trace amounts of explosives on people and objects at airports is a challenge in counterterrorism activities. In this regard, many trace explosive detectors have been developed for screening luggage and other objects at airports. Unfortunately, a number of technologies that can be used for scanning luggage cannot be used for screening passengers for health reasons [55].

1.2.2 Analysis of explosives

The trace analysis of explosives is an area of current interest and development, especially in view of the significant increase in terrorist activities in recent years, as described in the preceding section. The development of new, innovative detection approaches and the improvement of existing techniques are still highly important. The desired developments involve miniaturization, portability, low cost, fast analysis, ease of operation, high selectivity, and sensitivity [56].

The detection of explosives is achieved using various spectroscopic methods, such as IMS [57–59], MS [60,61], terahertz spectroscopy [62], infrared (IR) and Raman spectroscopy [51,54,63,64], as well as by chromatographic methods, such as ion chromatography (IC) [65,66] and HPLC [67,68]. However, other separation techniques, such as CE, have provided promising results for the analysis of explosives. CE has many advantages over more commonly used techniques, for instance, simple instrumental set-up, lower price, smaller solvent and sample requirements, and great versatility. This technique has high potential in on-field *in situ* analysis to avoid transportation of the sample. Several reviews of the advances in the use of CE in explosives analysis have been published [69–72]. The analysis of explosive residues by CE has been carried out using indirect photometric detection [73,74], laser induced fluorescence [75–78], MS [79], and C^{4}D [80–82]. C^{4}D has advantages over the other detection techniques, including its relatively simple electronic circuity, low cost, and low power consumption, and is therefore very well-suited for implementation in portable CE instruments. In light of these advantages, a portable CE instrument with a C^{4}D was implemented in this thesis for the analysis of explosives [82].

1.2.3 Fingerprint analysis

Fingerprints are one of the main means by which explosive traces are transferred [83]. Therefore, numerous articles have focused on developing methods to detect explosive traces in fingerprints [83–88]. Various spectroscopic, imaging, and microscopic techniques have been employed for this purpose, such as laser-induced breakdown spectroscopy [83,89,90], IR [52,53,88,91–93] and Raman spectroscopy [84,85,94–97]. However, chromatographic techniques have also been implemented [98–100]. All these studies focused mainly on detecting and identifying explosive residues in fingerprints on different materials, while the transfer of residues to different surfaces (on which they are detected) in consecutive fingerprints has scarcely been studied. In fact, this was one aim of this thesis, and was studied in the article of Lees *et al.* [101] using a simple approach involving multispectral imaging (MSI). Regarding the transfer of explosives, Turano [98] quantified and compared the amounts of the explosive precursors NH_4NO_3 and $KClO_3$ in consecutive fingerprints on three surfaces, filter paper, polypropylene, and polyurethane, using IC. Oxley *et al.* [100] quantified the amount of explosive residues remaining in the primary work area and in secondary transfer points during a simple manipulation process using GC and LC. Their results indicated that small percentage of the total amount of explosive might remain in the work area, and that secondary contamination is significantly lower. Choi and Son [59] used IMS to detect 1,3,5-trinitroperhydro-1,3,5-triazine (RDX) and 2,4,6-trinitrotoluene (TNT) after being transferred to three smear matrices, stainless steel mesh, cellulose paper, and cotton fabric, using a poly(tetrafluoroethylene) (PTFE) sheet. Explosive particles deposited on the PTFE sheet were transferred to the smear matrix using a stainless steel roller. Verkouteren *et al.* [102] described a method to perform automated mapping of RDX particles in consecutive C-4 fingerprints. They used polarized light microscopy and image analysis to map the entire fingerprint and the distribution of RDX particle in fifty consecutive fingerprints.

1.3 General aspects of the separation techniques used for method development

1.3.1 Capillary electrophoresis

In capillary electrophoresis (CE), separation is achieved via the differential migration of solutes in an electric field. Electrophoretic analysis is performed in a narrow-bore fused silica capillary, typically with an internal diameter of 50-75 µm. A high voltage of 10 to 30 kV is applied to the capillary. One of the main advantages of CE method is the overall simplicity of the instrumentation. The CE instrument consists only of a high voltage source, buffer vials with an anode and cathode, a sample vial, a capillary, a detector, and a computer [103].

CE has numerous operation modes, such as capillary zone electrophoresis (CZE), micellar electrokinetic chromatography (MEKC), capillary isoelectric focusing (CIEF), capillary gel electrophoresis (CGE), capillary electrochromatography (CEC), nonaqueous capillary electrophoresis (NACE), and capillary isotachophoresis (CITP). CZE is fundamentally the simplest and most widely used form of CE [103]. In CZE, the capillary is filled only with a buffer. Anions and cations are separated due to their different electrophoretic mobilities, while neutral molecules are not separated and elute together

with electroosmotic flow (EOF). EOF is the movement of the liquid (*i.e.* BGE) induced by an applied potential across a capillary. In MEKC mode, the separation of both neutral and charged molecules is possible. The separation of analytes in MEKC is achieved by hydrophobic/ionic interactions with the micelles. This is accomplished by the use of surfactants in the running buffer. At concentrations above the critical micelle concentration (CMC), the surfactant molecules aggregate to form micelles. Micelles are usually charged, and depending on their charge migrate either with or against the EOF [103].

When an ion with a charge of *q* is placed in an electric field *E* (V/m), it experiences an accelerating force, *qE*. In addition, a retarding frictional force, fv_{ep}, is also experienced by an ion in solution, where *f* is the friction coefficient and v_{ep} is the velocity of the ion. If the accelerating force is equal to the retarding frictional force, the ion begins to move at a steady speed:

$$f v_{ep} = qE$$

$$v_{ep} = \frac{q}{f}E = \mu_{ep}E \, , \tag{1}$$

where μ_{ep} is the electrophoretic mobility of the ion.

μ_{ep} is the proportionality constant between the ion velocity and the electric field strength (Equation 2) [104]. The friction coefficient *f* for a spherical particle with radius *r* moving through a solution with a viscosity *η* is:

$$f = 6\pi\eta r$$

$$\mu_{ep} = \frac{v_{ep}}{E} = \frac{q}{f} = \frac{q}{6\pi\eta r} \tag{2}$$

Similarly to Equation 2, the electroosmotic mobility, μ_{EOF}, is defined as

$$\mu_{EOF} = \frac{v_{EOF}}{E} \tag{3}$$

The velocity of the EOF, v_{EOF}, is defined as:

$$v_{EOF} = \frac{\varepsilon \zeta E}{4\pi\eta} \, , \tag{4}$$

where *ε* is the dielectric constant, *ζ* is the zeta potential, *E* is the strength of the applied electric field, and *η* is the viscosity of the separation buffer.

The apparent mobility, μ_{app}, of an ion is the sum of its electrophoretic mobility, μ_{ep}, and electroosmotic mobility, μ_{EOF}:

$$\mu_{app} = \mu_{ep} + \mu_{EOF} \tag{5}$$

Despite the many advantages of the CE method, it has some drawbacks, such as higher detection limits and poor reproducibility, compared to HPLC method [104–106].

1.3.2 High performance liquid chromatography

LC is a separation technique carried out in the liquid phase. The sample is separated into its constituent compounds through distribution between the mobile phase and a stationary phase. The mobile phase (the flowing liquid) is typically a mixture of an organic solvent (*e.g.* acetonitrile (ACN) or methanol) and water, while the stationary phase consists of chemically modified silica particles packed in a column. HPLC is a form of LC that uses columns packed with small particles through which the mobile phase is pumped at high pressure (typically, up to 400 bar). The HPLC system consists of a degasser, a pump, an injector (autosampler), a column, a column oven, a detector, and a data-

handling device. A typical HPLC column is a stainless steel tube filled with 3–5 μm particles with a length of 50–250 mm and an internal diameter (i.d.) of 2.0–4.6 mm [107].

HPLC has four major separation modes: normal-phase chromatography (NPC), reversed-phase chromatography (RPC), ion-exchange chromatography (IEC), and size-exclusion chromatography (SEC). More than half of modern HPLC analytical methods are based on RPC. In the case of RPC, the mobile phase is relatively polar (water, methanol, ACN) and the stationary phase is non-polar, typically silica gel with long hydrocarbon chains (C8–C18) attached to the surface. In RPC, separation takes place on the basis of the polarities of the analyte molecules, with compounds eluting in order of decreasing polarity [107].

HPLC separation can be performed under isocratic or gradient conditions. In isocratic analysis, the mobile phase composition remains constant throughout the analysis, while in gradient analysis, the strength of the mobile phase increases with time during sample elution. The latter is preferred for more complex samples containing analytes of different polarities [107].

There are several parameters that characterize the chromatographic separation, *e.g.*, the retention factor k, separation factor α, plate height H, plate number N, and resolution R_s. The number of theoretical plates (N) is a measure of the efficiency of the column, with an increase in the number of theoretical plates representing better efficiency. N is calculated as:

$$N = 16\left(\frac{t_R}{w_B}\right)^2 = 5.546\left(\frac{t_R}{w_{0.5}}\right)^2, \tag{6}$$

where t_R is the retention time, w_B is the peak width, and $w_{0.5}$ is the peak width at half-height.

The main purpose of chromatographic analysis is to separate two or more compounds in the solution. Resolution (R_s) is a quantitative measure of how well the two peaks are separated and is calculated as:

$$R_s = 2\left(\frac{t_{R2} - t_{R1}}{w_{B1} + w_{B2}}\right)^2 = \frac{2}{1.7}\left(\frac{t_{R2} - t_{R1}}{w_{0.5,1} + w_{0.5,2}}\right)^2, \tag{7}$$

where t_{R1} and t_{R2} are the retention times of the two peaks of interest, w_{B1} and w_{B2} are the peak widths measured at the baseline, and $w_{0.5,1}$ and $w_{0.5,2}$ are the peak widths measured at half-height.

Normally, data systems use the half-height method for measuring resolution since it is easier to measure the half-height width than the baseline width. The R_s should be at least 1.5-2.0 for the complete separation of compounds [107–109].

1.3.3 Detection

Liquid separation methods are implemented with a wide variety of detection techniques. The most popular detectors employed in CE and HPLC are based on UV/Vis absorption and fluorescence [105]. Instruments utilizing a diode array detector (DAD) record entire spectra, providing a 3D chromatogram showing absorbance as a function of wavelength and elution time [105]. Despite the fact that optical detection has proven to be of great importance, compounds that do not absorb UV radiation can only be detected using indirect methods, which are relatively insensitive. For sensitive fluorescence detection, derivatization is required for most of the analytes [110].

Another group of CE and HPLC detectors are based on electrochemical detection methods, among which amperometry and conductivity are the most common [105].

In CE, the capacitively coupled contactless conductivity detector (C^4D) is a highly suitable detection method for inorganic anions and cations, since these ions do not exhibit high enough absorptivity to be detected by UV/Vis absorption [111]. In the C^4D detection method, the capillary is placed through two metal tubes (electrodes) that act as two cylindrical capacitors. These detectors are located around the outer surface of the capillary, and can be located anywhere along the capillary. The detector operates in a non-contact manner, and therefore there is no need to clean or flush the detector [111]. The detector measures the change in the electrical conductivity of the solution in the detector gap between the electrodes. The signal is not measured radially across the capillary diameter, but axially along the capillary. Therefore, this method does not impose strict limits on the internal diameter of the capillary, and can also be used with small internal diameter capillaries and miniature instruments [111–113]. In fact, conductivity detection can be implemented very effectively in a portable CE device, because it can be easily miniaturized, its power consumption is minimal, and it is relatively sensitive [114].

In addition, MS detection is often employed in HPLC and CE analysis. MS detection is very sensitive and provides structural information that aids in identifying the analytes. The interface between CE/HPLC and mass spectrometer is more technically difficult because of the incompatibility of a BGE/liquid mobile phase with the high vacuum requirement of the mass spectrometer and therefore, benchtop instruments are mainly used [105]. However, HPLC-MS and CE-MS are now widely applied methods.

1.4 Spectral imaging

Visible light (VIS), the radiation that the human eye can perceive, consists of electromagnetic waves in the wavelength range of 380–780 nm, while the near-infrared (NIR) spectrum covers the 780-2500 nm range. VIS and NIR ranges are desirable in many applications. NIR light can penetrate more deeply into materials, for example, tissues, and may show information that is otherwise invisible to human eyes.

Spectral imaging is a combination of spectroscopy and photography that collects and processes information from across the electromagnetic spectrum [115]. The term has broad usage and can refer to hyperspectral imaging (HSI), multispectral imaging (MSI), imaging spectroscopy, or chemical imaging. MSI measures light in a small number (typically 3 to 15) of spectral bands, while HSI measures hundreds of contiguous spectral bands. Therefore, HSI obtains the spectrum for each pixel in the image with the aim of identification of the compound. The obtained data may be visualized as a hypercube, which is a 3D block of data spanning two spatial dimensions (x and y) together with a series of wavelengths (λ) making up the third spectral axis. Each hypercube can contain thousands of spectra. The obtained spatial and spectral information allows for the analysis, detection, and identification of the sample.

An illustration of how NIR-HSI is used to generate a 3D image containing the spatial and spectral information of the sample is shown in Figure 4 [53]. The spatial information in the HSI image corresponds to the digital image of the sample (x and y-axes), while the spectral data contains the spectra over the range of wavelengths (λ axis) for each pixel in the digital image. A pixel is the minimal sub-unit of an image [53].
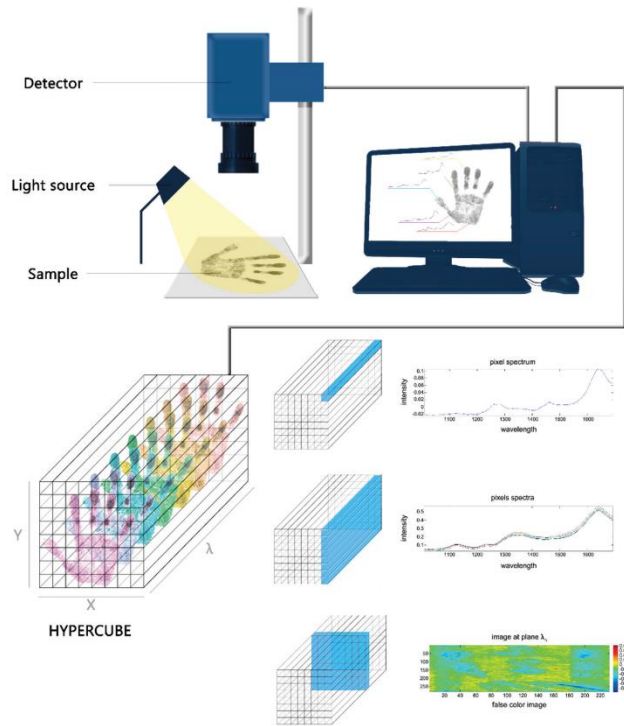
Figure 4. Schematic illustration of the experimental setup of an HSI system and the acquisition of the hyperspectral data cube (xyλ). Reprinted from ref. [53] with permission from Elsevier.

1.4.1 Multispectral imaging

As described in the preceding paragraph, a multispectral image captures image data within specific wavelength ranges across the electromagnetic spectrum. The information contained in a few wavelengths is quite often sufficient in specific applications in many different fields, for instance, food quality control [116–118], cultural heritage [119], medicine [120,121], and forensics [95,122–124]. The successful use of MSI in forensics was demonstrated by Zapata *et al.* [124], who recorded multispectral images of clothing targets shot from different distances (from 10 to 220 cm) at specific wavelengths. The pixels corresponding to gunshot residues in these images were counted, which allowed the shooting distance to be estimated. A simplified scheme of their image processing procedure is shown in Figure 5. Previous investigations, as well as the one presented in this thesis by Lees *et al.* [101], support the use of MSI as a fast and relatively inexpensive technique for a variety of forensic purposes.
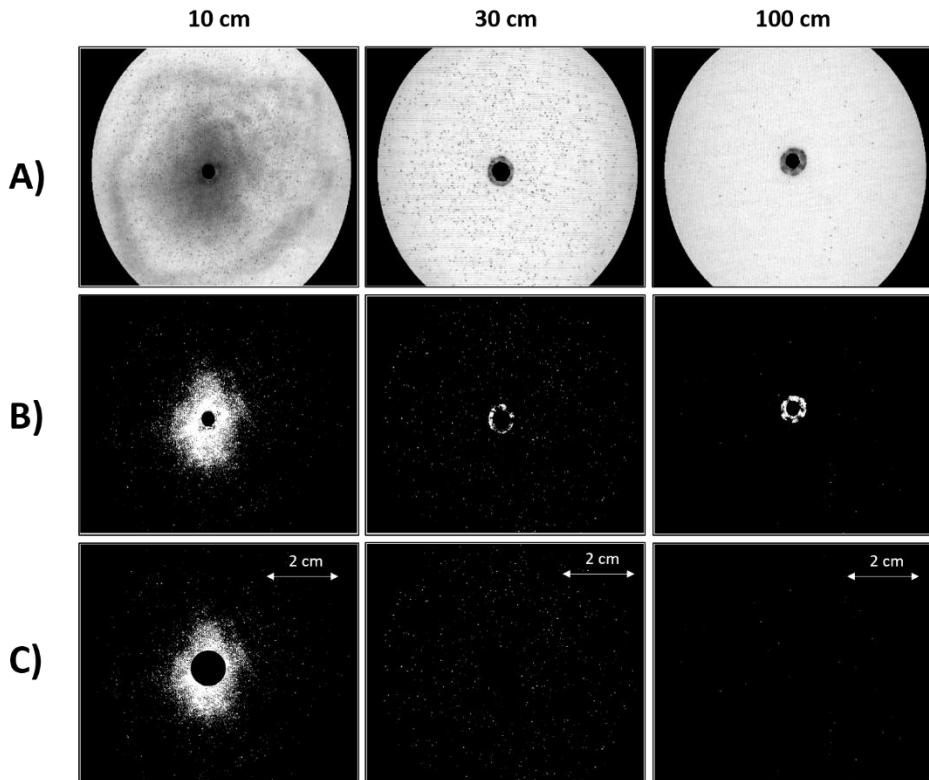
Figure 5. Image processing of multispectral images of clothing targets shot from distances of 10, 30, and 100 cm. (A) Gray-scale images of the blue RGB-frames (at 470 nm) after selecting the region of interest; (B) after binarizing and inverting the pixels corresponding to gunshot residues, and (C) after removal of the bullet wipe and the entrance hole. Reprinted from ref. [124] *with permission from Elsevier.*

Neither professional reflex cameras nor the cameras used in mobile phones record the true spectral reflectance of an object; such cameras record only the red (R), green (G), and blue (B) portions of the visual spectrum. Therefore, image reproduction is based on the trichromatic theory [120].

MSI is a fast, inexpensive, non-contact, non-destructive, and non-invasive technique [124]. Unfortunately, MSI does not provide identification of compounds; for qualitative analysis, selective spectral ranges using IR or Raman vibrational spectroscopy are needed. However, for the purposes of this thesis, the simplest visible MSI system consisting of RGB wavelengths was sufficient, since the aim was not the identification of compounds. One aim of this thesis was to study the transfer of known explosives to different materials through fingerprints. To date, no attempts have been made to study the transfer of explosive residues in consecutive fingerprints using MSI.

1.5 Data analysis

1.5.1 Principal component analysis

Interpretation of the obtained data is an important aspect of analytical chemistry. Principal component analysis (PCA) is one of the most common techniques used for data analysis. PCA analyzes a data table representing observations described by several dependent variables. Its purposes are to extract the most important information from the data table, to express this information as a set of new orthogonal variables known as principal components (PCs), and to simplify the description of the data [125]. PCs are obtained as linear combinations of the original variables. The first PC must have the largest possible variance. The second PC is calculated under the restriction of being orthogonal to the first one. PCA allows better visualization of data in exploratory analysis [125].

PCA results in a mathematical transformation of the original 2D matrix, which takes the form:

$$X = TP^T + E \qquad (8)$$

where T is a matrix of scores, P is a matrix of loadings, and E is an error matrix [126,127].

1.5.2 Analysis of variance

Analysis of variance (ANOVA) is a powerful statistical method used to separate and estimate the different causes of variation [128]. It is a method for testing the hypothesis that there is no difference between two or more population means. Several requirements must be fulfilled in order to use ANOVA. First, there must be only one independent variable (*e.g.* ethnicity) and there should be more than two levels for that independent variable (*e.g.* Estonian, Russian, Finnish, and American). Secondly, there must be only one dependent variable [129]. In addition, several assumptions are associated with one-way ANOVA. First, each population must be normally distributed with the same variance, *i.e.*, homogeneity of variance. Secondly, the groups under consideration must be independent.

The hypotheses for ANOVA are:
Null hypothesis H_0: The (population) means of all groups under consideration are equal: $\mu_1 = \mu_1 = \ldots = \mu_j$, where j is number of populations.
Alternative hypothesis H_1: The (population) means are not all equal (at least one mean differs from the others).

If m is the number of samples, and each sample has n members, the results form a table (matrix):

$$\begin{bmatrix} x_{11} & \cdots & x_{1m} \\ \vdots & \ddots & \vdots \\ x_{n1} & \cdots & x_{nm} \end{bmatrix}$$

The overall mean of the variable x is $\bar{\bar{x}}$ (all the values grouped together) and the mean value of kth sample is $\bar{x}_k$. We assume that all series of measurements are from the same population with a variation of σ^2. The total sum of squares (SST) is made up of two parts: the variation within each group (SSW) and the variation between the groups (SSB). The summary of the sums of squares and their equations are listed in Table 1.

Table 1. Summary of the sums of squares and degrees of freedom [128,130].

Source of variation	Sum of squares	Degrees of freedom
Sum of squares within groups (SSW)	$\displaystyle\sum_{k=1}^{m}\sum_{i=1}^{n}(x_{ki}-\bar{x}_k)^2$	m(n-1)=mn-m
Sum of squares between groups (SSB)	$\displaystyle n\sum_{k=1}^{m}(\bar{x}_k-\bar{\bar{x}})^2$	m-1
Total sum of squares (SST)	$\displaystyle\sum_{k=1}^{m}\sum_{i=1}^{n}(x_{ki}-\bar{\bar{x}})^2$	mn-1

Note: x_{ki} is the *i*th measurement of the *k*th sample.

In order to test whether the differences between SSW and SSB are significant, the F distribution is calculated:

$$F = \frac{variance\ between\ the\ groups}{variance\ within\ the\ groups} =$$
$$= \frac{SSB/(m-1)}{SSW/(n-1)m} \begin{cases} F < F^{crit}_{(1-\alpha),(m-1),m(n-1)} \Rightarrow H_0 \\ F > F^{crit}_{(1-\alpha),(m-1),m(n-1)} \Rightarrow H_1 \end{cases} \tag{9}$$

After the *F* value is calculated, it is compared with the critical value of the *F* distribution. $F^{crit}_{(1-\alpha),(m-1),m(n-1)}$ in Equation 9 is the critical value of *F* at confidence level (*1-α*). If the calculated value of *F* is much greater than F_{crit}, the null hypothesis (H_o) is rejected: the sample means do differ significantly, and thus, the alternative hypothesis (H_1) is accepted. If the calculated value of *F* is less than the F_{crit}, the null hypothesis (H_o) is accepted. In other words, if most of the variation comes from between groups, there is probably a significant effect, but if the variation between and within the groups is almost the same, there are no significant differences between sample means [128,130].

2 AIMS OF THE STUDY

The present dissertation had two main goals. The first was the development of rapid and simple analysis methods to detect degradation products of sulfur mustard (HD) in water samples. The second was the analysis of explosives for counterterrorism purposes.

The more specific aims of this thesis were as follows:

- Development of a protocol for the analysis of acyclic degradation products of HD using a CZE method with UV detection
- Development of a protocol for the analysis of cyclic degradation products of HD using MEKC and HPLC methods with UV detection
- Development of a rapid on-site analysis method for the detection of post-blast explosive residues using a portable CE instrument
- Development of a simple approach for acquiring fundamental knowledge about the transfer of explosive residues in consecutive fingerprints to different surfaces
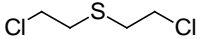
3 EXPERIMENTAL

3.1 Reagents and samples

3.1.1 Reagents
(Publications I, II and III)

The HD degradation products TDG, TDGO, TDGOO, 1,2,5-trithiepane, and 1,4,5-oxadithiepane were synthesized by Envilytix GmbH (Wiesbaden, Germany), while 1,4-thioxane, 1,3-dithiolane, and 1,4-dithiane were obtained from Sigma-Aldrich (Germany). All eight of the HD degradation products studied in **Publications I** and **II** are listed in Table 2. The BGE components (boric acid, sodium hydroxide, sodium tetraborate decahydrate, sodium dodecyl sulfate (SDS), 2-(*N*-morpholino)ethanesulfonic acid (MES), L-histidine (HIS), cetyltrimethylammonium bromide (CTAB), and 18-crown-6), as well as the internal standards (sinapinic acid, niacinamide, nicotinic acid, vanillin, and lithium formate) used in **Publications I-III** were purchased from Sigma-Aldrich. The ACN (HPLC grade, ≥99.99%) used as a mobile phase in **Publication II** was also obtained from Sigma-Aldrich.

Deionized (DI) water was supplied from a Milli-Q water purification system (Millipore S. A. Molsheim, France). All the BGEs and stock solutions used in **Publications I-III** were prepared in DI water. Chemicals were purchased from Sigma-Aldrich (Germany) unless otherwise stated. All reagents were of analytical grade.

Table 2. Chemical properties of HD and its degradation products.

Name	Structure	MW (g/mol)	Solubility in water (mg/mL)	logP	pKa
Sulfur mustard		159.08	0.39[a]	2.00[a] 1.98±0.34[b]	-
Thiodiglycol (TDG)		122.19	153.80[a]	-0.89[a] -0.71±0.35[b]	15.24-15.85[a]
Thiodiglycol sulfoxide (TDGO)		138.19	1972.15[a]	-2.66[a] -2.45± 0.37[b]	14.88-15.48[a]
Thiodiglycol sulfone (TDGOO)		154.18	1584.26[a]	-2.47[a] -1.99±0.35[b]	14.60-15.20[a]
1,4-thioxane		104.17	16.76[a]	0.25[a] 0.21±0.44[b]	-
1,3-dithiolane		106.21	2.13[a]	1.32[a] 0.71±0.58[b]	-
1,4-dithiane		120.24	2.20[a]	0.84[a] 1.12±0.58[b]	-
1,4,5-oxadithiepane		136.23	1.84[a]	0.47[a] 1.23±0.34[b]	-
1,2,5-trithiepane		152.29	0.24[a]	1.05[a] 2.11±0.52[b]	-
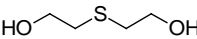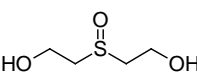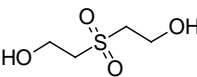
[a] estimated values derived from MarvinSketch version 16.2.1.0 (ChemAxon Ltd.)
[b] estimated values derived from ACD/ChemSketch (Freeware) 2015

3.1.2 Seawater and pore water samples for method development (Publications I and II)

The seawater and sediment samples were collected from the Baltic Sea. The sediment sample was taken from the bottom of the Baltic Sea at the port of Virtsu (Läänemaa, Estonia). The seawater sample was collected from the Gulf of Finland, 5 km from the coast of Tallinn. These samples were verified to be free of HD degradation products. The seawater sample was used as received, while the sediment sample was centrifuged for 20 min at 8500 rpm, after which the pore water was collected and filtrated for the analysis.

The water samples (seawater and pore water) were purified and concentrated in both publications using SPE. SPE based on carbon aerogels [131] was implemented (3 mL, 100 mg) in **Publication I**, while commercial Supelclean LC-18 SPE Tubes (3 mL, 500 mg, SUPELCO, Bellefonte, PA, USA) were used in **Publication II**.

3.1.3 Explosive samples (Publications III and IV)

The explosives used in **Publication III** were commercial products provided by OY Forcit AB (Hanko, Finland). The explosions were carried out on three different surfaces (sand, metal plate, and concrete) at the test site in Hanko. 50-100 g of the explosive was placed on the studied matrix, and the explosion was initiated using a detonator.

The organic explosives and explosive mixtures (TNT, HMTD, PETN, ANFO, dynamite, and black powder) in **Publication IV** were obtained from TEDAX, Spanish Explosive Ordnance Disposal, while the inorganic salts (NH_4NO_3, KNO_3, and $NaClO_3$) were purchased from Sigma-Aldrich.

The chemical composition of the explosives studied in **Publications III** and **IV** are indicated in Table 3.

Table 3. Studied explosives and their chemical composition.

Explosive residue	Chemical composition[a]
NH_4NO_3	Ammonium nitrate (100%)
KNO_3	Potassium nitrate (100%)
$NaClO_3$	Sodium chlorate (100%)
ANFO[a]	Ammonium nitrate (90%) + diesel (10%)
Dynamite[a]	Ammonium nitrate (66%) + ethylene glycol dinitrate (29%) + nitrocellulose (1%) + dibutyl phthalate (2.5%) + sawdust (1.2%) + calcium carbonate (0.3%)
Black powder[a]	Potassium nitrate (75%) + charcoal (15%) + sulfur (10%)
TNT[a]	2,4,6-Trinitrotoluene (100%)
HMTD[a]	Hexamethylene triperoxide diamine (100%)
PETN[a]	Pentaerythritol tetranitrate (100%)
C4[b]	RDX (91%)/ diethylhexyl or dioctyl sebacate (plasticizer, 5.3%)/ polyisobutylene (binder, 2.1%)/ non-detergent motor oil (1.6%)
PENO[b]	85% PETN /15% binder and detectant
RDX[b]	1,3,5-Trinitroperhydro-1,3,5-triazine (100%)
V40[b]	Reduced sensitivity RDX (RS-RDX), ammonium perchlorate, aluminum powder, binder

[a] Information provided by the manufacturer or by TEDAX (Spanish EOD).
[b] Information provided by the company OY Forcit AB (Hanko, Finland).

3.1.4 Sample preparation and fingerprint collection (Publication IV)

NH_4NO_3, KNO_3, $NaClO_3$, HMTD, PETN, ANFO, and black powder were obtained in powdered form and were used without pretreatment, while dynamite and TNT were powdered before the experiments.

Cotton fabric and polycarbonate plastic are the most common clothing and luggage materials, and thus were chosen for the study of the transfer of explosive residues through fingerprints. In order to obtain repeatable fingerprints, the initial explosive amount (10 mg), the applied force (1 kg), and time (3 sec) were fixed to control the transfer procedure. The standardized procedure for taking fingerprints is illustrated in Figure 6.
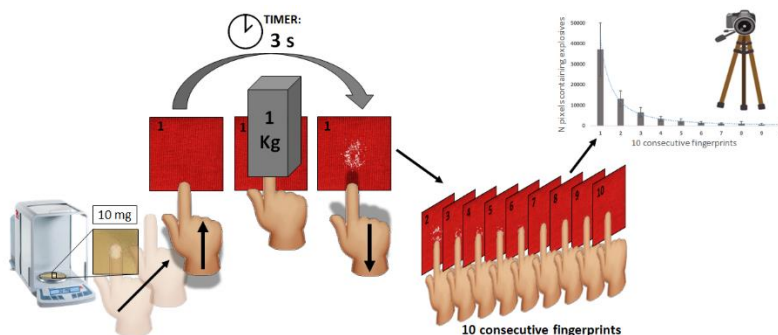

*Figure 6. Scheme of the standardized procedure for taking fingerprints (**Publication IV**).*

3.2 Instrumentation

3.2.1 Capillary electrophoresis
(Publications I, II and III)

An Agilent 3D instrument (Agilent Technologies) equipped with a diode array detector (DAD) was used for the capillary electrophoretic separation of the HD degradation products in **Publications I** and **II**. The detection wavelength in both publications was 200 nm. A portable CE instrument equipped with a C^4D was implemented for the experiments in **Publication III**. Uncoated fused-silica capillaries (Polymicro Technologies, Phoenix, AZ, USA) with an i.d. of 50 µm (**Publication I**) or 75 µm (**Publication II**) and a length of 51.5/60 cm (effective length/total length) were employed in the experiments. A capillary with a total length of 50 cm (i.d. of 50 µm) was used in **Publication III**. A BGE consisting of 30 mM borate buffer (pH 8.50) was used in **Publication I**, while 10 mM borate and 90 mM SDS were implemented as the BGE in **Publication II**. A BGE with low conductivity consisting of 20 mM MES/HIS, 30 µM CTAB, and 2 mM 18-crown-6 was used in **Publication III**. The samples were injected hydrodynamically under a pressure of 50 mbar for 5 sec (**Publication I**) or 3 sec (**Publication II**), while in **Publication III**, 500 µL of the sample was injected by manually applying pressure to the plastic syringe. In **Publication III**, dual opposite end injection (DOEI) was performed from both sides of the instrument. First, 500 µL of the sample followed by 1500 µL of BGE was injected from the positive side, and then 500 µL of the sample followed by 500 µL of BGE was injected from the negative side.

3.2.2 High performance liquid chromatography
(Publication II)

In addition to CE analysis, cyclic HD degradation products were also analyzed using an Agilent 1200 series HPLC instrument with a DAD (Agilent Technologies, Waldbronn, Germany). The detection wavelength was 200 nm. The samples were separated on a ZORBAX Eclipse Plus C18 column (Narrow Bore RR, 150 × 2.1mm i.d., 3.5 µm particle size). The mobile phase consisted of H_2O/ACN (55:45, v/v) with a flow rate 0.2 mL/min. The sample volume was 5 µL. Water samples were purified and concentrated before the HPLC analysis by using Supelclean LC-18 SPE Tubes (volume 3 mL, 500 mg, SUPELCO, Bellefonte, PA, USA).

3.3 Validation
(Publications I and II)

The methods developed in **Publications I** and **II** were validated by evaluating parameters such as the sensitivity, linearity, limits of detection and quantification (LOD and LOQ), precision, and recovery. All the calibration curves were constructed using different concentrations, and were obtained by plotting the response (ratio of the corresponding analyte peak area to the internal standard peak area) against the analyte concentration. The LOD and LOQ were obtained experimentally by measuring the signal-to-noise ratio (S/N). Precision was evaluated as intraday (repeatability) and interday (reproducibility) precision. The repeatability evaluation involved measuring the concentration of the control sample in six replicates during one day. Reproducibility was evaluated by analyzing the control sample in six replicates over a 5-day period.

3.4 Multispectral imaging
(Publication IV)

Explosive residues on the surfaces were imaged using a Nikon D5000 Digital SLR Camera. Image processing was carried out in MATLAB R2017a (MathWorks, USA). The pictures were processed as follows. First, the unnecessary image borders were removed by selecting the region of interest (ROI), which consisted of 1000 × 1000 pixels. Then, the RGB frames of each image were compared, and the frame that provided the sharpest contrast between the background material and the explosive was selected. After the selection of the proper frame, the amount of explosive residues was quantified by counting the pixels whose intensity values in the chosen frame exceeded a specific value. After quantifying the pixels, the image was transformed into black and white, *i.e.*, values of 0 and 1 only, for better visualization. A simplified scheme of the image processing performed in MATLAB is shown in Figure 7.
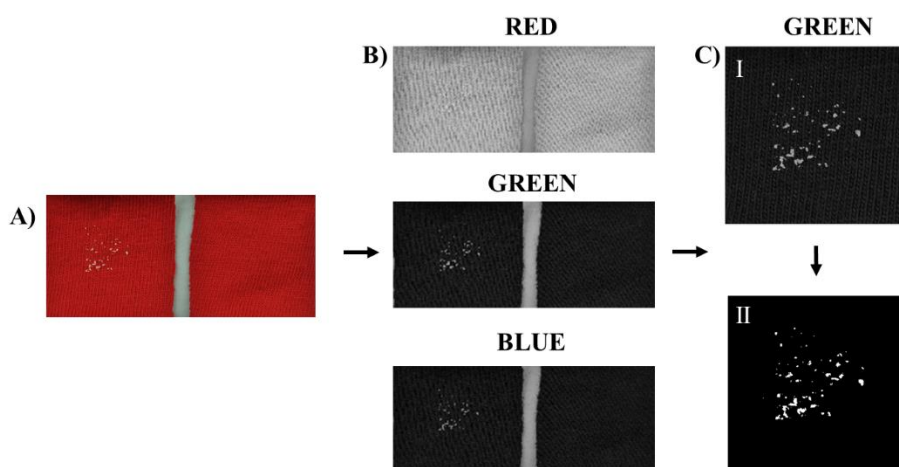

*Figure 7. Simplified scheme of image processing in MATLAB: A) explosive residues on cotton fabric (left) compared to a blank sample (right), B) RGB frames for estimation and selection, C) selection of the region of interest in the green frame (I), and conversion of the image to black and white only (II) (**Publication IV**).*

4 RESULTS AND DISCUSSION

The results presented in this dissertation are based on four publications. The first two studies, **Publication I** and **Publication II**, involve the development of methods to detect degradation products of HD in water samples. In this respect, **Publication I** covers the development of a method to analyze open-chain degradation products of HD, such as TDG and its oxidation products, while **Publication II** includes the analysis of cyclic degradation products of HD. The methodologies developed in these publications are based on CE and HPLC with UV detection. **Publications III** and **IV** cover the analysis of explosive residues. **Publication III** focused on analyzing the ionic content of post-blast explosive residues using a portable CE instrument with conductivity detection. **Publication IV** employed a simple approach to estimate the transfer of explosive residues in fingerprints to different surfaces.

All four studies focused on the development of new analysis methods to detect the use of explosives and CWAs.

4.1 Development of CE and HPLC methods for the analysis of sulfur mustard degradation products
(Publications I and II)

In **Publication I**, a CZE method with direct UV detection was developed for the analysis of three acyclic HD degradation products, namely TDG, TDGO, and TDGOO. In **Publication II**, HPLC and MEKC methods with UV detection were developed for the analysis of five cyclic HD degradation products (1,4-thioxane, 1,3-dithiolane, 1,4-dithiane, 1,2,5-trithiepane, and 1,4,5-oxadithiepane).

4.1.1 Optimization of the sample derivatization
(Publication I)

In **Publication I**, derivatization of the analytes was necessary, while in **Publication II** the chemical modification of analytes was not needed. The derivatization mixture was prepared as in the article of Vanhoenacker *et al.* [132]. Derivatization of the TDG, TDGO, and TDGOO samples with phthalic anhydride (Figure 8) was applied in **Publication I** to lower their high pK_a values ($pK_a > 14$, see Table 2) to enable the ionization of the analytes for electrophoretic analysis, as well as to lower the detection limit for UV detection by the addition of a chromophore into the molecule. The derivatization procedure enabled the LODs in **Publication I** to be lowered approximately 100 times in comparison to the previous work of Cheicante *et al.* [45], in which these neutral molecules were analyzed using MEKC. The derivatization procedure was carefully investigated, and the amount of derivatizing reactant, heating time, and temperature were optimized. The optimum derivatizaton conditions were obtained when 100 µL of the reactant was added to the solid analyte and heated for 20 min at 45 °C.
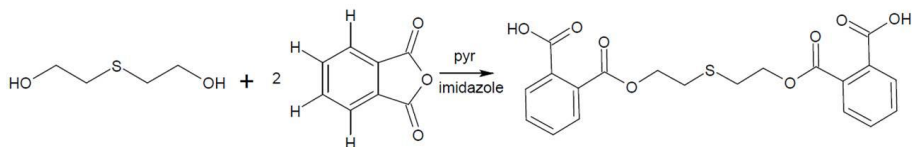

Figure 8. Derivatization reaction (using TDG as an example) with phthalic anhydride in the presence of pyridine and imidazole.

4.1.2 Optimization of the developed methods (Publications I and II)

The optimization of the CE methods in **Publications I** and **II** was performed by investigating the effect of the BGE concentration, pH, capillary temperature, and applied voltage. The optimized separation conditions are depicted in Table 4.

*Table 4. Optimized CE conditions for separation efficiency in **Publications I** and **II**.*

Studied condition	Publication I CZE method	Publication II MEKC method
BGE concentration	20-50 mM borate	10 mM borate, 50-100 mM SDS
pH	7.5-10.0	9.15
Capillary temperature	15-30 °C	15-25 °C
Applied voltage	15-25 kV	15-25 kV
Optimal conditions	30 mM borate, pH 8.50, 25 °C, 15 kV	10 mM borate, 90 mM SDS, 20 °C, 20 kV

After considering all the listed parameters, the optimal separation conditions in **Publication I** were found to be the following: a 30 mM borate buffer concentration, a pH of 8.50, a capillary temperature of 25 °C, and an applied voltage of 15 kV. A representative electropherogram in which the optimized separation conditions were applied to the three derivatives is shown in Figure 9.
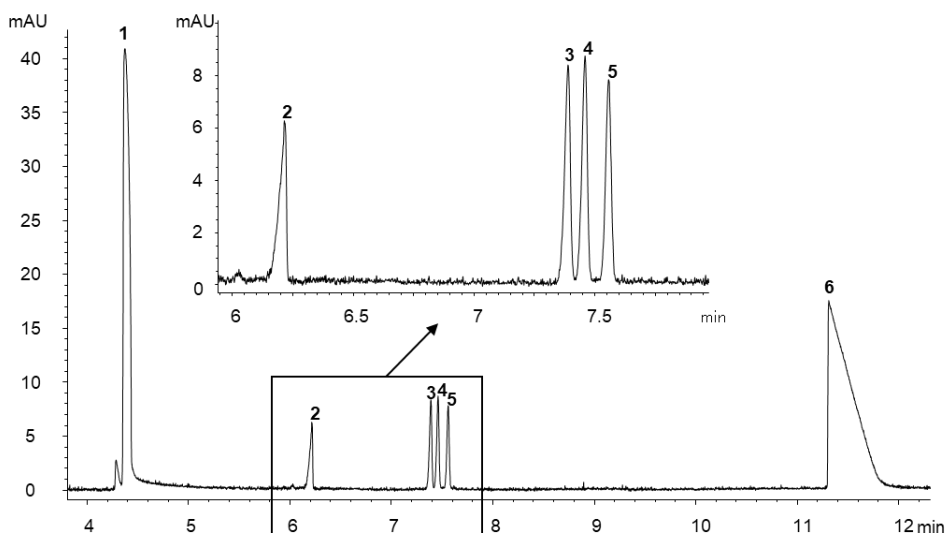
*Figure 9. Electropherogram of 25 µM of TDGO (3), TDG (4), and TDGOO (5) derivatives under optimized separation conditions: 30 mM borate buffer, pH 8.5, 15 kV, 25 °C. Additional peaks: (1) EOF, (2) sinapinic acid as IS, and (6) phthalic acid from the hydrolysis of unreacted phthalic anhydride (**Publication I**).*

In **Publication II**, the main criteria for selecting the optimum conditions for the separation of the five cyclic HD degradation products using MEKC was the complete resolution of 1,4-dithiane and 1,4,5-oxadithiepane. After carefully investigating all the listed conditions, the optimized conditions for the separation of compounds of interest

by MEKC were as follows: a 10 mM borate, 90 mM of SDS, an applied voltage of 20 kV, and a capillary temperature of 20 °C. Representative electropherograms in the three different matrices (distilled water, pore water, and seawater) are depicted in the Figure 10. As can be seen from Figure 10, the different matrices did not affect the separation of the analytes. Thus, this method is applicable to different water samples without the need for sample pretreatment (*i.e.*, purification of the sample by removing salts).
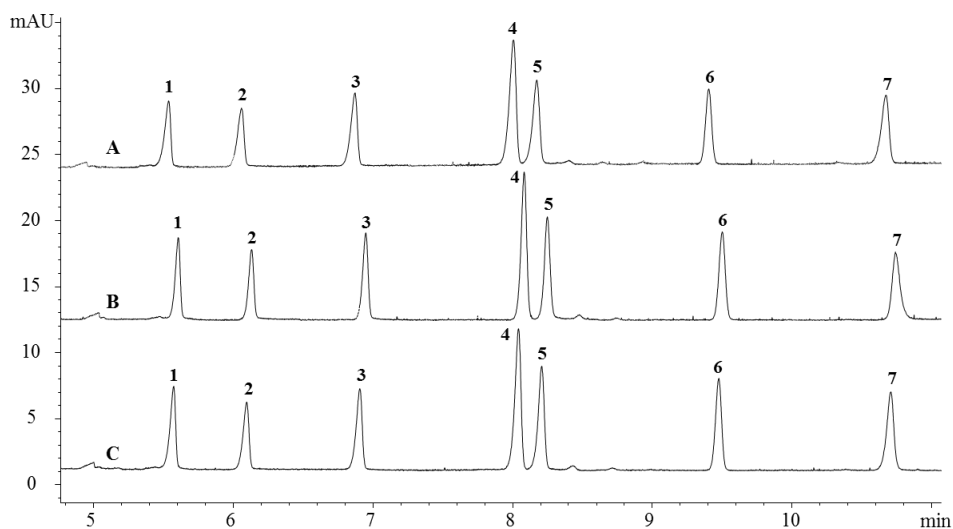
*Figure 10. Electropherograms of standards in (A) distilled water, (B) pore water, and (C) seawater. Identification of the peaks: (1) niacinamide (IS), (2) 1,4-thioxane, (3) 1,3-dithiolane, (4) 1,4-dithiane, (5) 1,4,5-oxadithiepane, (6) nicotinic acid (IS), and (7) 1,2,5-trithiepane. Optimized separation conditions: 10 mM borate, 90 mM SDS (pH 9.15), 20 kV, 20 °C (**Publication II**).*

In addition to the MEKC method, the cyclic degradation products of HD were analyzed using HPLC. Three variables were selected for the optimization of the HPLC method in **Publication II**: eluent strength, flow rate, and temperature. The ACN percentage was varied in the range 40-60% (step 5%). Figure 11 shows that all these mobile phase concentrations (40-60% of ACN) provided baseline separation of the five HD degradation products. The flow rate was varied in the range of 0.1-0.3 mL/min (in 0.05 mL/min steps). The temperature was varied from 25-40 °C (5 °C steps).
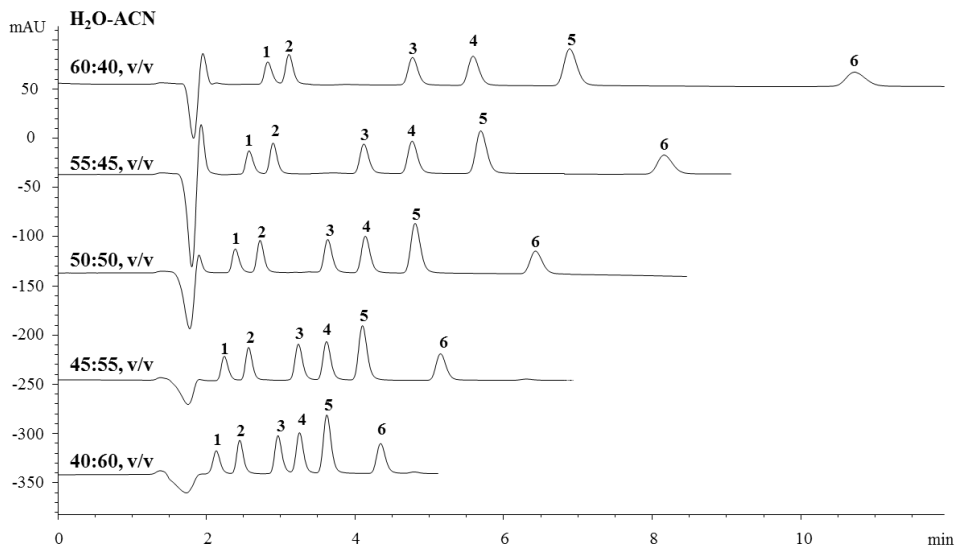
*Figure 11. Effect of the eluent strength on separation (40-60% ACN). Peaks: (1) vanillin (IS), (2) 1,4-thioxane, (3) 1,4,5-oxadithiepane, (4) 1,3-dithiolane, (5) 1,4-dithiane, and (6) 1,2,5-trithiepane. Flow rate: 0.2 mL/min, column temperature: 30 ˚C (**Publication II**).*

Figure 11 indicates that the optimum mobile phase for separating the analytes in distilled water would be 40% H_2O and 60% ACN, which resulted in the fastest time and best efficiency. However, the authors observed that the sample matrix (seawater or pore water) consisted of polar compounds, which resulted in a positive peak at the void time, which, in turn, affected the resolution of the first analytes. To ensure the baseline separation of all analytes in pore or seawater samples, H_2O-ACN (55:45, v/v) was selected as the optimum mobile phase (see Figure 12C). Therefore, the optimized HPLC conditions for separating cyclic HD degradation products were as follows: a mobile phase of H_2O-ACN (55:45, v/v), a flow rate of 0.2 mL/min, and a temperature of 30 °C.

Figure 12. Chromatograms of cyclic HD degradation products: (A) blank sample with an unknown peak (*); (B) 1 μM of each cyclic compound in distilled water; (C) seawater sample after the SPE proced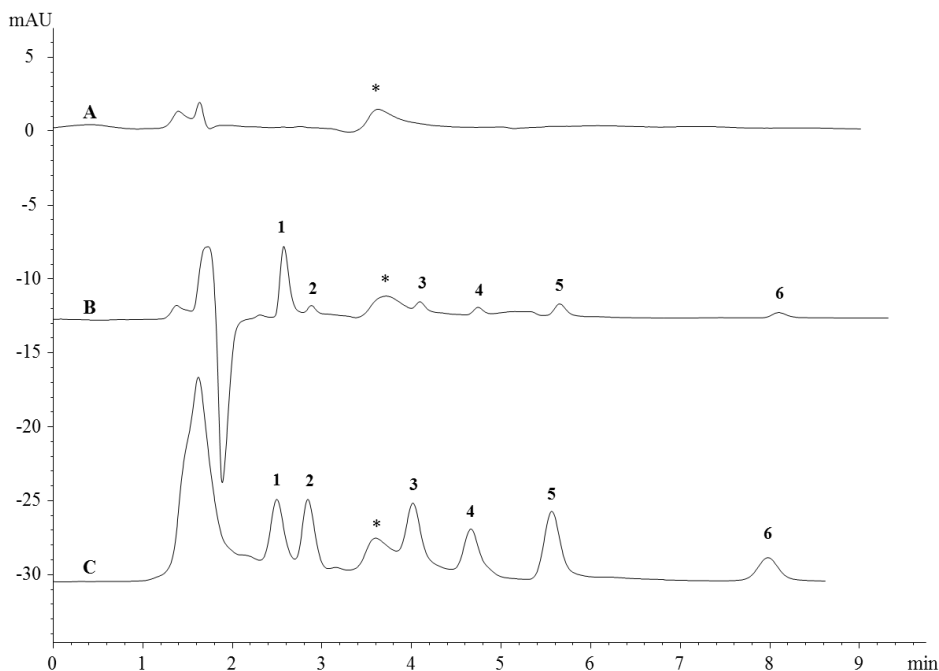ure (1 μM of the analytes concentrated 10 times). Peaks: (1) vanillin (IS), (2) 1,4-thioxane, (3) 1,4,5-oxadithiepane, (4) 1,3-dithiolane, (5) 1,4-dithiane, and (6) 1,2,5-trithiepane. Mobile phase: 55:45 (v/v) H_2O-ACN, flow rate: 0.2 mL/min, column temperature: 30 °C (Publication II).

The analysis of the cyclic HD degradation products in water samples using the developed HPLC method is depicted in Figure 12. In Figure 12A, the blank sample containing an unknown peak is shown. Figure 12B is a chromatogram of 1 μM of the standards in distilled water. Figure 12C shows the chromatogram obtained when 15 mL of seawater containing 1 μM of the standards was purified and concentrated 10 times using the optimized SPE procedure. It is important to note that it was not possible to inject the seawater or pore water samples into the HPLC system without sample pretreatment. The optimized ACN volume for eluting the analytes in the SPE procedure was 1.5 mL. Therefore, in the case of the 15 mL seawater sample, 1 μM of the analytes was concentrated 10 times. This means that in the case of 100% recovery, the concentration of these analytes should be 10 μM. The recoveries obtained using SPE depended on the sample volume and the analyte, and were in the range of 63-99%.

4.1.3 Validation and comparison of the CE and HPLC methods for quantitative analysis of HD degradation products
(Publications I and II)

The linearity range, regression equations, coefficients of determination (R^2), LOD, LOQ, and precision for each of the developed methodologies are given in Table 5. All the analytes in Table 5 are listed in their elution order with the specific method. The three methods in **Publications I** and **II** resulted in good linearity, with R^2 values higher than 0.99.

38

The LODs for the HD degradation products achieved using these methods were in the range of 0.08-20 µM. The lowest LODs, 0.08-0.10 µM, were achieved by the HPLC method for the cyclic compounds, while the highest LODs (10-20 µM) were obtained for the same compounds using the MEKC method. Even though the detection limits of the developed CE methods were one or two orders of magnitude higher than those of the HPLC method, each method has its advantages. In this respect, the HPLC method is very sensitive and could detect the leakage of HD munitions at low ppb levels. The cyclic compounds have been found in pore water fractions with concentrations of 0.02-0.14 µM [133], which are detectable by the developed HPLC method when the concentration procedure with SPE is included (at least 20-fold concentration was possible without affecting recoveries). However, one important advantage of the CE method is that it can easily be miniaturized and made portable. Thus, the analysis can be performed *in situ*, which is highly important due to the degradation of the analytes demonstrated in **Publication II**, in which the cyclic compounds were observed to undergo up to 15% degradation over a 5 h period (Section 3.5). However, due to the lower sensitivity of the CE method, this method is only applicable in cases when extreme sensitivity is not required. However, as the corrosion of CWs is still an ongoing process, in the future, higher concentrations of compounds may leak from the corroded shells into the sediment and seawater. Furthermore, the developed MEKC method did not require sample purification; salty water could be injected directly into the system, making the MEKC protocol significantly easier than the HPLC protocol, in which the purification step with SPE was essential.

In all three of the methods developed for the analysis of HD degradation products, the precision tests indicated RSDs of less than 1.2% and 7.7% for the migration times and peak areas, respectively. These RSD values indicate excellent repeatability and reproducibility for the migration times and peak areas of the analytes in the developed methods. The data presented in Table 5 demonstrates that the new methodologies performed well in the analysis of HD degradation products. The three developed methods were successfully applied to the analysis of eight HD degradation products in water samples.

Table 5. Performance characteristics of the developed CE and HPLC methods for the quantitative analysis of HD degradation products.

Analyte	Regression analysis					Precision I (peak areas)		Precision II (migration times)	
	Linear range, µM	Equation (*y=ax+b*)	R^2	LOD, µM	LOQ, µM	RSD (%), Intraday	RSD (%), Interday	RSD (%), Intraday	RSD (%), Interday
CZE									
TDGO derivative	1.0-20	y=0.1359x-0.0161	0.9997	1.0	3.3	2.4	5.4	0.6	0.8
TDG derivative	0.8-20	y=0.1517x+0.0017	0.9996	0.8	2.6	3.1	5.2	0.6	0.8
TDGOO derivative	1.0-20	y=0.1233x-0.0304	0.9994	1.0	3.3	2.7	6.3	0.6	1.2
HPLC									
1,4-thioxane	0.25-25	y=0.0606x-0.0116	0.9969	0.09	0.30	0.7	2.8	0.04	0.1
1,4,5-oxadithiepane	0.25-25	y=0.0798x+0.0524	0.9996	0.09	0.30	0.8	1.5	0.05	0.3
1,3-dithiolane	0.25-25	y=0.0814x-0.0198	0.9956	0.10	0.33	1.1	5.5	0.05	0.4
1,4-dithiane	0.25-25	y=0.1322x-0.0367	0.9974	0.08	0.26	1.0	4.0	0.06	0.5
1,2,5-trithiepane	0.25-25	y=0.080x+0.0056	0.9999	0.10	0.33	2.5	5.0	0.09	0.9
MEKC									
1,4-thioxane	50-500	y=0.0022x-0.0175	0.9980	20	66	2.2	4.3	0.6	1.1
1,3-dithiolane	50-500	y=0.0032x-0.0272	0.9990	15	50	2.2	7.7	0.6	1.0
1,4-dithiane	30-500	y=0.0057x-0.0325	0.9991	10	33	1.5	7.7	0.5	0.8
1,4,5-oxadithiepane	40-500	y=0.0035x-0.0095	0.9997	12	40	1.6	3.7	0.5	1.0
1,2,5-trithiepane	50-500	y=0.0039x+0.0154	0.9904	15	50	2.3	5.7	0.4	0.1

4.2 Fingerprinting of post-blast explosive residues
(Publication III)

In **Publication III**, a portable CE-C^{4}D system was used for fingerprint analysis of post-blast explosive residues. The identification of explosive residues based on their ionic content. For this purpose, eight different explosives (TNT, PETN, RDX, PENO, ANFO, dynamite, V40, and C4) were detonated on three different surfaces: sand, concrete, and metal. Analysis of post-blast explosive residues using CE is not novel; however, no systematic study on the effect of background ions from the surface (matrix) on which the explosion took place has been carried out. This is an important question since many of the ions used for identification are also present in the matrix. To obtain the analytes (ions) from the matrices, simple extraction methods were developed for each surface. The DOEI principle was used for the simultaneous separation of 10 anions and cations. The optimum position of the detector to enable the simultaneous separation of cations and anions was found to be 14 cm from the anodic side (for cation injection) and 36 cm from the cathodic side (for anion injection) (Figure 2 in **Publication III**). The cations were injected first. Altogether, ten cations and anions (NH_4^+, K^+, Ca^{2+}, Na^+, Mg^{2+}, Cl^-, NO_2^-, NO_3^-, SO_4^{2-}, and N_3^-) were separated in less than 4 minutes using DOEI (Figure 13).
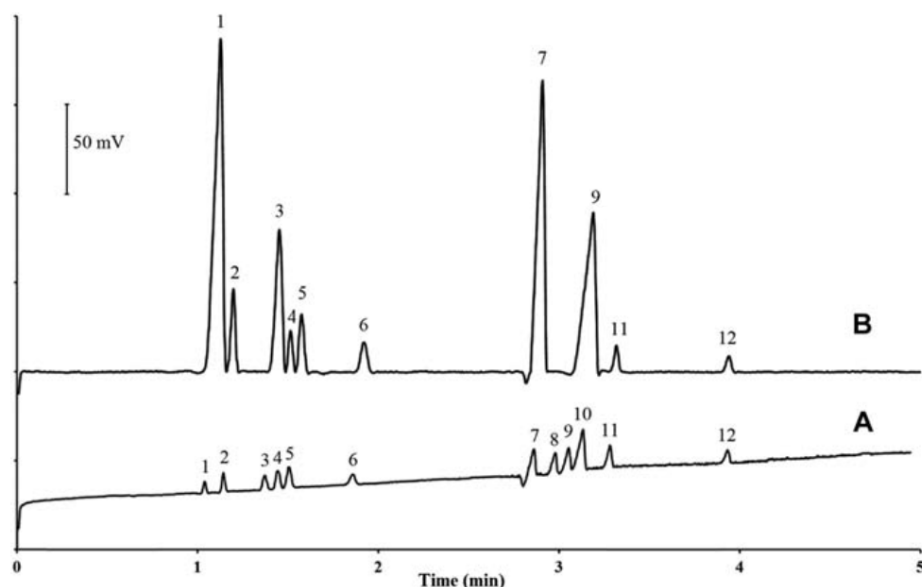
Figure 13. Simultaneous separation of cations and ions using DOEI. A) Standard solutions of ions. B) Analysis of post-blast residues of ANFO in a sand matrix (dilution 1:2). Identification of peaks: (1) NH_4^+, (2) K^+, (3) Ca^{2+}, (4) Na^+, (5) Mg^{2+}, (6) Li^+ (IS), (7) Cl^-, (8) NO_2^-, (9) NO_3^-, (10) SO_4^{2-}, (11) N_3^-, and (12) $HCOO^-$ (IS).

The developed CE method was validated for the simultaneous separation of cations and anions. The detection limits for the cations and anions were in the range of 3.7-35.7 µM. The precision tests resulted in RSDs of less than 9.9% for the peak areas. The method showed sufficient linear correlation ($R^2 \geq 0.87$) for the portable instrument without temperature control. The validated method was applied to the fingerprinting of eight explosives based on their ionic content. Based on the results, a flow chart was suggested

(Figure 14) for explosive identification on metal plate. However, this flow chart was valid only for the explosives under study, and only for the metal matrix. Therefore, the results clearly indicated that the matrix had a strong influence. In order to simplify the identification of explosives, PCA was applied to the data. PCA analysis revealed four significant PCs, which were responsible for 94% of the total variance. PCA also revealed that the influence of the matrix on the analysis of post-blast residues was strong. However, a combination of the information from PCA and electrophoretic analysis enabled partial identification of a specific explosive.
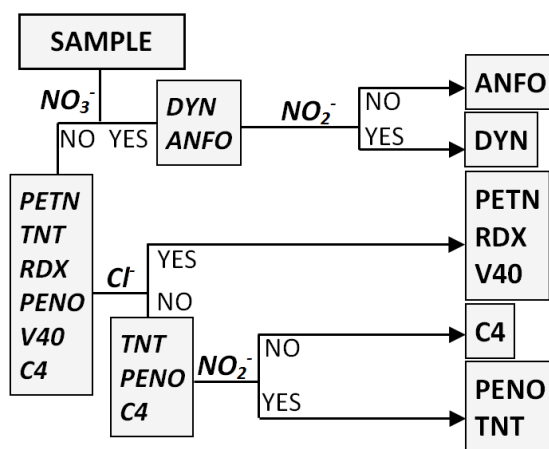

Figure 14. Flow chart for explosive identification on a metal matrix, based on the simultaneous separation of anions and cations.

4.3 Transfer of explosive residues in consecutive fingerprints
(Publication IV)

4.3.1 Transfer of PETN residues in consecutive fingerprints by different persons

In **Publication IV**, the influence of the subject providing the fingerprint on the transfer of explosive residues in successive fingerprints was studied. For this purpose, a test group consisting of ten persons was formed. All the subjects followed a standardized procedure for providing the fingerprints, which is described in more detail in Section 2.2 of **Publication IV**. Each person made ten successive fingerprints in triplicate. Subsequently, the fingerprints were imaged using a reflex camera, and the pixels corresponding to explosive residues in the images were counted in MATLAB. Via this data, the transfer patterns of PETN residues onto cotton fabric in consecutive fingerprints by different persons were evaluated. Surprisingly, the transfer pattern of the PETN residues in consecutive printings onto cotton fabric was similar for all subjects; the amount of explosive residues in the fingerprints decreased with increasing fingerprint number. In fact, this tendency perfectly followed the power function $y = 42556x^{-1.844}$ with an R^2 of 0.99 (Figure 15). The first column in Figure 15 represents the average number of pixels containing explosive residues in the first fingerprint given by the ten subjects with the calculated standard deviation; the second column represents the average number of pixels containing residues in the second fingerprints, *etc*.
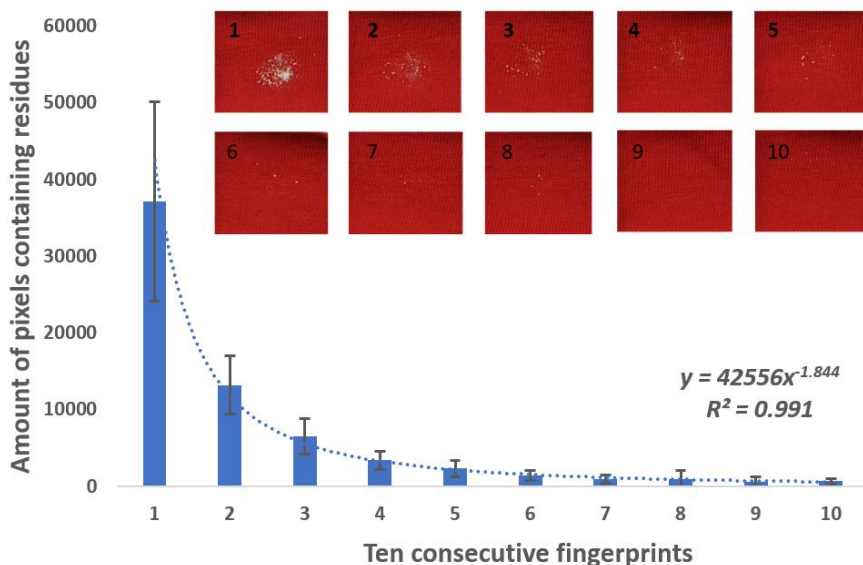
*Figure 15. The number of pixels corresponding to explosive residues in successive fingerprints of ten persons. Images of ten successive fingerprints of one person are shown as an example (**Publication IV**).*

However, the standard deviation bars in Figure 15 indicate that the amount of PETN in the successive fingerprints differed among the subjects. Statistical analysis was performed to determine whether the differences observed among the subjects were statistically significant. The analysis revealed that the differences in the amount of explosive residue transferred in the second to tenth fingerprints of the subjects were not statistically significant. Therefore, a multiple comparison procedure was applied to the ANOVA of the first fingerprint, which was found to be the variable that showed a statistically significant difference between the subjects at a 95% confidence level. The results revealed that even though there were significant differences between some subjects in the amount of explosive present in the first fingerprint, none of the subjects differed markedly from the others (see Table 3 of **Publication IV**). In conclusion, using PETN as an example, it was demonstrated that the subject did not significantly influence the transfer of explosives when following a standardized procedure.

4.3.2 Transfer of residues of explosives to different surfaces in successive fingerprints

The transfer of residues of nine explosives (NH_4NO_3, KNO_3, $NaClO_3$, HMTD, TNT, PETN, black powder, dynamite, and ANFO) via ten fingerprints onto cotton fabric and polycarbonate plastic was investigated. A single person made all the fingerprints (in three replicates per explosive and surface), as the study described in the preceding paragraph demonstrated that the transfer of explosive residues was not strongly influenced by the person providing the fingerprint when a controlled procedure was followed.

One replicate of consecutive fingerprints containing HMTD, TNT, black powder, and KNO_3 residues on cotton fabric and polycarbonate plastic is displayed in Figure 16. The figure clearly shows that the amount of residue transferred via fingerprints varies for each explosive. In order to better estimate the differences in the transfer of different

explosives, the number of pixels containing explosive residues in each image was quantified.
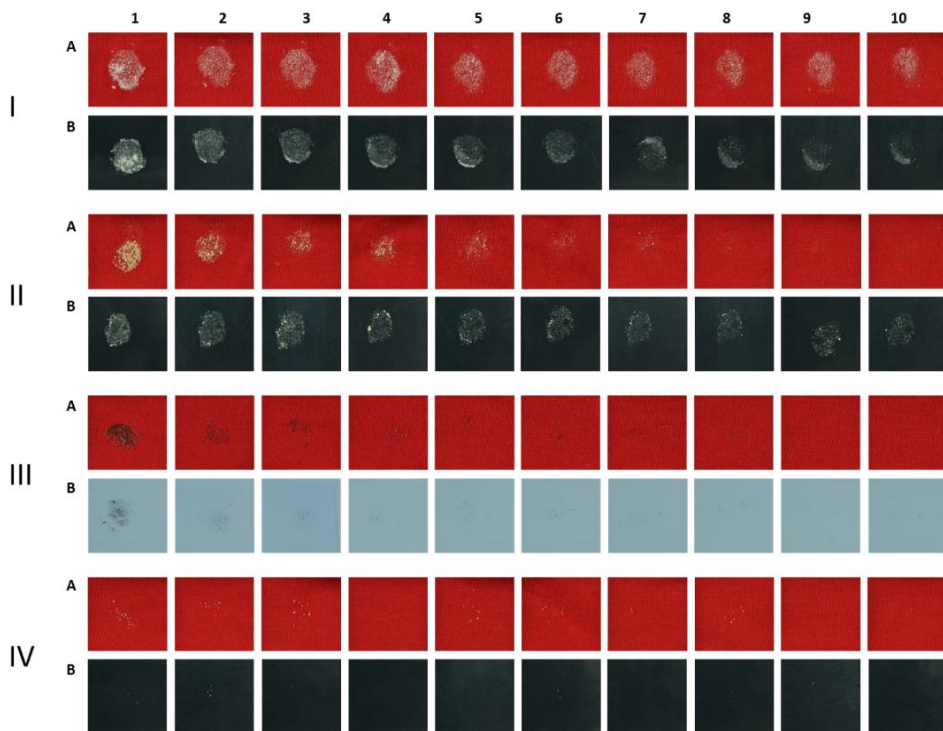
*Figure 16. Transfer of explosive residues via ten successive fingerprints onto cotton fabric (A) and polycarbonate plastic (B). I – HMTD, II – TNT, III – black powder, IV – KNO₃ (**Publication IV**).*

Two different tendencies were observed in the transfer of explosive residues through consecutive fingerprints using a standardized procedure. On one hand, the organic explosives (HMTD, TNT, and PETN), dynamite, and black powder showed a clear power or exponential decrease in the amount of residues transferred in consecutive fingerprints. On the other hand, no clear decrease in the amount of transferred residues of the oxidizing inorganic salts (NH_4NO_3, KNO_3, and $NaClO_3$) and ANFO (consisting of 90% NH_4NO_3) in consecutive fingerprints was noticed. The reason for their random transfer was probably the high hygroscopicity of the salt residues, which caused the particles to adhere to the bare finger rather than transfer to another material. Furthermore, the salts formed aggregates, which occasionally detached from the finger. The obtained graphs with the respective fitting functions for the transfer of each explosive are depicted in Figure 4 and 5 of **Publication IV**.

Regarding the effect of the cotton fabric and polycarbonate plastic surface, in general, higher amounts of explosive residues were transferred onto cotton. This was probably due to the stronger adhesion of the explosive residues to the cotton fibers than to the smooth surface of polycarbonate plastic. The transfer of inorganic salts and ANFO to polycarbonate was very low. In addition, a sharper decrease was observed in the amount of explosive residues transferred to polycarbonate plastic with successive fingerprints.

The results presented in **Publication IV** may significantly contribute to the scarcely investigated field of the transfer of explosives via fingerprints to different materials. To date, most investigations have dealt with the trace detection of explosive residues, but the study of their transfer has been overlooked. Although identification of the residues was not the aim of this research, the identification of the transferred explosive particles on both studied surfaces was achieved by using Raman spectroscopy. However, this data was not included in the manuscript.

5 CONCLUSIONS

The aim of this thesis was to develop and optimize new methodologies based on CE, HPLC and multispectral imaging (MSI) to determine the degradation products of CWAs and explosive residues.

The results of this thesis demonstrated that the developed CE and HPLC methods were very well suited for the detection of sulfur mustard (HD) degradation products and explosives, while MSI proved to be a simple approach for acquiring fundamental knowledge regarding the transfer patterns of different explosives.

The results of this thesis can be summarized as follows:

- A CE method with UV detection was optimized and validated for the determination of acyclic HD degradation products, namely TDG, TDGO, and TDGOO.
    - ✓ Pre-capillary derivatization with the strong UV chromophore phthalic anhydride enabled the detection limits of HD degradation products to be lowered by two orders of magnitude compared to the previously published work of Cheicante *et al.* [45].
    - ✓ The developed method was applicable to real seawater samples without interference from the sample matrix.
- HPLC and CE methods with UV detection were optimized and validated for the determination of cyclic HD degradation products, namely 1,4-thioxane, 1,3-dithiolane, 1,4-dithiane, 1,2,5-trithiepane, and 1,4,5-oxadithiepane in seawater and pore water samples.
    - ✓ The HPLC method enabled separation of all five cyclic compounds within 8 min by employing a simple isocratic mobile phase for elution.
    - ✓ The MEKC method provided separation of the five cyclic compounds in 11 min, did not require sample purification, and showed excellent efficiency.
    - ✓ Neither of the methods required sample derivatization.
    - ✓ With the HPLC method, the LODs were lowered by using SPE for sample purification and concentration.
    - ✓ The HPLC method had low detection limits, while the MEKC method could be adapted for *in situ* analysis, which is a highly important feature due to the instability of the studied compounds.
    - ✓ The HPLC method was applied to the analysis of two real samples collected near a dumped object located in the Bornholm Deep dumpsite.
- A portable CE method using conductivity detection was developed for the rapid analysis of post-blast explosive residues in three different matrices.
    - ✓ Simple methods were developed for the extraction of ions from metal, sand, and concrete surfaces.
    - ✓ Dual opposite end injection (DOEI) was implemented, enabling the simultaneous analysis of anions and cations in less than 4 min.
    - ✓ Partial identification of the explosives based on the ionic content of their post-blast residues was achieved.
    - ✓ The matrix effects were studied using principal component analysis.
- MSI was used for determining the transfer of explosive residues via ten consecutive fingerprints.
    - ✓ The transfer of nine different explosives to two different surfaces was investigated.

- ✓ A self-written code in MATLAB was used for semi-automatic image processing and pixel counting.
- ✓ The subject providing the fingerprint did not seem to have a significant impact on the transfer of explosive residues when following a standardized procedure. Similar transfer patterns of PETN residues were observed for all subjects.
- ✓ Two entirely different tendencies were observed in the transfer of explosive residues via consecutive fingerprints when using a standardized procedure. On the one hand, for organic explosives, black powder, and dynamite, the amount of explosive residues deposited in the ten successive fingerprints followed a particular power or exponential decrease. On the other hand, random transfer of residues of inorganic salts and ANFO (composed of 90% NH_4NO_3) was observed.

REFERENCES

[1]   G. Carton, A. Jagusiewicz, Historic Disposal of Munitions in U.S. and European Coastal Waters, How Historic Information Can be Used in Characterizing and Managing Risk, Mar. Technol. Soc. J. 43 (2009) 16–32.

[2]   J. Bełdowski, B. Robert, E.K. Turmus, Towards the Monitoring of Dumped Munitions Threat (MODUM), Springer, Dordrecht, The Netherlands, 2018.

[3]   Organisation for the Prohibition of Chemical Weapons (OPCW), About OPCW, [Online]. Available: https://www.opcw.org/about-opcw/.

[4]   Organisation for the Prohibition of Chemical Weapons (OPCW), About chemical weapons, [Online]. Available: https://www.opcw.org/about-chemical-weapons/what-is-a-chemical-weapon.

[5]   United Nations Office for Disarmament Affairs (UNODA), Geneva Protocol, [Online]. Available: http://disarmament.un.org/treaties/t/1925.

[6]   United Nations Treaty Collection, Chemical Weapons Convention, [Online]. Available: https://treaties.un.org/Pages/ViewDetails.aspx?src=TREATY&mtdsg_no=XXVI-3&chapter=26&lang=en.

[7]   International Maritime Organization, London Convention, [Online]. Available: http://www.imo.org/en/OurWork/Environment/LCLP/Pages/default.aspx.

[8]   HELCOM, Chemical Munitions Dumped in the Baltic Sea. Report of the *ad hoc* Expert Group to Update and Review the Existing Information on Dumped Chemical Munitions in the Baltic Sea (HELCOM MUNI), Baltic Sea Environment Proceeding (BSEP) No. 142, 2013.

[9]   James Martin Center for Nonproliferation Studies, Chemical Weapon Munitions Dumped at Sea, [Online]. Available: http://www.nonproliferation.org/chemical-weapon-munitions-dumped-at-sea/.

[10]   M.I. Greenberg, K.J. Sexton, D. Vearrier, Sea-dumped chemical weapons: Environmental risk, occupational hazard, Clin. Toxicol. 54 (2016) 79–91.

[11]   J. Bełdowski, Z. Klusek, M. Szubska, R. Turja, A.I. Bulczak, D. Rak, M. Brenner, T. Lang, L. Kotwicki, K. Grzelak, J. Jakacki, N. Fricke, A. Östin, U. Olsson, J. Fabisiak, G. Garnaga, J.R. Nyholm, P. Majewski, K. Broeg, M. Söderström, P. Vanninen, S. Popiel, J. Nawała, K. Lehtonen, R. Berglind, B. Schmidt, Chemical Munitions Search & Assessment - An evaluation of the dumped munitions problem in the Baltic Sea, Deep Sea Res. Part II. 128 (2016) 85–95.

[12]   A. Östin, Review of Analytical Methods for the Analysis of Agents Related to Dumped Chemical Weapons for the CHEMSEA project, CHEMSEA, Chemical Munitions Search & Assessment, 2012.

[13]   J.A. Romano, B.J. Lukey, H. Salem, Chemical warfare agents: chemistry, pharmacology, toxicology, and therapeutics, CRC Press, Florida, USA, 2008.

[14]   Agency for Toxic Substances and Disease Registry, Toxicological Profile for Sulfur Mustard (Update), Atlanta, Georgia, USA, 2003.

[15]   Organisation for the Prohibition of Chemical Weapons (OPCW), Mustard agents, [Online]. Available: http://www.opcw.org/protection/types-of-chemical-agent/mustard-agents/.

[16]   A.P. Watson, T.D. Jones, G.D. Griffin, Sulfur mustard as a carcinogen: application of relative potency analysis to the chemical warfare agents H, HD, and HT, Regul. Toxicol. Pharmacol. 10 (1989) 1–25.

[17] M.A. Williams, G. Reddy, M.J. Quinn Jr, M.S. Johnson, Wildlife Toxicity Assessments for Chemicals of Military Concern, Elsevier, 2015.

[18] W.E. Luttrell, W.W. Jederberg, K.R. Still, Toxicology Principles for the Industrial Hygienist, The American Industrial Hygiene Association, USA, 2008.

[19] A.P. Watson, G.D. Griffin, Toxicity of vesicant agents scheduled for destruction by the chemical stockpile disposal program, Environ. Health Perspect. 98 (1992) 259–280.

[20] N.B. Munro, S.S. Talmage, G.D. Griffin, L.C. Waters, A.P. Watson, J.F. King, V. Hauschild, The sources, fate, and toxicity of chemical warfare agent degradation products, Environ. Health Perspect. 107 (1999) 933–974.

[21] P. Vanninen, Recommended operating procedures for analysis in the verification of chemical disarmament, University of Helsinki, 2011.

[22] M. Söderström, WP3. Summary of chemical analysis of sediment samples, CHEMSEA, Chemical Munitions Search & Assessment, Helsinki, 2014.

[23] G. Reddy, M.A. Major, G.J. Leach, Toxicity assessment of thiodiglycol, Int. J. Toxicol. 24 (2005) 435–442.

[24] H.F.J. Smyth, J. Seaton, L. Fischer, The single dose toxicity of some glycols and derivatives, J. Ind. Hyg. Toxicol. 23 (1941) 259–268.

[25] G.O. Bizzigotti, H. Castelly, A.M. Hafez, W.H.B. Smith, M.T. Whitmire, Parameters for evaluation of the fate, transport, and environmental impacts of chemical agents in marine environments, Chem. Rev. 109 (2009) 236–256.

[26] T. Missiaen, M. Söderström, I. Popescu, P. Vanninen, Evaluation of a chemical munition dumpsite in the Baltic Sea based on geophysical and chemical investigations, Sci. Total Environ. 408 (2010) 3536–3553.

[27] R. Magnusson, T. Nordlander, A. Östin, Development of a dynamic headspace gas chromatography-mass spectrometry method for on-site analysis of sulfur mustard degradation products in sediments, J. Chromatogr. A. 1429 (2016) 40–52.

[28] B.T. Røen, E. Unneberg, J.A. Tørnes, E. Lundanes, Headspace-trap gas chromatography-mass spectrometry for determination of sulphur mustard and related compounds in soil, J. Chromatogr. A. 1217 (2010) 2171–2178.

[29] J. Bełdowski, J. Fabisiak, S. Popiel, A. Östin, U. Olsson, P. Vanninen, A. Lastumaki, T. Lang, N. Fricke, M. Brenner, R. Berglind, J. Baršiene, Z. Klusek, B. Pączek, M. Söderström, K. Lehtonen, M. Szubska, V. Malejevas, H. Koskela, J. Michalak, R. Turja, U. Bickmeyer, K. Broeg, A. Olejnik, J. Fidler, CHEMSEA FINDINGS: Results from the CHEMSEA project – Chemical munitions search and assessment, Gdańsk, 2014.

[30] E.W.J. Hooijschuur, C.E. Kientz, U.A.T. Brinkman, Analytical separation techniques for the determination of chemical warfare agents, J. Chromatogr. A. 982 (2002) 177–200.

[31] P.A. D'Agostino, C.L. Chenier, Analysis of Chemical Warfare Agents: General Overview, LC-MS Review, In-House LC-ESI-MS Methods and Open Literature Bibliography, Defence Research and Development Canada, Suffield, 2006.

[32] P.A. D'Agostino, L.R. Provost, Capillary column isobutane chemical ionization mass spectrometry of mustard and related compounds, Biomed. Mass Spectrom. 15 (1988) 553–564.

[33] P.A. D'Agostino, L.R. Provost, A.S. Hansen, G.A. Luoma, Identification of Mustard Related Cornpounds in Aqueous Samples by Gas Chromatography/Mass Spectrometry, Biomed. Environ. Mass Spectrom. 18 (1989) 484–491.

[34]   M. Mazurek, Z. Witkiewicz, S. Popiel, M. Śliwakowski, Capillary gas chromatography-atomic emission spectroscopy-mass spectrometry analysis of sulphur mustard and transformation products in a block recovered from the Baltic Sea, J. Chromatogr. A. 919 (2001) 133–145.

[35]   S. Popiel, J. Nawała, D. Dziedzic, M. Söderström, P. Vanninen, Determination of mustard gas hydrolysis products thiodiglycol and thiodiglycol sulfoxide by gas chromatography-tandem mass spectrometry after trifluoroacetylation, Anal. Chem. 86 (2014) 5865–5872.

[36]   U.C. Meier, Detection and identification of hydrolysis products of sulfur mustards at trace levels in environmental samples using liquid chromatography solid phase extraction combined with off-line nuclear magnetic resonance analysis, J. Chromatogr. A. 1286 (2013) 159–165.

[37]   M. Mesilaakso, Chemical Weapons Convention Chemicals Analysis: Sample Collection, Preparation and Analytical Methods, John Wiley & Sons, Ltd, Helsinki, 2005.

[38]   B.A. Tomkins, G.A. Sega, S.J. Macnaughton, The Quantitation of Sulfur Mustard By-Products, Sulfur-Containing Herbicides, and Organophosphonates in Soil and Concrete, Anal. Lett. 31 (1998) 1603–1622.

[39]   E.W.J. Hooijschuur, C.E. Kientz, U.A.T. Brinkman, Determination of the sulfur mustard hydrolysis product thiodiglycol by microcolumn liquid chromatography coupled on-line with sulfur flame photometric detection using large-volume injections and peak compression, J. Chromatogr. A. 849 (1999) 433–444.

[40]   E.W.J. Hooijschuur, C.E. Kientz, A.G. Hulst, U.A.T. Brinkman, Determination of hydrolysis products of sulfur mustards by reversed-phase microcolumn liquid chromatography coupled on-line with sulfur flame photometric detection and electrospray ionization mass spectrometry using large-volume injections and peak compression, Anal. Chem. 72 (2000) 1199–1206.

[41]   N. V. Beck, W.A. Carrick, D.B. Cooper, B. Muir, Extraction of thiodiglycol from soil using pressurised liquid extraction, J. Chromatogr. A. 907 (2001) 221–227.

[42]   G.R. Asbury, C. Wu, W.F. Siems, H.H. Hill Jr., Separation and identification of some chemical warfare degradation products using electrospray high resolution ion mobility spectrometry with mass selected detection, Anal. Chim. Acta. 404 (2000) 273–283.

[43]   P. Jõul, H. Lees, M. Vaher, E.-G. Kobrin, M. Kaljurand, M. Kuhtinskaja, Development of a capillary electrophoresis method with direct UV detection for the analysis of thiodiglycol and its oxidation products, Electrophoresis. 36 (2015) 1202–1207.

[44]   R.L. Cheicante, J.R. Stuff, H.D. Durst, Analysis of chemical weapons degradation products by capillary electrophoresis with UV detection, J. Capillary Electrophor. 2 (1995) 157–163.

[45]   R.L. Cheicante, J.R. Stuff, H.D. Durst, Separation of sulfur containing chemical warfare related compounds in aqueous samples by micellar electrokinetic chromatography, J. Chromatogr. A. 711 (1995) 347–352.

[46]   B.T. Røen, E. Unneberg, J.A. Tørnes, E. Lundanes, Trace determination of sulphur mustard and related compounds in water by headspace-trap gas chromatography-mass spectrometry, J. Chromatogr. A. 1217 (2010) 761–767.

[47] R.W. Read, R.M. Black, Rapid screening procedures for the hydrolysis products of chemical warfare agents using positive and negative ion liquid chromatography-mass spectrometry with atmospheric pressure chemical ionisation, J. Chromatogr. A. 862 (1999) 169–177.

[48] H. Lees, M. Vaher, M. Kaljurand, Development and comparison of HPLC and MEKC methods for the analysis of cyclic sulfur mustard degradation products, Electrophoresis. 38 (2017) 1075–1082.

[49] L. Türker, S. Variş, A review of polycyclic aromatic energetic materials, Polycycl. Aromat. Compd. 29 (2009) 228–266.

[50] J.P. Agrawal, High Energy Materials: Propellants, Explosives and Pyrotechnics, Wiley-VCH, Berlin, Germany, 2010.

[51] M. López-López, C. García-Ruiz, Infrared and Raman spectroscopy techniques applied to identification of explosives, Trends Anal. Chem. 54 (2014) 36–44.

[52] M.Á. Fernández de la Ossa, J.M. Amigo, C. García-Ruiz, Detection of residues from explosive manipulation by near infrared hyperspectral imaging: a promising forensic tool, Forensic Sci. Int. 242 (2014) 228–235.

[53] M.Á. Fernández de la Ossa, C. García-Ruiz, J.M. Amigo, Near infrared spectral imaging for the analysis of dynamite residues on human handprints, Talanta. 130 (2014) 315–321.

[54] F. Zapata, M.Á. Fernández de la Ossa, E. Gilchrist, L. Barron, C. García-Ruiz, Progressing the analysis of improvised explosive devices: comparative study for trace detection of explosive residues in handprints by Raman spectroscopy and liquid chromatography, Talanta. 161 (2016) 219–227.

[55] S. Singh, M. Singh, Explosives detection systems (EDS) for aviation security, Signal Processing. 83 (2003) 31–55.

[56] J.S. Caygill, F. Davis, S.P.J. Higson, Current trends in explosive detection techniques, Talanta. 88 (2012) 14–29.

[57] R.G. Ewing, D.A. Atkinson, G.A. Eiceman, G.J. Ewing, A critical review of ion mobility spectrometry for the detection of explosives and explosive related compounds., Talanta. 54 (2001) 515–529.

[58] S.D. Harvey, R.G. Ewing, M.J. Waltman, Selective sampling with direct ion mobility spectrometric detection for explosives analysis, Int. J. Ion Mobil. Spectrom. 12 (2009) 115–121.

[59] S.-S. Choi, C.E. Son, Analytical method for the estimation of transfer and detection efficiencies of solid state explosives using ion mobility spectrometry and smear matrix, Anal. Methods. 9 (2017) 2505–2510.

[60] I. Cotte-Rodríguez, Z. Takáts, N. Talaty, H. Chen, R.G. Cooks, Desorption electrospray ionization of explosives on surfaces: sensitivity and selectivity enhancement by reactive desorption electrospray ionization, Anal. Chem. 77 (2005) 6755–6764.

[61] N.L. Sanders, S. Kothari, G. Huang, G. Salazar, R.G. Cooks, Detection of Explosives as Negative Ions Directly from Surfaces Using a Miniature Mass Spectrometer, Anal. Chem. 82 (2010) 5313–5316.

[62] A.G. Davies, A.D. Burnett, W. Fan, E.H. Linfield, J.E. Cunningham, Terahertz spectroscopy of explosives and drugs, Mater. Today. 11 (2008) 18–26.

[63] F. Zapata, C. García-Ruiz, Determination of Nanogram Microparticles from Explosives after Real Open-Air Explosions by Confocal Raman Microscopy, Anal. Chem. 88 (2016) 6726–6733.

[64]   F. Zapata, C. García-Ruiz, Analysis of different materials subjected to open-air explosions in search of explosive traces by Raman microscopy, Forensic Sci. Int. 275 (2017) 57–64.

[65]   C. Johns, R.A. Shellie, O.G. Potter, J.W. O'Reilly, J.P. Hutchinson, R.M. Guijt, M.C. Breadmore, E.F. Hilder, G.W. Dicinoski, P.R. Haddad, Identification of homemade inorganic explosives by ion chromatographic analysis of post-blast residues, J. Chromatogr. A. 1182 (2008) 205–214.

[66]   B.R. McCord, K.A. Hargadon, K.E. Hall, S.G. Burmeister, Forensic analysis of explosives using ion chromatographic methods, Anal. Chim. Acta. 288 (1994) 43–56.

[67]   I.S. Krull, E.A. Davis, C. Santasania, S. Kraus, A. Basch, Y. Bamberger, Trace Analysis of Explosives by HPLC-Electron Capture Detection (HPLC-ECD), Anal. Lett. 14 (1981) 1363–1376.

[68]   D. Gaurav, A.K. Malik, P.K. Rai, High-performance liquid chromatographic methods for the analysis of explosives, Crit. Rev. Anal. Chem. 37 (2007) 227–268.

[69]   M. Pumera, Analysis of explosives via microchip electrophoresis and conventional capillary electrophoresis: A review, Electrophoresis. 27 (2006) 244–256.

[70]   M. Pumera, Trends in analysis of explosives by microchip electrophoresis and conventional CE, Electrophoresis. 29 (2008) 269–273.

[71]   M. Calcerrada, M. González-Herráez, C. García-Ruiz, Recent advances in capillary electrophoresis instrumentation for the analysis of explosives, TrAC - Trends Anal. Chem. 75 (2016) 75–85.

[72]   C. Sarazin, N. Delaunay, A. Varenne, C. Costanza, V. Eudes, P. Gareil, Capillary and microchip electrophoretic analyses of explosives and their residues, Sep. Purif. Rev. 39 (2010) 63–94.

[73]   J.P. Hutchinson, C.J. Evenhuis, C. Johns, A.A. Kazarian, M.C. Breadmore, M. Macka, E.F. Hilder, R.M. Guijt, G.W. Dicinoski, P.R. Haddad, Identification of inorganic improvised explosive devices by analysis of postblast residues using portable capillary electrophoresis instrumentation and indirect photometric detection with a light-emitting diode, Anal. Chem. 79 (2007) 7005–7013.

[74]   K.G. Hopper, H. Leclair, B.R. McCord, A novel method for analysis of explosives residue by simultaneous detection of anions and cations via capillary zone electrophoresis, Talanta. 67 (2005) 304–312.

[75]   M.Á. Fernández de la Ossa, M. Torre, C. García-Ruiz, Determination of nitrocellulose by capillary electrophoresis with laser-induced fluorescence detection, Anal. Chim. Acta. 745 (2012) 149–155.

[76]   M.Á. Fernández de la Ossa, F. Ortega-Ojeda, C. García-Ruiz, Discrimination of non-explosive and explosive samples through nitrocellulose fingerprints obtained by capillary electrophoresis, J. Chromatogr. A. 1302 (2013) 197–204.

[77]   C.G. Bailey, S.R. Wallenborg, Indirect laser-induced fluorescence detection of explosive compounds using capillary electrochromatography and micellar electrokinetic chromatography, Electrophoresis. 21 (2000) 3081–3087.

[78]   S. Kennedy, B. Caddy, J.M.F. Douse, Micellar electrokinetic capillary chromatography of high explosives utilising indirect fluorescence detection, J. Chromatogr. A. 726 (1996) 211–222.

[79]   K. Brensinger, C. Rollman, C. Copper, A. Genzman, J. Rine, I. Lurie, M. Moini, Novel CE-MS technique for detection of high explosives using perfluorooctanoic acid as a MEKC and mass spectrometric complexation reagent, Forensic Sci. Int. 258 (2016) 74–79.

[80]   J.P. Hutchinson, C. Johns, M.C. Breadmore, E.F. Hilder, R.M. Guijt, C. Lennard, G. Dicinoski, P.R. Haddad, Identification of inorganic ions in post-blast explosive residues using portable CE instrumentation and capacitively coupled contactless conductivity detection, Electrophoresis. 29 (2008) 4593–4602.

[81]   G.A. Blanco, Y.H. Nai, E.F. Hilder, R.A. Shellie, G.W. Dicinoski, P.R. Haddad, M.C. Breadmore, Identification of inorganic improvised explosive devices using sequential injection capillary electrophoresis and contactless conductivity detection, Anal. Chem. 83 (2011) 9068–9075.

[82]   E.-G. Kobrin, H. Lees, M. Fomitšenko, P. Kubáň, M. Kaljurand, Fingerprinting postblast explosive residues by portable capillary electrophoresis with contactless conductivity detection, Electrophoresis. 35 (2014) 1165–1172.

[83]   P. Lucena, I. Gaona, J. Moros, J.J. Laserna, Location and detection of explosive-contaminated human fingerprints on distant targets using standoff laser-induced breakdown spectroscopy, Spectrochim. Acta - Part B: At. Spectrosc. 85 (2013) 71–77.

[84]   E.D. Emmons, A. Tripathi, J.A. Guicheteau, S.D. Christesen, A.W. Fountain III, Raman chemical imaging of explosive-contaminated fingerprints, Appl. Spectrosc. 63 (2009) 1197–1203.

[85]   A. Tripathi, E.D. Emmons, P.G. Wilcox, J.A. Guicheteau, D.K. Emge, S.D. Christesen, A.W. Fountain, Semi-automated detection of trace explosives in fingerprints on strongly interfering surfaces with Raman chemical imaging, Appl. Spectrosc. 65 (2011) 611–619.

[86]   Y. Mou, J.W. Rabalais, Detection and identification of explosive particles in fingerprints using attenuated total Reflection-Fourier transform infrared spectromicroscopy, J. Forensic Sci. 54 (2009) 846–850.

[87]   S. Almaviva, S. Botti, L. Cantarini, A. Palucci, A. Puiu, F. Schnuerer, W. Schweikert, F.S. Romolo, Raman spectroscopy for the detection of explosives and their precursors on clothing in fingerprint concentration: a reliable technique for security and counterterrorism issues, Proc. SPIE. 8901 (2013) 890102/1-890102/9.

[88]   P.H.R. Ng, S. Walker, M. Tahtouh, B. Reedy, Detection of illicit substances in fingerprints by infrared spectral imaging, Anal. Bioanal. Chem. 394 (2009) 2039–2048.

[89]   M. Abdelhamid, F.J. Fortes, M.A. Harith, J.J. Laserna, Analysis of explosive residues in human fingerprints using optical catapulting-laser-induced breakdown spectroscopy, J. Anal. At. Spectrom. 26 (2011) 1445–1450.

[90]   J. Moros, J. Serrano, F.J. Gallego, J. Macías, J.J. Laserna, Recognition of explosives fingerprints on objects for courier services using machine learning methods and laser-induced breakdown spectroscopy, Talanta. 110 (2013) 108–117.

[91]   A. Banas, K. Banas, M.B.H. Breese, J. Loke, B. Heng Teo, S.K. Lim, Detection of microscopic particles present as contaminants in latent fingerprints by means of synchrotron radiation-based Fourier transform infra-red micro-imaging, Analyst. 137 (2012) 3459–3465.

[92]   N.J. Crane, E.G. Bartick, R.S. Perlman, S. Huffman, Infrared spectroscopic imaging for noninvasive detection of latent fingerprints, J. Forensic Sci. 52 (2007) 48–53.

[93]   T. Chen, Z.D. Schultz, I.W. Levin, Infrared spectroscopic imaging of latent fingerprints and associated forensic evidence, Analyst. 134 (2009) 1902–1904.

[94]   A. Tripathi, E.D. Emmons, J.A. Guicheteau, S.D. Christesen, P.G. Wilcox, D.K. Emge, A.W. Fountain III, Trace explosive detection in fingerprints with Raman chemical imaging, Proc. SPIE. 7665 (2010) 76650N/1-76650N/6.

[95] H. Östmark, M. Nordberg, T.E. Carlsson, Stand-off detection of explosives particles by multispectral imaging Raman spectroscopy, Appl. Opt. 50 (2011) 5592–5599.

[96] I. Malka, A. Petrushansky, S. Rosenwaks, I. Bar, Detection of explosives and latent fingerprint residues utilizing laser pointer-based Raman spectroscopy, Appl. Phys. B: Lasers Opt. 113 (2013) 511–518.

[97] M.R. Almeida, L.P.L. Logrado, J.J. Zacca, D.N. Correa, R.J. Poppi, Raman hyperspectral imaging in conjunction with independent component analysis as a forensic tool for explosive analysis: The case of an ATM explosion, Talanta. 174 (2017) 628–632.

[98] M.A. Turano, Transfer of Residues in Fingerprints, University of Rhode Island, Kingston, Rhode Island, USA, 2013.

[99] G.L. Gresham, J.P. Davies, L.D. Goodrich, L.G. Blackwood, B.Y.H. Liu, D. Thimsem, S.H. Yoo, S.F. Hallowell, Development of particle standards for testing detection systems: mass of RDX and particle size distribution of composition 4 residues, Proc. SPIE. 2276 (1994) 34–44.

[100] J.C. Oxley, J.L. Smith, E. Resende, E. Pearce, T. Chamberlain, Trends in explosive contamination, J. Forensic Sci. 48 (2003) 334–342

[101] H. Lees, F. Zapata, M. Vaher, C. García-Ruiz, Simple multispectral imaging approach for determining the transfer of explosive residues in consecutive fingerprints, Talanta. 184 (2018) 437–445.

[102] J.R. Verkouteren, J.L. Coleman, I. Cho, Automated mapping of explosives particles in composition C-4 fingerprints, J. Forensic Sci. 55 (2010) 334–340.

[103] D. Heiger, High-performance capillary electrophoresis, Agilent Technologies, Germany, 2000.

[104] D.C. Harris, Quantitative Chemical Analysis, W. H. Freeman and Company, New York, 2007.

[105] D. Harvey, Modern Analytical Chemistry, The McGraw-Hill Companies, DePauw University, USA, 2000.

[106] A. Manz, N. Pamme, D. Iossifidis, Bioanalytical Chemistry, Imperial College Press, London, 2004.

[107] M.W. Dong, Modern HPLC for Practicing Scientists, John Wiley & Sons, Inc., Hoboken, New Jersey, 2006.

[108] L.R. Snyder, J.J. Kirkland, J.L. Glajch, Practical HPLC Method Development, John Wiley & Sons, New York, USA, 1997.

[109] J.W. Dolan, Peak Tailing and Resolution, LC Troubl. (2002) 1–4.

[110] P. Kubán, P.C. Hauser, Fundamental aspects of contactless conductivity detection for capillary electrophoresis. Part I: Frequency behavior and cell geometry, Electrophoresis. 25 (2004) 3387–3397.

[111] A.J. Zemann, E. Schnell, D. Volgger, G.K. Bonn, Contactless conductivity detection for capillary electrophoresis, Anal. Chem. 70 (1998) 563–567.

[112] P. Kubán, P.C. Hauser, A review of the recent achievements in capacitively coupled contactless conductivity detection, Anal. Chim. Acta. 607 (2008) 15–29.

[113] A.J. Zemann, Capacitively coupled contactless conductivity detection in capillary electrophoresis, Electrophoresis. 24 (2003) 2125–2137.

[114] P. Kubán, A. Seiman, N. Makarõtseva, M. Vaher, M. Kaljurand, In situ determination of nerve agents in various matrices by portable capillary electropherograph with contactless conductivity detection, J. Chromatogr. A. 1218 (2011) 2618–2625.

[115] Y. Garini, I.T. Young, G. McNamara, Spectral imaging: Principles and applications, Cytom. Part A. 69A (2006) 735–747.

[116] M. Vaher, M. Kaljurand, The development of paper microzone-based green analytical chemistry methods for determining the quality of wines, Anal. Bioanal. Chem. 404 (2012) 627–633.

[117] T. Aid, M. Kaljurand, M. Vaher, Colorimetric determination of total phenolic contents in ionic liquid extracts by paper microzones and digital camera, Anal. Methods. 7 (2015) 3193–3199.

[118] C.-H. Feng, Y. Makino, S. Oshita, J.F. García Martín, Hyperspectral imaging and multispectral imaging as the novel techniques for detecting defects in raw and processed meat products: Current state-of-the-art research advances, Food Control. 84 (2018) 165–176.

[119] J. Li, X. Wan, Superpixel segmentation and pigment identification of colored relics based on visible spectral image, Spectrochim. Acta Part A Mol. Biomol. Spectrosc. 189 (2018) 275–281.

[120] J.R. Mansfield, V.A. Bochko, Multispectral Imaging, in: Handb. Digit. Imaging, John Wiley & Sons, Ltd., United Kingdom, 2015: pp. 185–210.

[121] C. Fernandez-Maloigne, ed., Advanced Color Image Processing and Analysis, Springer, New York, 2013.

[122] H.C. Schau, Remote detection of explosives with multispectral imaging, Proc. SPIE. 7304 (2009) 730414/1-730414/9.

[123] H. Bandey, S. Bleay, V. Bowman, L. Fitzgerald, A. Gibson, A. Hart, V. Sears, Fingerprint imaging across EM spectrum, Imaging Sci. J. 54 (2006) 211–218.

[124] F. Zapata, M. López-López, J.M. Amigo, C. García-Ruiz, Multi-spectral imaging for the estimation of shooting distances, Forensic Sci. Int. 282 (2018) 80–85.

[125] H. Abdi, L.J. Williams, Principal component analysis, Wiley Interdiscip. Rev. Comput. Stat. 2 (2010) 433–459.

[126] R.G. Brereton, Data analysis for the laboratory and chemical plant, John Wiley & Sons, Ltd., United Kingdom, 2003.

[127] R.G. Brereton, Applied Chemometrics for Scientists, John Wiley & Sons Ltd, United Kingdom, 2007.

[128] J.N. Miller, J.C. Miller, Statistics and Chemometrics for Analytical Chemistry, Sixth, Pearson, United Kingdom, 2010.

[129] R. Ho, Handbook of univariate and multivariate data analysis and interpretation with SPSS, Taylor & Francis Group, Florida, USA, 2006.

[130] M. Kaljurand, Kemomeetria, Tallinna Tehnikaülikooli Kirjastus, Tallinn, 2008.

[131] P. Jõul, M. Vaher, M. Kuhtinskaja, Evaluation of carbon aerogel-based solid-phase extraction sorbent for the analysis of sulfur mustard degradation products in environmental water samples, Chemosphere. 198 (2018) 460–468.

[132] G. Vanhoenacker, D. De Keukeleire, P. Sandra, Capillary zone electrophoresis for the analysis of phthalate-derivatized hydroxyl- and amino- containing compounds, J. Sep. Sci. 24 (2001) 651–657.

[133] I.M.A. Christensen, M.S. Storgaard, S.F. Hansen, E. Baatrup, H. Sanderson, Acute toxicity of sea-dumped chemical munitions: luminating the environmental toxicity of legacy compounds, Glob. Secur. Heal. Sci. Policy. 1 (2016) 39–50.

APPENDIX

Publication I

P. Jõul, **H. Lees**, M. Vaher, E.-G. Kobrin, M. Kaljurand, M. Kuhtinskaja, Development of a capillary electrophoresis method with direct UV detection for the analysis of thiodiglycol and its oxidation products, Electrophoresis. 36 (2015) 1202–1207.

Piia Jõul
Heidi Lees
Merike Vaher
Eeva-Gerda Kobrin
Mihkel Kaljurand
Maria Kuhtinskaja

Department of Chemistry, Tallinn
University of Technology, Tallinn,
Estonia

Research Paper

Development of a capillary electrophoresis method with direct UV detection for the analysis of thiodiglycol and its oxidation products

A novel method based on CE with precolumn derivatization and direct UV detection for the determination of thiodiglycol (TDG), TDG sulfoxide, and TDG sulfone in water samples was developed. The lack of a UV chromophore of target analytes was overcome by derivatization with phthalic anhydride. The reactant concentrations, as well as the derivatization dependence on heating temperature and time, were carefully investigated. The baseline separation of three derivatives was achieved in less than 8 min by applying a simple BGE composed of a 30 mM borate buffer at pH 8.5. Several parameters affecting the separation efficiency (buffer pH and concentration, capillary temperature, and applied voltage) were evaluated. Calibration curves of all compounds showed good linear correlations ($R^2 > 0.9994$). The LODs of the TDG and its oxidation products were in the range of 98–154 ng/mL. The precision tests resulted in RSDs for migration times and peak areas of less than 1.2 and 3.6%, respectively. The developed method was successfully applied for the analysis of TDG and oxidation products in seawater, utilizing the carbon aerogel-based adsorbents for sample purification and concentration. Additionally, the method has the potential to be transformed into a portable CE format.

1 Introduction

At the end of World War II it was necessary to dispose of large quantities of conventional and chemical munitions left over from German and allied stocks. Dumping at sea was considered the most appropriate solution at this time. Thus, around 50 000 tons of chemical munitions were dumped in the Baltic Sea (mostly bombs and shells) [1]. After almost 70 years of such dumping, human health and the entire Baltic marine ecosystem might be at serious risk due to the corrosion of the shells, which has led to a constantly increasing release of highly toxic compounds into the seawater.

A large number of the dumped munitions contain yperite, commonly known as sulfur mustard (HD). The compound itself is a vesicant that causes chemical burns on skin and is an eye and lung irritant [2]. In an aqueous environment, HD rapidly hydrolyses to nontoxic thiodiglycol

(TDG) and then slowly oxidizes to TDG sulfoxide (TDGO) and TDG sulfone (TDGOO). In addition, HD hydrolysis leads to the formation of a variety of degradation products, such as cyclic and open chain compounds [3]. It should be noted that potential ecological and health risks are associated primarily with sulfur mustard itself, and the importance of analysis of HD degradation products is that they act as a markers of the HD leakage locations.

Based on the recommended operating procedure for analysis in the verification of chemical disarmament [4], the most frequently used methods for the identification of a sulfur-containing precursor and breakdown products in aqueous samples are based on GC, in combination with MS and/or MS/MS. Due to the low or nonvolatility of the TDG and its oxidation products, derivatization is an essential step in sample preparation prior to GC analysis. Silylation is a widely used derivatization process for GC and, in the case of HD degradation products, *N,O*-bis(trimethylsilyl)trifluoroacetamide [5] and *N*-methyl-*N*-(tertbutyldimethylsilyl)trifluoroacetamide [6] are the most common derivatizing reactants. There are some disadvantages in the application of silylation. The most critical point here is that silyl derivatives tend to be highly moisture sensitive, which leads to derivative decomposition and, thus,

Correspondence: Dr. Maria Kuhtinskaja, Department of Chemistry, Tallinn University of Technology, Akadeemia tee 15, 12618 Tallinn, Estonia
E-mail: mariab@chemnet.ee
Fax: + 372 620 2828

Abbreviations: CWA, chemical warfare agent; **HD**, sulfur mustard; **TDG**, thiodiglycol; **TDGO**, TDG sulfoxide; **TDGOO**, TDG sulfone

---

Colour Online: See the article online to view Figs. 2 in colour.

requires strict control under derivatization conditions [7]. Another problem is the appearance of a large number of artificial peaks on the total ion chromatogram caused by the indiscriminate property of these derivatization reactants when they react with hydroxyl as well as carboxylic groups. Moreover, the reactant itself is prone to form clusters and contaminate the total ion chromatogram [8]. 1-(trifluoroacetyl)imidazole also demonstrated its high potential for TDG and TDGO derivatization. Trifluoroacetylation is less demanding, but the derivative is still sensitive to water traces and storage time [9].

Besides GC, LC coupled with MS [10], NMR spectrometry [11] or sulfur flame photometric detection [12] are also used for the analysis of water-soluble degradation products. In this context, the application of new analytical techniques, such as CE, could be the next promising step in the field of chemical warfare agents (CWAs) analysis.

However, the advantages of CE, such as simplicity of instrumentation and operation procedure as well as high separation efficiency, have not fully been realized yet and there is an urgent need to be more closely evaluated regarding, e.g. the screening of seawater quality as pointed out above. To the authors' knowledge, there are a very limited number of scientific articles on the utilization of CE for the analysis of HD and its degradation products. The neutral degradation products of HD can be analyzed by direct UV detection using micellar electrokinetic capillary chromatography (MEKC) [13, 14]. Separation was achieved through a running buffer of 10 mM borate and 100 mM SDS. The moderate sensitivity was due to the lack of UV chromophore sites on analyte molecules.

Moreover, unlike other separation methods (GC and HPLC), the simplicity and robustness of CE (besides its other features) allow for miniaturization of instrumentation and, as a consequence, the design of portable field analyzers [15]. Such instruments can be used in situ, at the point of care. This in turn provides a fast response when information is urgently needed. Although portable GC and HPLC instruments have been developed, the need to use compressed gases or pumps and solvents makes the construction of portable GC and HPLC instruments a difficult task. In contrast, a couple of successful portable CE instruments have been reported [16–18]. In terms of CWA screening, some examples are already available. The excellent separation performance of a portable CE has been confirmed by the separation of alkylphosphonic acids using a contactless conductivity detection system [19, 20]. The separation of other critical compounds of military and forensic interest has been demonstrated by Hauser's group (nitrogen mustard) [21] and Breadmore's group (explosives) [22].

In spite of that the GC-MS/MS protocol still outperforms the CE protocol proposed here on LOD as was pointed above, the portable GC is more difficult to operate in the field and its eventual usefulness of the portable CE instrument will depend on real concentrations that are present at the point of care. The information about the real concentration of TDG and its oxidation products in near-bottom water or sediments is very limited. Thus, the measured concentrations of WW II

CWA munitions near the Gotland and Gdansk dumping sites in the Baltic have been reported to be about 20–250 µg/kg of sediment (for sulfur compounds) [9]. In this respect, the proposed CE technology seems to be a very promising and reliable alternative to conventional GC-MS analysis.

In the present study, a CE method with direct UV detection for the analysis of TDG and its oxidation was developed and validated. The proof of the principle was demonstrated on a commercial lab scale instrument (Agilent), with the goal of transforming it further to a portable format. A CZE separation method with direct UV detection after precapillary derivatization with strong UV chromophore (phthalic anhydride) is described. A method validation in terms of specificity, precision, linearity and limits of quantification and detection was performed. The BGE contained only boric acid adjusted with sodium hydroxide, making it simple and easy to use. The developed method was used to determine the low amounts of TDG and its oxidation products in seawater.

2 Materials and methods

2.1 Chemicals

Boric acid, sodium hydroxide, acetonitrile, sinapinic acid (internal standard, IS) and imidazole were purchased from Sigma-Aldrich (Germany). Phthalic anhydride and pyridine were obtained from Merck KGaA (Darmstadt, Germany). TDG, TDGO, and TDGOO were synthesized by Envilytix (Wiesbaden, Germany). All chemicals were of analytical grade and used as received. BGE was prepared in DI water from a Milli-Q water purification system (Millipore S. A. Molsheim, France).

2.2 Instrumentation

An Agilent 3D instrument (Agilent Technologies, Waldbronn, Germany) equipped with a diode array UV/Vis detector (DAD) was used for the separation of TDG and its oxidation products. All electropherograms were recorded and integrated with Agilent ChemStation software. Uncoated fused-silica capillaries (Polymicro Technologies, Phoenix, AZ, USA) with an internal diameter of 50 µm and a length of 52/60 cm (effective length/total length) were employed in the experiments. Samples were injected hydrodynamically by applying a pressure of 50 mbar for 5 s. Separation process was monitored at 200 nm. The pH value of the electrolyte solution was measured with a Metrohm 744 pH meter equipped with a combination electrode (Metrohm, Herisau, Switzerland), which had been calibrated with commercial buffers at pH 7.00 ($\pm$0.01), pH 10.00 ($\pm$0.01), and pH 12.00 ($\pm$0.01) (Sigma-Aldrich). Empty SPE tube (polypropylene, tube volume 3 mL, Phenomenex) was used for SPE cartridge preparation.
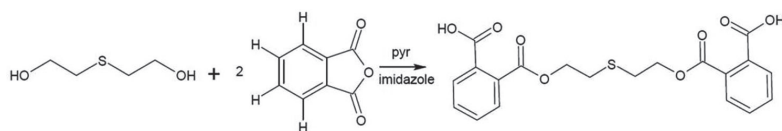
Figure 1. Derivatization reaction of TDG with phthalic anhydride.

2.3 Sample preparation

One liter of seawater (from the Baltic Sea) was spiked with TDG, TDGO, and TDGOO standard solutions to obtain the final concentrations of 0.12, 0.14, and 0.15 µg/mL, respectively. For the target analytes extraction, an SPE cartridge based on powdered carbon aerogels [23] was used (100 mg of powder per cartridge). Fifty milliliters of spiked seawater was run through the SPE cartridge using a vacuum system, then the sorbent was washed with 10 mL of DI water and, finally, the compounds of interest were eluted with 1.5 mL of acetonitrile. Then the solvent was evaporated under a gentle steam of nitrogen till dryness. Finally, 20 µL of derivatizing mixture was added to the solid residue and the sample was treated as described below.

2.4 Derivatization procedure

The derivatizing mixture was prepared in accordance with the literature [24]. Briefly, 1.61 g of phthalic anhydride was dissolved in 10 mL of pyridine, and then 0.24 g of imidazole was added to catalyze the reaction. The mixture was sealed with septum and stored in a desiccator in the dark. For derivatization, 100 µL of phthalic mixture was added to each 2.5 mg of analyte of interest, sealed and heated at 45°C for 20 min. Then the mixture was cooled and the same amount of water was added to stop the derivatizing reaction. Finally, the mixture was diluted by DI water in accordance with need, an IS of sinapinic acid was added, and the sample was introduced into the CE system (Fig. 1).

3 Results and discussion

3.1 Sample derivatization

To obtain reproducible results from the sample derivatization procedure, a careful optimization of several reaction parameters was needed. The effects of the amount of the derivatizating reactant, and the heating time and heating temperature were examined. Each time sample was injected into an electrophoretic system, the average peak area ($n = 3$) was measured and the condition that gave maximum response (peak area) was selected. Based on the stoichiometry of the derivatizing reaction, the required minimum amount of reactant was calculated (∼40 µL per 2.5 mg of TDG). Then two-, three-, and fourfold volume excess of reactant was applied for the derivatization of each analyte. Based on the average peak
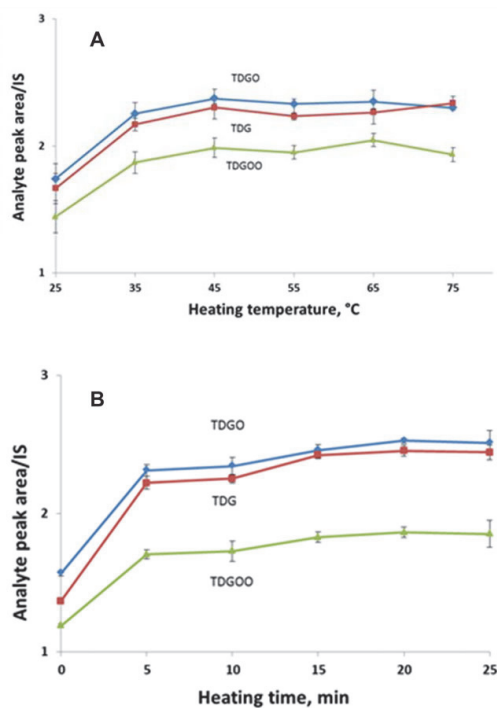
Figure 2. Effect of heating temperature (A) and time (B) on derivatization efficiency.

area measurements, the maximum response was achieved applying the twofold volume excess of phthalic mixture. The appearance of the phthalic acid peak on an electropherogram (unreacted phthalic anhydride) acted as an indicator of a sufficient excess of derivatizing reactant. For future experiments, 100 µL of reactant per each 2.5 mg of analyte was selected to avoid the lack of derivatizing reactant in samples.

In the presence of imidazole, the derivatization reaction was quite fast. To find the optimal derivatization temperature and heating time, a set of additional experiments was carried out, varying the temperature in a range of 25–75°C and the heating time in a range of 0–25 min. Keeping the temperature constant (85°C, in accordance with the literature source [24]), the maximum response was achieved within 5 min (Fig. 2A). The effect of the heating temperature was evaluated, keeping the reaction time (20 min) constant. The best response was obtained at 45°C and further temperature increases did not

Figure 3. Representative electropherograms obtained after derivatization of 3.05 μg/mL of TDG (4), 3.45 μg/mL of TDGO (3), and 3.85 μg/mL of TDGOO (5) under optimized separation conditions: borate buffer concentration 30 mM, buffer pH 8.5, applied voltage 15 kV, and capillary temperature 25°C. Additional peaks: EOF (1), IS (2), and phthalic acid (6).
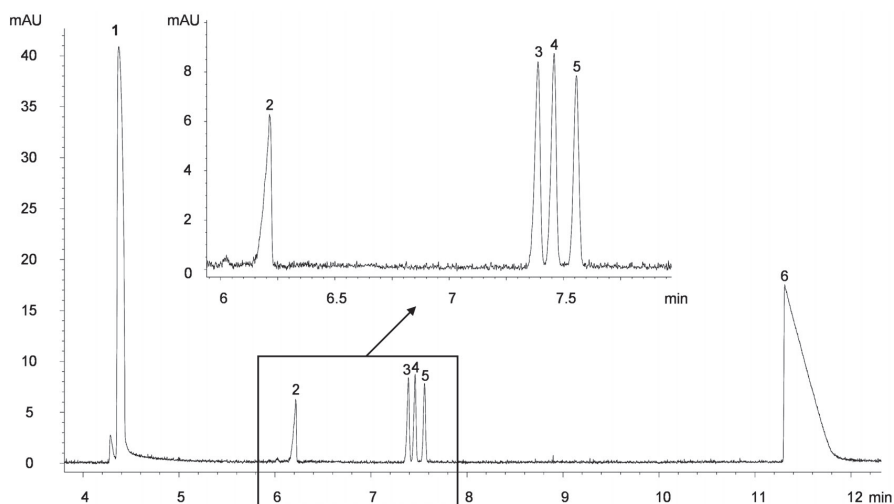
affect the result (Fig. 2B). Finally, the derivatization conditions were as follows: the amount of reactant 100 μL per each analyte, derivatization temperature 45°C, and derivatization time 20 min.

The stability of derivatives was investigated. For this, target analytes (3.1, 3.5, and 3.9 μg/mL for TDG, TDGO, and TDGOO, respectively) were derivatized as described above and after IS addition the mixture was divided into two equal aliquots. The first aliquot was stored at room temperature (23 ± 1°C) and under light (mostly halogen lamps), and the second aliquot was kept in a refrigerator (4°C, in darkness). Systematic sampling over 5 days was performed to measure the peak areas of the derivatives. In the case of TDG and TDGO, there were no systematic changes in the peak areas and shapes during the evaluation period for the first aliquot (kept at room temperature) or for the second one (kept at 4°C). The RSD of the peak areas did not exceed 3.2% ($n = 5$, one analysis per day), which indicated the high stability of the derivatives. TDGOO samples kept at room temperature showed a slight peak area decrease (RSD = 5.7%), but the refrigerated samples demonstrated stability.

3.2 Choice of BGE

Underivatized TDG and its oxidation products are neutral at pH below 9 and, thus, can be analyzed using the MEKC separation technique. Applying 10 mM borate buffer with 100 mM SDS and direct UV detection at 200 nm, TDG and TDGO could be separated within 6 min. The calculated LOD for TDG and TDGO was 10 μg/mL [14]. The high values of LOD are logically justified due to the absence of strong

UV-absorbing sites. In this work, an improved method for the analysis of target sulfur compounds involved derivatization with phthalic anhydride incorporating chromophore sites into the analyte structure and, at the same time, affecting the pK_a value of the formed derivatives and giving a charge to the molecules that, in own turn, allows to use borate buffer for analyte separation. The optimization of the separation conditions was carried out by the investigation of the effect of buffer pH, concentration, capillary temperature, and applied voltage on separation efficiency.

It is well known that buffer pH plays the key role in optimization of a separation process affecting the EOF velocity and degree of analyte ionization. So, in the present work, a 30 mM borate buffer with a pH range of 7.5–10.0 was investigated to evaluate the impact on separation results. At buffer pH values below 8.0, the derivatized analytes were unresolved and the peak shapes were asymmetric. An increase in the buffer pH value to 8.5 led to improvement in analysis time and all analytes were baseline separated. Further, pH change to 9.5 resulted in an increase in the electrophoretic mobility of the analytes. Baseline separation was still achieved and the analysis time was the shortest. Unfortunately, starting at pH 9.0, the sulfone peak area was prone to rapid decrease and at pH 10 almost disappeared, which is, obviously, associated with instability of TDGOO at pH 9 and above.

The influence of borate buffer concentration on separation was studied in the range of 20–50 mM at pH 8.5. By increasing the buffer concentration from 20 to 50 mM, the migration times of all analytes were also significantly increased. Nevertheless, the best separation efficiency was achieved at 30 mM and further concentration increase led to peak broadening without a remarkable change in peak separation.

Table 1. Regression data for the calibration curves

Derivative	Linearity range (µg/mL)	Regression equation	Regression coefficient (R^2)	LOD (µg/mL)	Limit of quantification (µg/mL)
TDG	0.10–2.44	$y = 0.1517x + 0.0017$	0.9996	0.10	0.31
TDGO	0.14–2.76	$y = 0.1359x - 0.0161$	0.9997	0.14	0.42
TDGOO	0.15–3.08	$y = 0.1233x - 0.0304$	0.9994	0.15	0.46
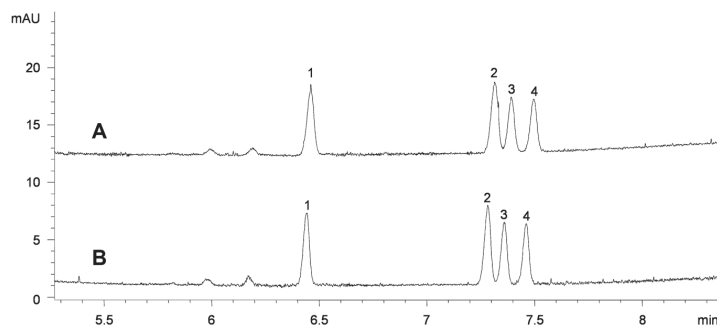
Figure 4. Electropherograms of (A) distilled water and (B) seawater samples. Separation conditions: borate buffer concentration 30 mM, buffer pH 8.5, applied voltage 15 kV, and capillary temperature 25°C. Peaks: IS (1), TDGO (2), TDG (3), TDGOO (4).

Additionally, the effect of the applied voltage over the range 15–25 kV and capillary temperature (15–30°C) was also investigated in terms of separation efficiency and migration times. Voltage values above 20 kV resulted in faster migration times of analytes, but the separation efficiency was not sufficient. All derivatives were baseline resolved at 15 kV, but the analysis time was extended by several minutes. The increase in capillary temperature also noticeably improved the migration time of the derivatives. Thus, the temperature increase from 15 to 30°C decreased the analysis time by a quarter, keeping the separation efficiency at a reasonable level.

Finally, the optimized separation conditions for the separation of three derivatives were as follows: borate buffer concentration 30 mM, buffer pH 8.5, applied voltage 15 kV, and capillary temperature 25°C. The representative electropherogram is shown in Fig. 3.

3.3 CE method validation

The precision of the developed method was investigated. All precision tests were based on optimized BGE and a standard mixture of derivatives. The tests were performed for the run-to-run and day-to-day variations of the migration times and peak areas. Run-to-run precision resulted in maximum RSD values of 0.6% ($n = 6$) and 3.1% ($n = 6$) for the migration time and peak area, respectively. Additionally, day-to-day results showed RSD values of 1.2% ($n = 6$) for the migration times and 3.6% ($n = 6$) for the peak areas. There were no systematic changes in peak shape during the precision tests.

The linearity was evaluated in the range of 0.10–2.44 µg/mL for TDG, 0.14–2.76 µg/mL for TDGO, and 0.15–3.08 µg/mL for TDGOO. Calibration curves were constructed using five concentration levels and were based on the ratio of the corresponding derivative to IS peak area versus concentration. The linearity range, regression equations, and regression coefficients are shown in Table 1.

The LOD and limit of quantitation (LOQ) were obtained experimentally by measuring the S/N. The lowest LOD and LOQ were obtained for TDG and calculated as 98 ng/mL (S/N = 3) and 305 ng/mL (S/N = 10), respectively.

To evaluate the specificity of the developed method, a blank sample was treated as described in Sections 2.3 and 2.4 and then injected into the CE system. There were no interfering peaks observed in the resulting electropherogram.

3.4 Spiked seawater analysis

To demonstrate the method applicability for real sample analysis, seawater was spiked with a standard mixture of free underivatized analytes (TDG, TDGO, and TDGOO) to get the final concentrations of 0.12, 0.14, and 0.15 µg/mL, respectively. The extraction of analytes and the derivatization process are described Sections 2.3 and 2.4. The same sample preparation procedure was carried out for spiked distilled water to evaluate the seawater as a matrix influence on the extraction and derivatization processes. Figure 4 shows the electropherograms of the separation performance of seawater as well as distilled water samples. In all cases, TDG, TDGO, and TDGOO were baseline separated. The RSD of the migration times between all analytes in spiked sea and distilled water samples resulted in 0.4% and the RSD of the peak areas was below 5%. These results show no evident influence of seawater matrix on the extraction and derivatization processes.

4 Concluding remarks

The results of the study show that precolumn derivatization by phthalic anhydride can be used for the significant reduction of LOD of TDG, TDGO, and TDGOO by applying capillary zone electrophoresis with direct UV detection. It also was demonstrated that sample purification and concentration on carbonaceous adsorbent allows for the quantitative analysis of mustard gas hydrolysis and oxidation products in seawater. Nevertheless, it should be noted that the obtained detection limits are less reliable than GC-MS results, but can still be considered acceptable. Moreover, the miniaturization benefits of CE allow translation onto a truly portable instrument, thus making the method more attractive for in-field use.

Transforming the protocol to a portable instrument involves another problem. Contemporary LED sources can generate radiation with wavelengths above 240 nm while the protocol reported in this study requires radiation of 200 nm. Thus, the UV detector implemented in the portable CE instrument must employ a miniature deuterium lamp which somewhat reduces the robustness of the instrument. We believe, however, that this is not a serious obstacle to its design.

The authors have declared no conflict of interest

5 References

[1] CHEMSEA (Chemical Munitions Search & Assessment) project, The Baltic Sea Region Programme 2007–2013. www.chemsea.eu.

[2] Shakarjian, M. P., Heck, D. E., Gray, J. P., Sinko, P. J., Gordon, M. K., Casillas, R. P., Heindel, N. D., Gerecke, D. R., Laskin, D. L., Laskin, J. D., *Toxicol. Sci.* 2010, *114*, 5–19.

[3] Muntro, N. B., Talmage, S. S., Griffin, G. D., Waters, L. C., Watson, A. P., King, J. F., Hauschild, V., *Environ. Health Perspect.* 1999, *107*, 933–974.

[4] Vanninen, P. (Ed.), *Recommended Operating Procedures for Analysis in the Verification of Chemical Disarmament*, The Ministry for Foreign Affairs of Finland, University of Helsinki, Helsinki, 2011 Edition.

[5] Mesilaakso, M. (Ed.), *Chemical Weapons Convention Chemicals Analysis: Sample Collection, Preparation and Analytical Methods*, John Wiley and Sons Ltd, Chichester 2005.

[6] Ohsawa, I., Kanamori-Kataoka, M., Tsuge, K., Seto, Y., *J. Chromatogr. A* 2004, *1061*, 235–241.

[7] Kayser, O., Warzecha, H., *Pharmaceutical Biotechnology: Drug Discovery and Clinical Applications*, WILEY-VHC Verlag GmbH, Weinheim 2012.

[8] Pardasani, D., Palit, M., Gupta, A. K., Kanaujia, P. K., Dubey, D. K., *J. Chromatogr. A* 2004, *1059*, 157–164.

[9] Popiel, S., Nawala, J., Dziedzic, D., Söderström, M., Vanninen, P., *Anal.Chem* 2014, *86*, 5865–5872.

[10] Read, R. W., Black, R. M., *J. Chromatogr. A* 1999, *862*, 169–177.

[11] Meier, U. C., *J. Chromatogr. A* 2013, *1286*, 159–165.

[12] Hooijschuur, E. W. J., Kientz, C. E., Brinkman, U. A. T. h., *J. Chromatogr. A* 1999, *849*, 433–444.

[13] Cheicante, R. I., Stuff, J. R., Durst, H. D., *J. Capillary Electrophor.* 1995, *2*, 157–163.

[14] Cheicante, R. I., Stuff, J. R., Durst, H. D., *J. Chromatogr. A*, 1995, *711*, 347–352.

[15] Lewis, A. P., Cranny, A., Harris, N. R., Green, N. G., Wharton, J., Wood, A. R. J. K., Stokes, K. R., *Meas. Sci. Technol.* 2013, *24*, 042001.

[16] Mai, T. D., Pham, T. T. T., Sáiz, J., Hauser, P. C., *Anal. Chem.* 2013, *85*, 2333–2339.

[17] da Costa, E. T., Neves, C. A., Hotta, G. M., Vidal, D. T. R., Barros, M. F., Ayon, A. A., Garcia, C. D., do Lago, C. L., *Electrophoresis*, 2012, *33*, 2650–2659.

[18] Kuban, P., Seiman, A., Kaljurand, M., *J. Chromatogr. A* 2011, *1218*, 1273–1280.

[19] Seiman A., Jaanus, M., Vaher, M., Kaljurand, M., *Electrophoresis* 2009, *30*, 507–514.

[20] Kuban, P., Seiman, A., Makarõtseva, N., Vaher, M., Kaljurand, M., *J. Chromatogr. A* 2011, *1218*, 2618–2625.

[21] Sáiz, J., Mai, T. D., Hauser, P. C., Garcia-Ruiz, C., *Electrophoresis* 2013, *34*, 2078–2084.

[22] Hutchinson, J. P., Johns, C., Breadmore, M. C., Hilder, E. F., Guijt, R. M., Lennard, C., Dicinoski, G., Haddad, P. R., *Electrophoresis* 2008, *29*, 4593–4602.

[23] Pérez-Caballero, F., Peikolainen, A-L., Uibu, M., Kuusik, R., Volobujeva, O., Koel, M., *Micropor. Mesopor. Mater.* 2008, *108*, 230–236.

[24] Vanhoenacker, G., DeKeukeleire, D., *Pat, S., J. Sep. Sci.* 2001, *24*, 651–657.

Publication II

H. Lees, M. Vaher, M. Kaljurand, Development and comparison of HPLC and MEKC methods for the analysis of cyclic sulfur mustard degradation products, Electrophoresis. 38 (2017) 1075–1082.

Heidi Lees
Merike Vaher
Mihkel Kaljurand

Department of Chemistry, Tallinn
University of Technology, Tallinn,
Estonia

Research Article

Development and comparison of HPLC and MEKC methods for the analysis of cyclic sulfur mustard degradation products

In this study, novel, fast, and simple methods based on RP-HPLC and MEKC with DAD are developed and validated for the qualitative and quantitative determination of five cyclic sulfur mustard (HD) degradation products (1,4-thioxane, 1,3-dithiolane, 1,4-dithiane, 1,2,5-trithiepane, and 1,4,5-oxadithiepane) in water samples. The HPLC method employs a C18 column and an isocratic water-ACN (55:45, v/v) mobile phase. This method enables separation of all five cyclic compounds within 8 min. With the CE method, the baseline separation of five compounds was achieved in less than 11 min by applying a simple BGE composed of a 10 mM borate buffer and 90 mM SDS (pH 9.15). Both methods showed good linear correlation ($R^2 > 0.9904$). The detection limits were in the range of 0.08–0.1 μM for the HPLC method and 10–20 μM for MEKC. The precision tests resulted in RSDs for migration times and peak areas less than 0.9 and 5.5%, respectively, for the HPLC method, and less than 1.1 and 7.7% for the MEKC method, respectively. The developed methods were successfully applied to the analysis of five cyclic HD degradation products in water samples. With the HPLC method, the LODs were lowered using the SPE for sample purification and concentration.

Keywords:

HPLC / MEKC / SPE / Sulfur mustard degradation products / UV detection

DOI 10.1002/elps.201600418

Additional supporting information may be found in the online version of this article at the publisher's web-site

1 Introduction

After World War II, large amounts of munitions were dumped in the sea. At that time, it was considered the easiest and cheapest way to dispose of the toxic substances. It is estimated that around 50 000 tons of chemical munitions were dumped in the Baltic Sea, which contained approximately 15 000 tons of chemical warfare agents (CWAs). Among the munitions dumped in the Baltic Sea, sulfur mustard (HD) is the most abundant CWA. For example, HD accounts for two-thirds of the munitions dumped near Gotland and Bornholm [1, 2]. The munitions have been lying in the seabed for almost 70 years by now, meaning that the shells containing CWAs are corroding and leaking. The leakages cause

the chemical pollution of the marine environment and, unfortunately, its full risks are not yet entirely understood [2–4].

HD is a blister agent that possesses strong alkylating properties and, consequently, demonstrates systemic toxicity in addition to its unfavorable effect on the skin, eyes, and the respiratory tract [5]. It is also considered a known human carcinogen [6]. In an aqueous environment, HD hydrolyzes to many complex degradation products [7]. HD degrades predominantly by hydrolysis to thiodiglycol (TDG). TDG may be oxidized to thiodiglycol sulfoxide (TDGO) and, more slowly, to thiodiglycol sulfone (TDGOO) [3, 8]. HD and its degradation products TDG, TDGO, and TDGOO are surprisingly rarely found in the sediment and water samples from the dumpsites [9,10], whereas the cyclic compounds are quite frequently found in the real samples from the dumpsites [10–12]. The analysis of HD degradation products indicates the presence and leakage of HD from the corroded shells.

The most frequently used methods for the identification of HD degradation products are based on GC and LC in combination with MS [8, 13–15], but ion mobility spectroscopy (IMS) has also been used [16]. Besides GC and LC coupled with MS, other detection techniques have been employed,

Correspondence: Heidi Lees, Department of Chemistry, Tallinn University of Technology, Akadeemia tee 15, 12618 Tallinn, Estonia
E-mail: heidilees90@gmail.com
Fax: +37-26-202-828

Abbreviations: CWA, chemical warfare agent; **HD**, sulfur mustard; **TDG**, thiodiglycol

such as NMR [17], atomic emission detection (AED) [18], flame photometric detection (FPD) [19], and amperometric detection [20]. Alternatively, CE has been applied to the detection of HD degradation products as well [21–23].

GC-MS is used for the detection of cyclic HD degradation products [2,24]. Røen et al. [11,25] have developed methods for the trace determination of cyclic HD degradation compounds in soil and water samples using headspace-trap in combination with GC-MS. The cyclic sulfur compounds 1,4-thioxane, 1,3-dithiolane, and 1,4-dithiane could be detected at 0.2–0.7 ng/g in soil samples and at 0.1 ng/mL in water samples. Magnusson et al. [12] developed an analytical method for the onsite identification and quantification of cyclic degradation products of HD (1,4-thioxane, 1,3-dithiolane, 1,4-dithiane, 1,4,5-oxadithiepane, and 1,2,5-trithiepane) in sediment samples using a HAPSITE field-portable GC-MS instrument equipped with a headspace sampler. Their workgroup verified the leakages from HD munitions in the Bornholm Basin CW dumping site and detected four cyclic HD degradation products in the sediments at concentrations ranging from 15 to 308 μg/kg dry weight.

Doster and Zentner [26] have reported separation of TDG, dithiodiglycol, 1,4-thioxane, 1,3-dithiane, and 1,4-dithiane standard solutions in methanol. The separation was accomplished using a gradient elution with water and methanol on a semi-microbore ODS RP column. The chromatograms were obtained by recording a blank solvent run and then subtracting the solvent absorption from the sample run.

Cheicante et al. [21,23] separated sulfur-containing chemical warfare related compounds, including 1,4-thioxane and 1,4-dithiane, within 10 min, applying a buffer consisting of 10 mM borate with 100 mM SDS. The LODs for 1,4-thioxane and 1,4-dithiane were 8.0 and 4.1 μg/mL, respectively.

In light of the Chemical Weapons Convention and the environmental concerns of dumped CWA, the need of new analytical methods for determination of HD and related compounds has increased [25]. In the present study, HPLC and MEKC methods with DAD at 200 nm are applied for the first time for the determination of five cyclic HD degradation products (1,4-thioxane, 1,3-dithiolane, 1,4-dithiane, 1,2,5-trithiepane, and 1,4,5-oxadithiepane), which previously have been found in the real samples from the dumpsites [10–12]. To the authors' knowledge, the above-mentioned cyclic HD degradation products have not been separated with isocratic elution before, which enables to detect low absorbing analytes at 200 nm without subtracting the solvent absorption. Developed HPLC method with sample concentration step is sensitive and therefore suitable for detecting small-scale leakages from munitions. CE could be used for detecting large-scale leakages due to its lower sensitivity. However, great advantage of the developed CE method is that it does not need sample purification step. Furthermore, CE is a green analytical chemistry method—currently the utilization of green chemistry concept is very actual [27]. CE does not require toxic reagents; consumption of sample, solvents, and energy is low; and waste is minimal. This makes it one of the best candidate

techniques for miniaturization and portable instrumentation construction.

In this research, the developed methods were validated in terms of sensitivity, linearity, LOD, LOQ, recovery, and precision. These methods are very simple and rapid, presenting a good alternative to the commonly used GC-MS method.

2 Materials and methods

2.1 Chemicals

1,4-Thioxane (98% purity), 1,3-dithiolane (97%), and 1,4-dithiane (97%) were obtained from Sigma-Aldrich (Germany). 1,2,5-Trithiepane (99%) and 1,4,5-oxadithiepane (99%) were synthesized by Envilytix GmbH (Wiesbaden, Germany). Sodium tetraborate decahydrate, SDS, vanillin (internal standard (IS) for the HPLC method), niacinamide (IS for the CE method), nicotinic acid (IS for the CE method), sodium hydroxide (NaOH), and ACN (HPLC grade, ≥ 99.99%) were purchased from Sigma-Aldrich. Deionized water was supplied from a Milli-Q water purification system (Millipore S. A. Molsheim, France). Some chemical properties of the target cyclic HD degradation products are listed in Supporting Information Table S1.

2.2 Seawater and pore water samples for method development

The sediment and seawater sample were collected from the Baltic Sea. It was verified that these samples did not contain any degradation products of HD. The sediment sample was collected from the bottom of the Baltic Sea at the port of Virtsu (Läänemaa, Estonia) by the Marine Systems Institute at Tallinn University of Technology. The seawater sample was taken from the Gulf of Finland, 5 km from the coast of Tallinn, and was used as received. The sediment sample was centrifuged for 20 min at 8500 rpm, after that the pore water was collected and filtrated and then used for the analysis. The remaining samples were stored in a freezer. The developed HPLC method was tested with two sediment samples taken near a wreck located in the Bornholm Deep dumpsite.

2.3 Instrumentation

2.3.1 HPLC instrumentation

Analysis of HD degradation products was performed on HPLC equipment of the Agilent 1200 series with DAD (Agilent Technologies, Waldbronn, Germany). The samples were separated on a ZORBAX Eclipse Plus C18 column (Narrow Bore RR, 150 × 2.1 mm i.d., 3.5 μm particle size). The mobile phase consisted of two solvents: Milli-Q water and ACN. Following conditions were used for analysis: mobile phase H_2O-ACN (55:45, v/v), flow rate 0.2 mL/min, column temperature 30°C, and injection volume 5 μL. The detection wavelength was 200 nm.

2.3.2 CE instrumentation

An Agilent 3D instrument (Agilent Technologies) equipped with DAD was used for the capillary electrophoretic separation of cyclic HD degradation products. All electropherograms were recorded and integrated with Agilent ChemStation software. Uncoated fused-silica capillaries (Polymicro Technologies, Phoenix, AZ, USA) with an i.d. of 75 μm and a length of 51.5/60 cm (effective length/total length) were employed in the experiments. The BGE was prepared containing 10 mM borate buffer and 90 mM SDS (pH 9.15) in Milli-Q water. The sample was injected hydrodynamically under a pressure of 50 mbar for 3 sec. Separations were performed at 20°C at a voltage 20 kV. The detection wavelength was 200 nm. Before each run, the capillary was flushed with 1 M NaOH for 3 min, with Milli-Q water for 3 min and with the BGE for 5 min. Water samples were directly injected without pretreatment (only filtration).

2.4 Validation

Parameters such as sensitivity, linearity, LOD, LOQ, precision, and recovery were evaluated. LOD and LOQ were experimentally calculated from the analysis of spiked samples, giving the S/N of 3 and 10, respectively. Precision was evaluated at two levels, repeatability as intraday precision and reproducibility as interday precision. Repeatability was determined by measuring the concentration of the control sample containing analytes in six replicates during one day, under the same experimental conditions. Reproducibility was calculated over the 5-day observation period for six replicates each day.

2.5 Solid-phase extraction (SPE)

The water samples (seawater and pore water) were purified and concentrated using Supelclean LC-18 SPE Tubes (volume 3 mL, 500 mg, SUPELCO, Bellefonte, PA, USA). Prior to extraction, the sorbent was conditioned with 2 mL of ACN followed by 2 mL of deionized water. After conditioning, the sample solution (15–30 mL) was passed through the cartridge by using a vacuum system at a flow rate of 1.0 mL/min. After that the cartridge was washed with 2 mL of distilled water to remove the unwanted materials from the cartridge. Then the cartridge was dried for 5 min under vacuum. The analytes retained on the sorbent were eluted with 1.5 mL of ACN.

3 Results and discussion

3.1 SPE

RP-SPE (Supelco LC-18) was used for sample purification and concentration before the HPLC analysis. This sample preparation was used to minimize the values of LOD and to remove the unwanted salts from the sample before the injection into the HPLC system.

According to the SPE procedure outlined in Section 2.5, 1 μM 1,4-thioxane, 1,3-dithiolane, 1,4-dithiane, 1,4,5-oxadithiepane, and 1,2,5-trithiepane in 15 mL seawater were passed through the SPE cartridge. ACN was used as an elution solvent. The effect of the eluent volume (1, 1.5, 2, and 2.5 mL) on extraction efficiency was investigated. The seawater was chosen for the sample matrix because preliminary studies showed that with UV detection there is no significant difference between seawater and pore water as a matrix. The extraction efficiencies for five cyclic compounds with 1.0–2.5 mL elution volumes can be seen in Supporting Information Fig. S1A ($n = 6$). The purpose was to keep the elution volume as low as possible to concentrate the sample as much as possible. The results showed that 1.5 mL of ACN was just sufficient to elute all the cyclic compounds from the sorbent without a great loss of the analytes. Higher volumes did not affect the extraction efficiency. It can be seen from Supporting Information Fig. S1A that even 1 mL of ACN resulted in good recoveries but the extraction efficiencies with some compounds rose slightly with elution of 1.5 mL of ACN and therefore, to be sure that all the compounds of interest were extracted at their maximum level, 1.5 mL was selected. The recoveries were in the range of 60.8–98.8% ($n = 6$). Stronger eluents such as acetone, THF, and mixture of acetone and ACN were also tested but did not enhance extraction efficiency, yet resulted in an intensive positive peak eluting at the void time. Supporting Information Fig. S2 depicts the chromatogram that was obtained when 15 mL of 1 μM standards in seawater were extracted with SPE and analyzed with the HPLC instrument.

The next step was to determine the maximum sample volume that can be extracted. The cartridges were loaded with 15–30 mL volumes of standard solutions in seawater. The optimized ACN volume (1.5 mL) was used for elution. To determine the maximum sample volume that can be extracted, the cartridges were loaded with 15, 22.5, and 30 mL volumes (concentrating the sample 10, 15, and 20 times, respectively) of standard solutions in seawater containing 1 μM of each cyclic compound. The recoveries obtained using this procedure are illustratively shown in Supporting Information Fig. S1B. Satisfactory results were achieved using ACN as an eluting solvent, with recoveries ranging from 62.9 to 99.4% ($n = 6$).

3.2 Optimization of HPLC separation conditions

For the optimization of the HPLC method three variables were selected: eluent strength, flow rate, and temperature. The ACN percentage was varied from 40 to 60% with a step of 5% to increase the elution strength. With these selected mobile phase variations (40–60% ACN), all five HD degradation products and IS were baseline separated ($R_s > 1.5$). With the mobile phase of 60% water and 40% ACN, all analytes were separated within 11 min while with the mobile phase
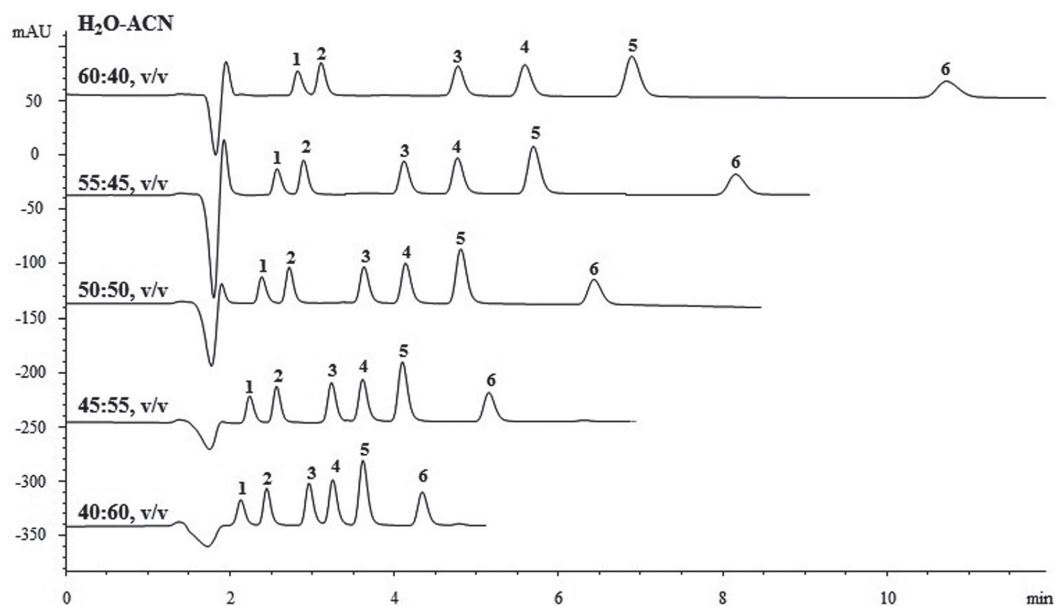
Figure 1. Effect of the eluent strength on separation (40-60% ACN). Peak identifications: (1) vanillin (IS), (2) 1,4-thioxane, (3) 1,4,5-oxadithiepane, (4) 1,3-dithiolane, (5) 1,4-dithiane, (6) 1,2,5-trithiepane. Flow rate: 0.2 mL/min, column temperature: 30°C.

consisting of 40% water and 60% ACN the separation was achieved in less than 4.5 min (Fig. 1). The optimum mobile phase for the analytes in distilled water would be 40% H_2O and 60% ACN (the best efficiency and fastest time), but due to the complexity of the sample matrix (seawater or pore water) the different composition of the mobile phase had to be used. The authors observed that the sample matrix consisted of polar compounds, which resulted in a positive peak in the beginning of the chromatogram. The retention time of these compounds was the same as the void time and due to this, the first analytes were interfered with the mobile phase 40% H_2O and 60% ACN. Therefore, to make the elution of the analytes longer and to ensure that all the analytes are baseline separated, the optimum mobile phase composition for the seawater and pore water matrix was 55% H_2O and 45% ACN (see Supporting Information Fig. S2).

The flow rates were investigated in the range of 0.1–0.3 mL/min with a step of 0.05 mL/min. The flow rate 0.2 mL/min was chosen because retention times were desirable and the pressure was optimal. The temperature was varied between 25 and 40°C with a step of 5°C. With all temperatures the baseline resolution of the analytes was achieved. The higher temperature resulted in slight decrease in retention times. The temperature 30°C was chosen as an optimal because as it turned out later, higher temperatures (35 and 40°C) affected the stability of the analytes.

The optimized HPLC conditions for separating five cyclic HD degradations products were as follows: mobile phase H_2O-ACN (55:45, v/v), flow rate 0.2 mL/min, and column temperature controlled at 30°C. The optimized separation conditions were used for the analysis of two real samples collected from the chemical weapon dumping site in the Bornholm Basin. The sediment samples were prepared as described in Section 2.2 and the sample was concentrated with SPE 20 times (30 mL of pore water). No HD cyclic degradation products were found in the pore water of collected sediments.

3.3 Optimization of CE separation conditions

The optimization of the separation conditions was carried out by investigation of the effect of SDS concentration, capillary temperature, and applied voltage on separation efficiency. The main aspect of selecting optimum conditions for separation was the complete resolution of 1,4-dithiane and 1,4,5-oxadithiepane because these two analytes migrated closely and the baseline separation of these compounds was critical. For the sufficient separation of the analytes, the resolution value should be higher than 1.5 to measure the peak areas accurately.

The influence of SDS concentration on separation was studied in the range of 50–100 mM; the borate buffer concentration was kept 10 mM as in the work of Cheicante et al. [21]. With SDS concentrations of 50 to 80 mM, 1,4-dithiane and 1,4,5-oxadithiepane were not baseline separated ($R_s < 1.5$). With 90 mM SDS the baseline separation of these two compounds was achieved ($R_s > 1.5$), while 100 mM SDS

resulted in an increase in the migration times without a significant increase in the resolution of 1,4-dithiane and 1,4,5-oxadithiepane. Therefore, 90 mM was chosen as the optimum SDS concentration.

Additionally, the effect of the capillary temperature over the range 15–25°C was optimized in terms of separation efficiency and migration times. The fastest migration times of the analytes were achieved with 25°C, but the separation of 1,4-dithiane and 1,4,5-oxadithiepane was not sufficient ($R_s = 1.3$). All analytes were baseline resolved with the capillary temperatures of 15 and 20°C, but with 20°C the migration times of the analytes were faster. Thus, 20°C was chosen as the optimum temperature.

Furthermore, the voltage in the range of 15–25 kV was used to evaluate its impact on separation results. With voltage values of 15 and 20 kV 1,4-dithiane and 1,4,5-oxadithiepane were baseline separated ($R_s > 1.8$), while with 25 kV the resolution value of these two peaks was 1.3. With the voltage value of 15 kV, the analysis time was 5 min longer than with 20 kV; therefore, 20 kV was chosen as the optimum voltage.

Several ISs were tested but it was calculated that the quotient of niacinamide and nicotinic acid gave the most accurate result. Finally, the optimized conditions for the separation of five cyclic HD degradation products were as follows: 10 mM borate buffer, 90 mM SDS, applied voltage 20 kV, capillary temperature 20°C, 100 µM niacinamide and nicotinic acid as ISs.

The same sample preparation (SPE) as used in the developed HPLC method was not possible because the injection of the extract in ACN into the CE system resulted in an unstable and noisy baseline, which led to an insufficient resolution of the cyclic sulfur compounds. The evaporation (under a gentle stream of nitrogen or with the rotary evaporator) of the extract in ACN till dryness and dissolution in water resulted in a major loss of the analytes. Therefore, the proposed sample preparation with the SPE before the CE analysis was assessed ineffective. However, the great advantage of the CE

method was that the sample preparation was not needed—it was possible to inject the sample (salty water) straight into the system.

3.4 Validation of the HPLC and MEKC methods

3.4.1 Sensitivity, linearity, LOD, LOQ, and precision

The sensitivity of the developed methods was evaluated as the slope of the calibration curve. With HPLC method, the calibration curves were constructed using eight concentrations (0.25–25 µM) and were obtained by plotting the response (ratio of the corresponding analyte peak area to the IS peak area) against the analyte concentration. With CE method, the calibration curves were constructed using five concentrations (50–500 µM) and were obtained by plotting the response (ratio of the corresponding analyte to the ratio of two IS peak areas) against the analyte concentration. The linearity range, regression equations, coefficients of determination (R^2), LOD, and LOQ are presented in Table 1. The acquired LODs are compared to the previously developed methods in Supporting Information Table S2. All analytes in Table 1 are listed in their elution order with the specific method. With both methods, the values of R^2 were greater than 0.99, resulting in good linearity. It can be seen from the data that the new methodologies give good performance.

All precision tests were based on optimized conditions and a standard sample. The tests were performed as intraday (repeatability) and interday (reproducibility) variations of the peak areas and migration times. For the HPLC method, the precision tests resulted in RSD values of less than 5.5 and 0.9% for the peak areas and migration times, respectively. For the MEKC method, the precision tests resulted in RSD values of less than 7.7 and 1.1% for the peak areas and migration times, respectively. The results of the precision tests are given in Table 1. The RSD values show excellent repeatability and

Table 1. Performance characteristics of the HPLC and MEKC methods for the quantification of HD degradation products

Analyte	Regression analysis					Precision I (peak areas)		Precision II (migration times)	
	Linear range (µM)	Equation ($y = ax + b$)	R^2	LOD (µM)	LOQ (µM)	RSD (%), intraday	RSD (%), interday	RSD (%), intraday	RSD (%), interday
HPLC									
1,4-Thioxane	0.25–25	$y = 0.0606x - 0.0116$	0.9969	0.09	0.30	0.66	2.8	0.04	0.1
1,4,5-Oxadithiepane	0.25–25	$y = 0.0798x + 0.0524$	0.9996	0.09	0.30	0.77	1.5	0.05	0.3
1,3-Dithiolane	0.25–25	$y = 0.0814x - 0.0198$	0.9956	0.10	0.33	1.11	5.5	0.05	0.4
1,4-Dithiane	0.25–25	$y = 0.1322x - 0.0367$	0.9974	0.08	0.26	0.97	4.0	0.06	0.5
1,2,5-Trithiepane	0.25–25	$y = 0.080x + 0.0056$	0.9999	0.10	0.33	2.46	5.0	0.09	0.9
MEKC									
1,4-Thioxane	50–500	$y = 0.0022x - 0.0175$	0.9980	20	66	2.2	4.3	0.6	1.1
1,3-Dithiolane	50–500	$y = 0.0032x - 0.0272$	0.9990	15	50	2.2	7.7	0.6	1.0
1,4-Dithiane	30–500	$y = 0.0057x - 0.0325$	0.9991	10	33	1.5	7.7	0.5	0.8
1,4,5-Oxadithiepane	40–500	$y = 0.0035x - 0.0095$	0.9997	12	40	1.6	3.7	0.5	1.0
1,2,5-Trithiepane	50–500	$y = 0.0039x + 0.0154$	0.9904	15	50	2.3	5.7	0.4	0.1

Table 2. Recoveries (*R*) obtained for each sulfur compound at different spiked levels in seawater and pore water samples, *n* = 6

			1,4-Thioxane	1,3-Dithiolane	1,4-Dithiane	1,4,5-Oxadithiepane	1,2,5-Trithiepane
Seawater	100 μM	*R* (%)	101.0	91.7	98.4	103.2	96.3
		RSD (%)	1.98	1.74	0.59	0.47	3.21
	250 μM	*R* (%)	99.5	99.0	100.9	101.0	102.9
		RSD (%)	0.80	2.67	1.90	1.67	0.96
	400 μM	*R* (%)	96.6	95.1	98.7	99.5	96.3
		RSD (%)	0.69	3.75	1.83	0.11	1.88
Pore water	100 μM	*R* (%)	99.6	91.3	98.1	102.6	101.9
		RSD (%)	1.28	2.17	1.84	0.96	2.17
	250 μM	*R* (%)	98.2	98.7	100.3	99.2	99.8
		RSD (%)	1.00	0.94	1.33	1.92	1.49
	400 μM	*R* (%)	96.5	95.9	99.0	98.1	96.8
		RSD (%)	1.28	1.60	1.03	0.26	0.44

reproducibility for the analytes' migration times and peak areas with both methods.

3.4.2 Recovery

For the HPLC analysis, sample preparation was needed. Therefore, SPE was used for the extraction of the analytes from the sample matrix. The recovery was determined by comparing the response of the extract with the response of the reference material (standard) dissolved in water. The HPLC method recovery study showed that the extraction efficiencies were 62.9–99.4% (*n* = 6) for all the analytes, which is indicative of an excellent suitability of this method for the analysis of the compounds of interest. The obtained recoveries are represented in Supporting Information Fig. S1B.

As mentioned in Section 3.3, the sample preparation with SPE was not possible (and not necessary) with the developed CE method. Therefore, the MEKC method recovery studies were evaluated by determining the recovery of a spiked sample of the analyte into the matrix of the sample to be analyzed. The samples were spiked at three different concentration levels. The recoveries are shown in Table 2. The values varied from 91.3 to 103.2% with RSDs less than 3.2% showing excellent recoveries in different sample matrices. The electropherograms in different matrices are depicted in Fig. 2.

3.5 Stability of cyclic sulfur compounds

The stability of cyclic sulfur compounds in water solutions was investigated at two levels: over a 7-day period kept in a refrigerator (+4°C) and over a 5-h period kept at room temperature (23 ± 1°C). Systematic sampling over 7 days (every day) and 5 h (every 30 min) was performed to measure the peak areas of the analytes. It was observed that 1,4-thioxane and 1,4,5-oxadithiepane were stable in water solutions kept in a refrigerator for 7 days and RSDs of the peaks areas did not exceed 3.2%. Nevertheless, over a 7-day period, 1,4-dithiane, 1,3-dithiolane, and 1,2,5-trithiepane were degraded 11.2, 14.5, and 9.0%, respectively. Over a 5-h period

at room temperature, the degradation of 1,4-thioxane and 1,4,5-oxadithiepane was 9.6 and 4.2%, respectively, while 1,4-dithiane, 1,3-dithiolane, and 1,2,5-trithiepane degraded 11.5, 15.0, and 10.1%, respectively. However, the analytes showed stability for 1 h at room temperature (RSD < 1.3%). Based on these results, it can be concluded that the compounds should be kept in the refrigerator and warmed up to room temperature just prior to the analysis to avoid degradation. Also, it must be noted that for better reproducibility new solutions should be made every day.

3.6 Comparison of the developed methods

Comparison of HPLC and MEKC methods reveals that both demonstrate approximately the same precision for analysis of cyclic HD degradation products. The only difference, and not surprisingly, is that the detection limit of the HPLC method is two orders of magnitude lower than that of the MEKC method. The opportunity to use the SPE technology in the HPLC analysis for sample concentration enables lowering the detection limits even more (at least 20 times), making this method sensitive and therefore effective in case the leakages of the chemical munitions are minimal. This method could detect the leakages of HD munitions at low ppb levels. The compounds of interest have been found in the pore water fractions with concentrations 0.02–0.14 μM [28]. This is achievable with developed HPLC method when concentration step with SPE is applied. MEKC did not tolerate the direct injection of a nonaqueous sample solution, and drying and reconstitution of the sample before the MEKC analysis led to the loss of the analytes. However, the MEKC protocol does not require the purification of the sample with SPE, making it remarkably simpler than the HPLC protocol, which obligatorily needs the purification step. With MEKC the pore water or seawater sample can be injected directly into the system, resulting in good separation without interferences from the water samples.

Also, as is well known, the CE technology can be easily miniaturized and thus, made portable. Due to the danger of sample degradation during the storage and transport to the
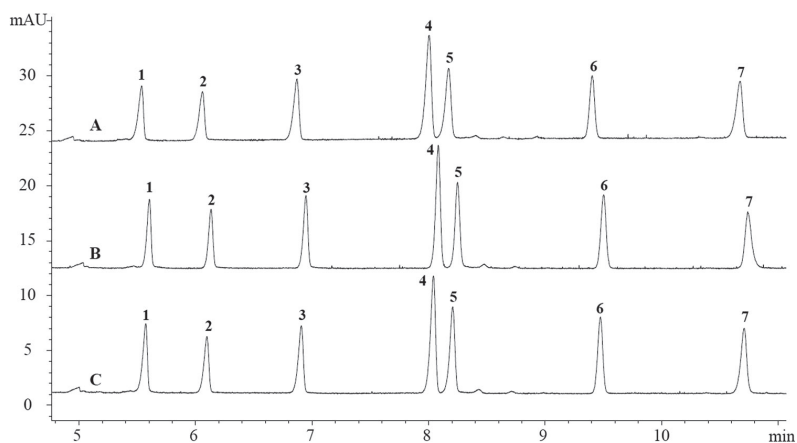
Figure 2. Electropherograms of 400 μM standards in (A) distilled water, (B) pore water, (C) seawater. Peaks identified: (2) 1,4-thioxane, (3) 1,3-dithiolane, (4) 1,4-dithiane, (5) 1,4,5-oxadithiepane, and (7) 1,2,5-trithiepane. Optimized separation conditions used: 10 mM borate buffer, 90 mM SDS (pH 9.15), applied voltage 20 kV and capillary temperature 20°C, injection hydrodynamically 50 mbar 3 sec. Absorbance detected at 200 nm, capillary length 60 cm. ISs: 100 μM (1) niacinamide and (6) nicotinic acid.

laboratory for analysis, as demonstrate the results of Section 3.5, a miniaturized MEKC instrument can perform analysis in situ, immediately. Portable CE instruments have demonstrated excellent performance in various situations (although with conductivity detection but development of CE instruments with optical detectors is ongoing in our and other laboratories) [29–33]. The MEKC technology for CWAs monitoring is successfully applicable to cases when extreme sensitivities are not required (e.g., detection of hazardous concentrations of HD degradation products).

4 Concluding remarks

HPLC and MEKC methods with UV detection for the determination of five cyclic HD degradation products were developed and validated. Validation of these methods showed their good performance. Two water matrices (seawater and pore water from the Baltic Sea) were employed in the method development. The developed HPLC method was applied to the analysis of real samples from the chemical warfare dumpsite. HPLC method with sample concentration step is sensitive while MEKC method could easily be made portable and adapted to onsite analysis. Furthermore, the developed MEKC method requires no sample purification step (only filtration) and shows excellent efficiency. MEKC would be the method of choice in case of large-scale leakages of HD munitions. Being rapid and simple, the developed methods offer a good alternative to the commonly used GC-MS method.

The authors have declared no conflict of interest.

5 References

[1] HELCOM, *Chemical Munitions Dumped in the Baltic Sea*, HELCOM – Baltic Marine Environment Protection Commission, Helsinki 2013.

[2] Bełdowski, J., Klusek, Z., Szubska, M., Turja, R., Bulczak, A. I., Rak, D., Brenner, M., Lang, T., Kotwicki, L., Grzelak, K., Jakacki, J., Fricke, N., Östin, A., Olsson, U., Fabisiak, J., Garnaga, G., Nyholm, J. R., Majewski, P., Broeg, K., Söderström, M., Vanninen, P., Popiel, S., Nawała, J., Lehtonen, K., Berglind, R., Schmidt, B., *Deep Sea Res. Part II Top. Stud. Oceanogr.* 2016, *128*, 85–95.

[3] Bizzigotti, G. O., Castelly, H., Hafez, A. M., Smith, W. H. B., Whitmire, M. T., *Chem. Rev.* 2009, *109*, 236–256.

[4] Sanderson, H., Fauser, P., Thomsen, M., Vanninen, P., Söderström, M., Savin, Y., Khalikov, I., Hirvonen, A., Niiranen, S., Missiaen, T., Gress, A., Borodin, P., Medvedeva, N., Polyak, Y., Paka, V., Zhurbas, V., Feller, P., *Environ. Sci. Technol.* 2010, *44*, 4389–4394.

[5] Watson, A. P., Griffin, G. D., *Environ. Health Perspect.* 1992, *98*, 259–280.

[6] Watson, A. P., Jones, T. D., Griffin, G. D., *Regul. Toxicol. Pharmacol.* 1989, *10*, 1–25.

[7] Munro, N. B., Talmage, S. S., Griffin, G. D., Waters, L. C., Watson, A. P., King, J. F., Hauschild, V., *Environ. Health Perspect.* 1999, *107*, 933–974.

[8] Vanninen, P. (Ed.), *Recommended Operating Procedures for Analysis in the Verification of Chemical Disarmament*, University of Helsinki, Helsinki 2011.

[9] Missiaen, T., Söderström, M., Popescu, I., Vanninen, P., *Sci. Total Environ.* 2010, *408*, 3536–3553.

[10] Söderström, M., *WP3. Summary of Chemical Analysis of Sediment Samples*, CHEMSEA, Helsinki 2014.

[11] Røen, B. T., Unneberg, E., Tørnes, J. A., Lundanes, E., *J. Chromatogr. A* 2010, *1217*, 2171–2178.

[12] Magnusson, R., Nordlander, T., Östin, A., *J. Chromatogr. A* 2016, *1429*, 40–52.

[13] Read, R. W., Black, R. M., *J. Chromatogr. A* 1999, *862*, 169–177.

[14] Hooijschuur, E. W. J., Kientz, C. E., Brinkman, U. A. T., *J. Chromatogr. A* 2002, *982*, 177–200.

[15] D'Agostino, P. A., Chenier, C. L., *Analysis of Chemical Warfare Agents: General Overview, LC-MS Review, In-House LC-ESI-MS Methods and Open Literature Bibliography*, DRDC, Suffield 2006.

[16] Asbury, G. R., Wu, C., Siems, W. F., Hill Jr., H. H., *Anal. Chim. Acta* 2000, *404*, 273–283.

[17] Meier, U. C., *J. Chromatogr. A* 2013, *1286*, 159–165.

[18] Mazurek, M., Witkiewicz, Z., Popiel, S., Śliwakowski, M., *J. Chromatogr. A* 2001, *919*, 133–145.

[19] Tomkins, B. A., Sega, G. A., Macnaughton, S. J., *Anal. Lett.* 1998, *31*, 1603–1622.

[20] Mahyari, M., *Microchim. Acta* 2016, *183*, 2395–2401.

[21] Cheicante, R. L., Stuff, J. R., Durst, H. D., *J. Chromatogr. A.* 1995, *711*, 347–352.

[22] Jõul, P., Lees, H., Vaher, M., Kobrin, E.-G., Kaljurand, M., *Electrophoresis* 2015, *36*, 1202–1207.

[23] Cheicante, R. L., Stuff, J. R., Durst, H. D., *J. Capillary Electrophor.* 1995, *2*, 157–163.

[24] Östin, A., *Review of Analytical Methods for the Analysis of Agents Related to Dumped Chemical Weapons for the CHEMSEA project*, CHEMSEA, Umeå 2012.

[25] Røen, B. T., Unneberg, E., Tørnes, J. A., Lundanes, E., *J. Chromatogr. A* 2010, *1217*, 761–767.

[26] Doster, D. E., Zentner, M., *J. Chromatogr.* 1989, *461*, 293–303.

[27] Gałuszka, A., Migaszewski, Z., Namieśnik, J., *TrAC* 2013, *50*, 78–84.

[28] Christensen, I. M. A, Storgaard, M. S., Hansen, S. F., Baatrup, E., Sanderson, H., *Glob. Secur. Health Sci. Policy* 2016, *1*, 39–50.

[29] Kubáň, P., Seiman, A., Makarõtševa, N., Vaher, M., Kaljurand, M., *J. Chromatogr. A* 2011, *1218*, 2618–2625.

[30] Sáiz, J., Mai, T. D., Hauser, P. C., García-Ruiz, C., *Electrophoresis* 2013, *34*, 2078–2084.

[31] Mai, T. D., Pham, T. T. T., Pham, H. V., Sáiz, J., García-Ruiz, C., Hauser, P. C., *Anal. Chem.* 2013, *85*, 2333–2339.

[32] Seiman, A., Jaanus, M., Vaher, M., Kaljurand, M., *Electrophoresis.* 2009, *30*, 507–514.

[33] Li, Y., Nesterenko, P. N., Paull, B., Stanley, R., Macka, M., *Anal. Chem.* 2016. DOI:10.1021/acs.analchem.6b02832

Publication III

E.-G. Kobrin, **H. Lees**, M. Fomitšenko, P. Kubáň, M. Kaljurand, Fingerprinting postblast explosive residues by portable capillary electrophoresis with contactless conductivity detection, Electrophoresis. 35 (2014) 1165–1172.

Eeva-Gerda Kobrin[1]
Heidi Lees[1]
Maria Fomitšenko[1]
Petr Kubáň[1,2]
Mihkel Kaljurand[1]

[1]Department of Chemistry,
 Tallinn University of
 Technology, Tallinn, Estonia
[2]Department of Chemistry,
 Masaryk University, Brno, Czech
 Republic

Research Article

Fingerprinting postblast explosive residues by portable capillary electrophoresis with contactless conductivity detection

A portable capillary electrophoretic system with contactless conductivity detection was used for fingerprint analysis of postblast explosive residues from commercial organic and improvised inorganic explosives on various surfaces (sand, concrete, metal witness plates). Simple extraction methods were developed for each of the surfaces for subsequent simultaneous capillary electrophoretic analysis of anions and cations. Dual-opposite end injection principle was used for fast (<4 min) separation of 10 common anions and cations from postblast residues using an optimized separation electrolyte composed of 20 mM MES, 20 mM L-histidine, 30 μM CTAB and 2 mM 18-*crown*-6. The concentrations of all ions obtained from the electropherograms were subjected to principal component analysis to classify the tested explosives on all tested surfaces, resulting in distinct cluster formations that could be used to verify (each) type of the explosive.

Additional supporting information may be found in the online version of this article at the publisher's web-site

1 Introduction

The analysis of postblast explosive residues is important to trace the origin and source of the chemical compounds in explosive devices that are used in the acts of terrorism. Especially in the latest years, the incidence of terrorist attacks using such devices has increased and targeted major cities, such as Madrid, Spain (2004). London, England (2005), Prune, India (2010), Oslo, Norway (2011), and most recently Boston, USA (2013). Although mainly improvised inorganic explosives based on easily accessible chemicals, such as ammonium nitrate/fuel oil (ANFO), black powder, or sodium chlorate-type devices were employed, the use of other types of explosives (i.e. organic high explosives) cannot be completely ruled out. The chemical trace that each explosive device leaves after detonation can lead to quicker identification of possible

Correspondence: Eeva-Gerda Kobrin, Institute of Chemistry, Tallinn University of Technology, Akadeemia tee 15, 12618 Tallinn, Estonia
E-mail: eevagerda@gmail.com
Fax: +372-6202828

Abbreviations: ANFO, ammonium nitrate/fuel oil; **DOEI**, dual-opposite end injection; **IS**, internal standard; **PCA**, principal component analysis

suspects and prevent additional attacks. The obtained data may function not only as a "fingerprint" of the explosive itself but also of a particular constructor. It has been shown that most inorganic explosives produce an ionic postblast residue that is composed of a few distinct inorganic anions and cations. On the contrary, however, very little knowledge is available on the chemical traces that organic high explosives leave.

Currently used techniques for the analysis of postblast explosive residues include a wide range of spectroscopic techniques, such as atomic absorption spectroscopy [1], SEM, energy dispersive X-ray detection [2, 3], X-Ray diffraction [4], MS [5], ion mobility spectrometry [6], as well as chromatographic techniques, such as HPLC [7] and ion chromatography [8, 9]. Many of the above mentioned techniques are not easily portable and the sample must be taken to the laboratory for analysis, resulting in increased risk of contamination and significant delays in the analysis and data processing.

CE, on the contrary is easily amenable for field analyses. The analysis of postblast explosive residues has been carried out by conventional CE with indirect absorbance [10], direct [11] and indirect laser induced fluorescence [12]. Electrochemical detection [13], and particularly capacitively coupled contactless conductivity detection (C^4D), [14, 15] have been recently used [16]. For the detection of small inorganic ions, C^4D is more sensitive than indirect UV detection, has

simple electronic circuitry, relatively low cost, and low power consumption. It is thus ideally suited for implementation in portable CE instruments. Moreover, CE is even applicable for postblast explosive analysis on a chip [17]. The edge that CE can offer in terms of portability for postblast explosive residue analysis has been first realized by Hutchinson et al. in 2008 [18]. They used a commercially available portable CE instrument (http://www.ce-resources.com) for sensitive determination of inorganic anions and cations in residues from inorganic homemade explosives. Two separate methods for analysis of anions and cations were developed employing two different separation electrolytes at different pH. Hopper and co-workers [19] have proceeded one step further toward a comprehensive ionic analysis and optimized a CE method with indirect UV detection for simultaneous separation of anions and cations in low explosive residues employing the dual-opposite end injection (DOEI) approach [20, 21]. In this mode, the sample is injected sequentially into both ends of the separation capillary and during the electrophoretic run, cations and anions migrate toward the detector placed in an optimized position (typically in the centre of the separation capillary). With indirect UV detection, as used by Hopper et al. [19], the choice of separation electrolyte for DOEI is rather difficult, requiring complex BGE containing anionic and cationic indirect detection probes, cation complexation agents, organic modifier, and an EOF modifier. Despite the BGE complexity, six cations and eight anions could be separated in less than 6 min.

In this work, we show simultaneous separation of postblast explosive residues using portable CE with C^4D. The choice of electrolyte for simultaneous CE separation with C^4D detection is much easier than with indirect UV detection and a portable CE system recently developed in our laboratory [22–24] was shown to be able to differentiate between postblast residues resulting from various commonly encountered explosives on various matrices. While postblast residue analysis by CE has been reported several times there is virtually no systematic study on the effect of background ions from the matrix where the explosion took place. This is an important problem to address since many analytes that can be used in identification of a particular explosive are frequently found also in the matrix itself. More importantly, this study deals not only with inorganic improvised devices, but also with organic high explosives. By applying simple chemometrics (principal component analysis (PCA)) to the obtained data, explosives can be, at least partly, classified regardless of the matrix complexity.

2 Materials and methods

2.1 Electrophoretic system

A purpose-built portable CE instrument was fitted into a watertight, crush-proof, dust-proof case made of durable plastic (Peli 1200 Case©, Peli Products, Barcelona, Spain). The in-
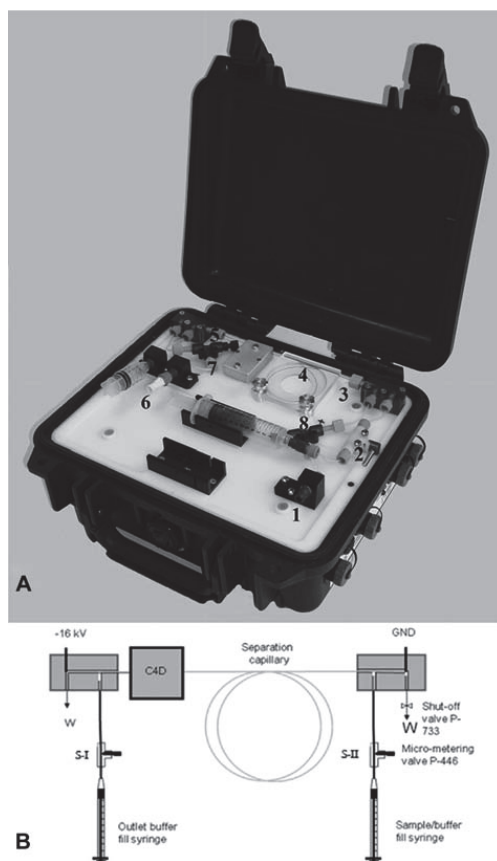

Figure 1. (A) A photo of the portable instrument (1) syringe socket, (2) shut off valve, (3) inlet end of the capillary, (4) the separation capillary, (5) outlet end of the capillary, (6) syringe socket, (7, 8) metering valve. (B) A schematic of the separation compartment of the portable instrument ("W"—output to waste, GND—grounding, S-I and S-II—interfaces, micro flow-metering valves (P-446)).

strument was equipped with an HV safety interlock and included a negative high-voltage power supply (EMCO, Sutter Creek, CA, USA) capable of delivering voltages up to −25 kV, an in-house built C^4D detector operating at 200 kHz and a voltage of 60 Vp-p, and a data acquisition system. The instrument was controlled by an in-house written software and the signal was obtained through a USB connection of a notebook computer.

The schematic of the experimental set up and a photograph of the instrument is shown in Fig. 1. The sample injection units placed at both capillary ends include each a splitter interface machined to $35 \times 15 \times 15$ mm from a block of polyimide. Each splitter interface has a 2 cm long

horizontal flow-through channel of 1 mm id. to which two vertical channels of the same diameter are connected. A separation capillary is inserted from the side of the interface with its tip positioned exactly at the cross-section of the vertical and horizontal channel. A grounding and a high voltage electrode (made of Pt wire) are inserted into the second vertical channel of the respective interface. Both the capillary and the Pt electrodes are secured with 1/16″ flangeless fittings (Upchurch Scientific, Oak Harbor, WA, USA). Two in-line micro flow-metering valves (P-446, Upchurch Scientific) are used to precisely regulate the flow rates with manual syringe injection [25].

2.2 Dual opposite end injection

During DOEI process, a 500 μL volume of sample is injected manually into the first splitter interface (S-I) using a 1 mL disposable plastic syringe (Omnifix 100 Duo, Braun, Melsungen, Germany) followed by an injection of 1500 μL of the BGE solution. Then another sample aliquot of 500 μL is injected into the second splitter interface (S-II), followed by an injection of 500 μL of the BGE solution. This sequence allows (i) simultaneous injection of sample into both capillary end and (ii) removal of any remaining sample from the splitter interfaces before the separation takes place.

2.3 Separation capillary conditioning

Fused-silica capillaries (50 μm id, 375 μm od, 50 cm total length, Polymicro Technologies, AZ, USA) were used. Capillary rinsing was performed by manually applying the pressure to the syringe with appropriate solution inserted in the splitter interface S-II with the shut-off valve (P-733, Upchurch Scientific) closed. Prior to the first use, the separation capillaries were preconditioned with 0.1 M NaOH for 30 min, DI water for 10 min, and BGE solution for 10 min. Before each analysis sequence, the capillaries were manually washed with approximately 150 column volumes of DI water and 150 column volumes of the BGE. Between two successive injections, the capillary was flushed with 100 column volumes of the BGE solution (1 min). At the end of each day, the capillaries were washed with at least 150 column volumes of DI water and kept in DI water overnight.

2.4 Chemicals

Stock solutions of standards, 100 mM for each inorganic ion, were prepared from reagent grade chemicals (Sigma-Aldrich, Steinheim, Germany) by dissolving them in DI water (MilliQ Water System, Millipore, Molsheim, France). Lithium formate (Sigma-Aldrich, 98% purity), 5 mM stock solution, was used as internal standard to spike the sample and standard solutions. BGE for CE measurements was prepared daily by diluting 100 mM stock solutions of MES (Sigma-

Aldrich), 100 mM L-histidine (HIS, Sigma-Aldrich) and 18-*crown*-6 (Sigma-Aldrich) to the required concentration. CTAB (Sigma–Aldrich) was prepared as 10 mM stock solution in 5% acetonitrile and was added to the BGE. The optimized BGE composition used in this work was 20 mM MES, 20 mM HIS, 30 μM CTAB, and 2 mM 18-*crown*-6 at pH 6.

2.5 Explosives

All used explosives with their approximate chemical composition are listed in Table 1 in the Supporting information. They were commercial products, regulated by national authorities and were kindly provided by Forcit OY, (Hanko, Finland). Electrically initiated detonators (No. 8 Al, Sellier & Bellot JSC, Czech Republic) were used to trigger the explosive devices.

2.6 Field analysis

The explosions were carried out at the test site of Forcit OY company, Hanko, Finland. Typically 50 to 100 g of the selected explosive was placed on the investigated matrix and the explosion was initiated with an electrically connected detonator. The detonators contained lead azide (45 mg) and lead styphnate (105 mg) as primary explosive and small amounts of PETN (0.72 g) and TNT (0.08 g) as secondary explosive. In a detonator the primary explosive is the more sensitive part which is initiated electrically and gives enough energy to ignite the secondary explosive. The secondary explosive is then enough to ignite the charge that is handled.

2.7 Sampling and sample preparation

The explosions were performed on three different surfaces—sand, metal plate, and concrete that represent the three common matrices similar to those that can be encountered in a real terrorist attack. The matrices were selected as they are readily available and were used to test the applicability of the proposed approach to identify the explosive type. However, the matrices used herein should not be considered universal and a more detailed study addressing the effect of other possible matrices will be required. Here, we provide just the initial results and a proof of concept. Thus a fresh sand bead, a concrete plate (25 × 25 cm, 5 cm thick) or a metal witness plate (10 × 10 cm, 8 mm steel) was used for each explosive. Each explosion was done in triplicate. Only one blank sample from each matrix was taken, while two parallel samples were taken after explosion. The total amount of blank samples taken for one explosive and one surface was three and the amount of postblast explosive residue samples was six.

2.7.1 Blank samples

Blank samples were collected from the explosion sites before the detonation of each explosive. For sand matrix, 4 g of the sand directly from the sand bead was transferred into
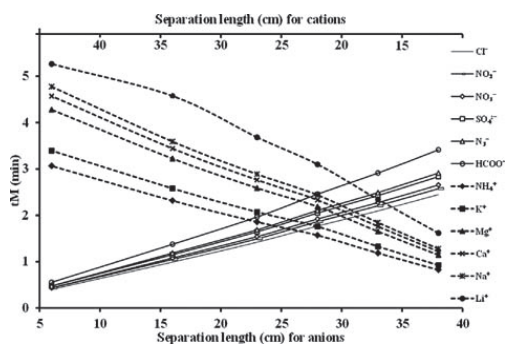
Figure 2. Dependence of migration times of anions and cations on the separation distance from the detector. Total capillary length was 50 cm and the detector was consecutively positioned 6, 16, 23, 28, and 38 cm from one injection end. The separation of anions was carried from the negative end, while the separation of cations was carried from the positive end.

a 50 mL sampling container and 10 mL of DI water was added. For concrete and metal plates, cotton pads (purchased from local pharmacy) were first washed with 30 mL of DI water and dried to remove any background ions. Right before sampling, the pre-processed cotton pads were moisturized by 1 mL DI water and the surface was wiped utilising NIOSH surface wipe sampling technique (http://www.bnl.gov/esh/shsd/sop/pdf/ih_sops/ih75190.pdf). The cotton pad was then transferred into a 50 mL sampling container and 10 mL of DI water was added. All samples were shaken for 1 min and the aqueous extract was filtered through the 0.45 μm filter (Filtropur S (Sarstedt, Germany)) and the filtrate was used for the CE analysis.

2.7.2 Sand sampling after detonation

After each set of explosions, 4 g of postblast sand was collected from the remaining sand and processed in the same way as the blank samples. Typically about one half of the total sample weight was taken from the centre and another half was collected from the areas about 10–20 cm from the centre. When the explosion has left an obvious trace (light ash, dark ash etc.) this type of residue was preferentially collected.

2.7.3 Metal and concrete plate sampling after detonation

Two samples were taken from each metal witness plate or each concrete plate, by wiping one half of the plate surface with one cotton pad and second half with another one. Depending on the explosive strength, the concrete plate either remained whole or was shattered into several pieces. In case of shattering, the pieces were collected together and their surface was wiped. Again, two parallel samples were taken from

each concrete block. The cotton pads with collected residues were processed in the same way as blank samples.

3   Results and discussion

3.1   Optimization of the separation electrolyte for DOEI

The optimization of the simultaneous separation of anions and cations consisted of injecting anions and cations separately from opposite capillary ends with a C^4D detector positioned at different positions along the separation capillary [26]. Only those ions that were detected in the samples of explosive residues were separated in the model mixture, thus 12 ions in total, including lithium formate as internal standard were evaluated. Due to the specific construction of the instrument the minimum possible effective length of capillary from anodic and cathodic end is 13 and 6 cm, respectively. The graph in Fig. 2 shows the migration times versus the effective separation capillary length from the respective injection point to the detector. A previously optimized [27] separation electrolyte consisting of 20 mM MES, 20 mM HIS, 30 μM CTAB, and 2 mM 18-crown-6 was used. A suitable position of the detector can be selected from a graph in Fig. 2. The minimum detector distance from the anodic side that allows full separation of selected cations with the shortest analysis time is 14 cm, while for full separation of all selected anions the minimum distance from the cathodic side is around 36 cm. This gives an optimum position of the detector to be 14 cm from the anodic side (right) and 36 cm from the cathodic side (left) and this configuration was used throughout this study. An electropherogram of a standard solution containing all selected ions and two internal standards is shown in Fig. 3A. Note that all ions are fully baseline-separated in less than 4 min.

3.2   Performance data

The developed CE method for simultaneous determination of anions and cations was validated using a set of standard solutions prepared in DI water (a matrix that is very similar to the sample matrix). Table 1 lists the most important figures of merit, such as repeatability of peak areas ($n = 3$), linearity and LODs. The calibration curves were constructed by using lithium formate as an internal standard (IS). Lithium formate was added to the cationic and anionic standard solution to yield final concentration of 50 μM and the ratio of peak areas of each analyte to peak area of IS was plotted against the analyte concentration. The same amount of IS was also added to the postblast explosive residue samples and blank samples for qualitative and quantitative analysis. The linearity was measured in the range of the concentrations of ions found in most of the samples. A variable dilution of the samples (1:2–1:500) was used to fit the measured peak areas within the calibration curve. The LODs were between 12.2 and 35.7 μM
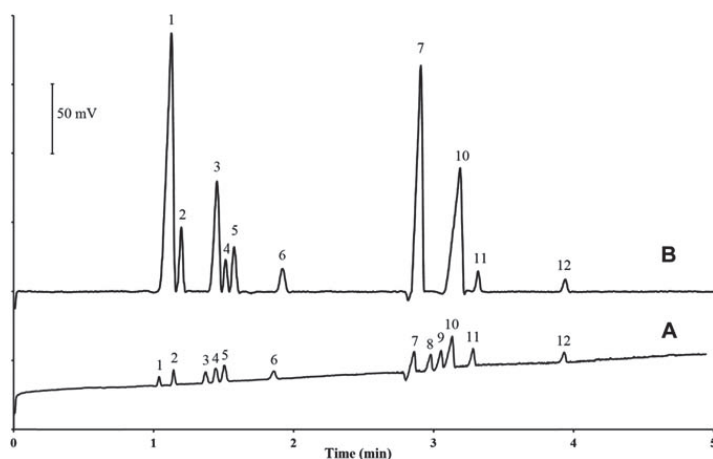
Figure 3. (A) Separation of standard solution with IS using DOE injection. Simultaneous separation of anions and cations. Cations injected first (3 s, hand pressure injection of 500 μL standard solution and 1500 μL BGE), followed by anions (3 s, hand pressure injection of 500 μL standard solution, BGE 500 μL). CE conditions: −16 kV, contactless conductivity detection. Peaks: (1) NH_4^+, (2) K^+, (3) Ca^{2+}, (4) Na^+, (5) Mg^{2+}, (6) Li^+, (7) Cl^-, (8) NO_2^-, (9) NO_3^-, (10) SO_4^{2-}, (11) N_3^-, (12) $HCOO^-$. Detector position: 36 cm from the positive side and 14 cm from the negative side. (B) Simultaneous separation of anions and cations in postblast residue from ANFO explosion. ANFO sand sample diluted 1:2. Simultaneous injection in the following sequence and side: 500 μL sample (positive side)−1500 μL BGE (positive side) 500 μL sample (negative side)−500 μL BGE (negative side). Peaks: (1) NH_4^+, (2) K^+, (3) Ca^{2+}, (4) Na^+, (5) Mg^{2+}, (6) Li^+, (7) Cl^-, (8) NO_3^-, (9) SO_4^{2-}, (10) $HCOO^-$. CE conditions: the same as in 3(A).

for anions and 3.8 and 7.3 μM for cations. The optimized and validated CE method was then used for detailed screening of ionic content of 8 different explosives.

3.3 Postblast explosive analysis

3.3.1 Analysis of blank samples

As most of ions used in this work, are also ubiquitous in nature and on various surfaces it is important to determine

Table 1. Figures of merit of the developed CE-C⁴D method for simultaneous determination of inorganic anions and cations in explosives residues, *n* = 3

Ion	RSD (%) P.A.	Calibration range (μM)	r^2	LOD (μM)
NH_4^+	5.5	1–500	0.9960	7.3
K^+	4.4	1–250	0.9969	3.7
Na^+	5.0	1–250	0.9928	7.1
Ca^{2+}	5.7	1–250	0.9982	3.8
Mg^{2+}	3.6	1–250	0.9968	5.8
Cl^-	7.1	1–250	0.8707	35.7
NO_2^-	9.9	1–75	0.9900	11.0
NO_3^-	7.8	1–75	0.9889	15.6
SO_4^{2-}	7.1	1–75	0.9953	12.2
N_3^-	9.1	1–250	0.9900	12.8

P.A., peak area.

the extent of matrix effects and subtract it from the measured data. For this reason blank sample from each matrix was taken and analyzed as described previously. Blank concentration levels of most anions were lower than their LOD, only in concrete blank samples traces of NO_3^- and SO_4^{2-} between 19 and 51 μM were detected. On the other hand all cations (measured in our work) were present in all blank samples and ranged between 6 and 272 μM.

3.3.2 Analysis of inorganic and organic explosive postblast residues

Analysis of post blast residues of eight explosives: Dynamite, PETN, TNT, RDX, PENO, ANFO, V40, C4 from three different surfaces (except for V40, which was not tested on concrete due to the safety reasons) showed the majority of inorganic ions described previously in the literature. As an example, simultaneous analysis of postblast residue in an ANFO sample from sand matrix is shown in Fig. 3B.

3.4 Fingerprinting the postblast explosive residues

In a simple case, when improvised inorganic explosive is premixed from raw chemicals, such as perchlorate, chlorate, and nitrate the identification can indeed be based on either anionic or cationic trace. Significant research effort has been devoted to identify these types of explosives. On the contrary, very little knowledge is available on the traces that organic
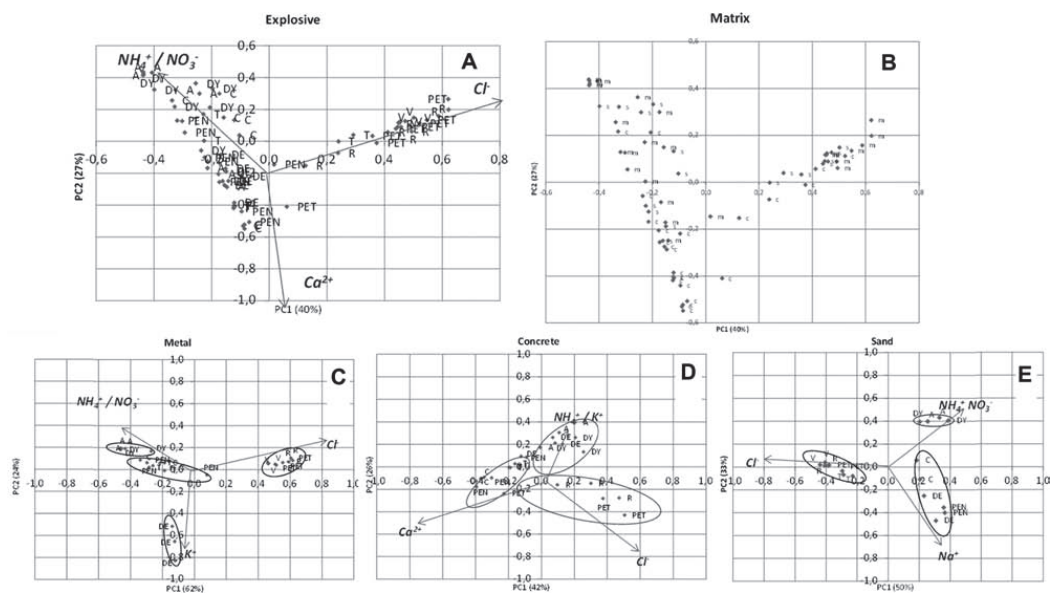
Figure 4. Ion intensity data from all explosives in different matrices analyzed by standard principal component analysis (PCA). (A) Score plots of all samples labeled by matrix type (s, sand; c, concrete; m, metal). (B) Score plots of all samples labeled by explosive: Dynamite (DY); PETN (PET), TNT (T), RDX (R), PENO (PEN), ANFO (A), V40 (V), C4 (C), detonator (DE). (C–E) Distribution of the ions on metal, concrete, and sand, respectively.

high explosives leave. In a paper by Hutchinson et al. [10] two organic devices (a mixture of PETN/RDX and TNT) were tested with no apparent inorganic residues left. This observation is consistent with our initial observations; however, other organic high explosives do leave a significant inorganic ion trace that may help to identify them. Separate analysis of anions or cations may not be sufficient for correct identification of the explosive. The complexity of the ionic traces is demonstrated in Fig. 1 (see the Supporting information) that shows bar graphs of cation and anion concentrations in each of the tested explosives and each matrix. When looking at the anionic graphs it is clearly visible, for instance, that high concentrations of nitrate are present in dynamite and ANFO traces. The same can be seen for ammonia cation. The other ions do not exert such a clear difference, but can be still used to at least partially characterize the postblast residues. This is shown in an example in Fig. 2 (Supporting information) that suggests a flow chart that could be used for explosive identification. The flow chart is however valid only for the selected group of explosives and only applies for metal matrix, while the other two matrices do not provide similar results. It is apparent that the matrix has an influence on the data. Chemometric approaches, such as PCA, are known to eliminate matrix effects, at least to some extent, and eventually may simplify the identification. That is why in the next step, we have applied PCA to the measured data.

3.4.1 PCA analysis and clustering of the explosives

Before applying the PCA procedure the peak areas of all the ions from blank samples were subtracted from the peak areas of the ions in the corresponding postblast explosive residue samples. The obtained peak areas of all ions from all explosives in different matrices were then combined into a matrix of data which was initially analyzed by standard PCA. However, as the ionic concentrations of the postblast explosive residues are very similar and the matrix (concrete, sand, and metal surface) contains frequently the same ions, the identification was difficult. Moreover, the spread of the ion concentrations is extremely heterogeneous, so the samples taken from different locations differ significantly not only in concentrations levels but also in composition. Thus, to establish whether the pattern of ions in an electropherogram is characteristic of the used explosive or not, the peak areas were normalized to the sum of the total peak areas in each electropherogram. The resulting table consisted of 70 rows (samples of different explosives detonated on different matrices and obtained in different locations around the blast) and 10 columns of corresponding ion peak areas. The table was subjected to mean centered PCA procedure. The "leave-one-out" cross-validation procedure was used to determine the number of significant principal components. The "predicted residual error sum of squares" or PRESS was calculated according

to [28] . If the ratio PRESS(n)/PRESS($n-1$) exceeds one, then the use of $n-1$ principal components in the model is recommended. This procedure revealed four significant principal components that accounted for 94% of the total variance. Results of first two—most vivid components—PC1 and PC2 are shown in Fig. 4. PCA is a tool that allows better visualization of data in exploratory analysis. This is demonstrated in Fig. 4, where definite patterns can be identified, which highlight similarities and differences between the electropherograms of different explosive residues. In Fig. 4A and B are score plots of all samples. The figures are essentially the same except the labeling of points for clarity. The figures reveal the distinctive structure of postblast electropherograms. Two big clusters can be recognized which are located almost orthogonally to each other. Loading vectors plot (Fig. 4A) indicates that the separation of the clusters is due to the domination of Cl^- ion peak on the electropherogram. Figure 4B demonstrates that when using normalized data in PCA, the sample matrix has little influence on the clustering; on the contrary, the nature of the explosive (Fig. 4A) correlates loosely with the location of clusters. The structure of the PCA plots suggests that there is an opportunity to use electropherograms of postblast explosive extracts in classification algorithms for further identification of the explosives. Clustering becomes even more distinctive when one looks at the distribution of the ions on different matrices (Fig. 4C–E). Here again the results are represented in the first most significant PC coordinates. In all score plots the explosives can be divided into three distinctive clusters. V40, PETN, RDX form one cluster which is separated from the rest by the dominance of the Cl^- ion (note that on concrete matrix V40 was not determined). Although the dispersion of this cluster is wide on concrete matrix it still can be easily differentiated from the others. The second cluster is formed by the Dynamite and ANFO and it is separated from the rest by the dominance of the NH_4^+ ion (the other loadings depend on the matrix). The last cluster is formed by C4 and PENO, the position of which is however matrix dependent. Detonator and TNT location seems to depend on the matrix.

To summarize, the matrix influence on the postblast sample electropherogram pattern is strong. Concrete is an especially difficult matrix. Reproducibility is low and due to that, the clusters are not well "focused." Ca^{2+} influence on the distribution of clusters seems to contribute much to the location of clusters. On the other hand, however, the matrix can be considered as such in the particular situation. Well defined clusters on the corresponding scores plot mean that the electropherograms are characteristic for the detonated explosive on the given matrix and can be used for their identification.

4 Concluding remarks

Field detection of postblast residues to identify the origin of explosive devices is of uttermost importance with regard to the civil safety and subsequent police investigation. Portable CE with C^4D and DOEI sample introduction presents a suitable, fast, and sensitive method for the analysis of total ionic trace of the postblast explosive residue. A rapid separation of ten most commonly present ions (both cations and anions) was achieved in <4 min and can be used for preliminary fingerprinting of the explosives. Additionally, PCA analysis shows three main matrix-dependent and ion specific clusters formed from different explosives. By combination of the information obtained from the electropherogram and the PCA analysis, the identification of a specific explosive can be made. The identification has been tested on postblast residues of eight selected inorganic and organic high explosives, which suggests that the methodology may in general be applicable for the sensitive, field-based identification of a wide range of other explosive types.

The authors have declared no conflict of interest.

5 References

[1] Beveridge, A. D., Audette, R. J., Shaddick, R. C., *J. Forensic Sci.* 1975, *20*, 431–454.

[2] Kuila, D. K., Chakrabortty, A., Sharma, S. P., Lahiri, S. C., *Forensic Sci. Int.* 2006, *159*, 127–131.

[3] Royds, D., Lewis, S. W., Taylor, A. M., *Talanta.* 2005, *67*, 262–268.

[4] Green, M. C., Partain, L. D, in: Steven, R., Bar-Cohen, Y., Aktan, A. E. (Eds.), *High-throughput baggage scanning employing x-ray diffraction for accurate explosives detection*, Nondestructive Detection and Measurement for Homeland Security, San Diego, CA 2003, *5048*, pp. 63–72.

[5] Burns, D. T., Lewis, R. J., Doolan, K., *Anal. Chim. Acta.* 1997, *349*, 333–337.

[6] Harvey, S. D., Ewing, R. G., Waltman, M. J., *Int. J. Ion Mobil. Spec.* 2009, *12*, 115–121.

[7] Kanu, A. B., Hill, H. H. Jr., *J. Chromatogr. A* 2008, *1177*, 12–27.

[8] McCord, B. R., Hargadon, K. A., Hall, K. E., Burmeister, S. G., *Anal. Chim. Acta.* 1994, *288*, 43–56.

[9] Johns, C., Shellie, R. A., Potter, O. G., O'Reilly, J. W., Hutchinson, J. P., Guijt, R. M., Breadmore, M. C., Hilder, E. F., Dicinoski, G. W., Haddad, P. R., *J. Chromatogr. A* 2008, *1182*, 205–214.

[10] Hutchinson, J. P., Evenhuis, C. J., Johns, C., Kazarian, A. A., Breadmore, M. C., Macka, M., Hilder, E. F., Guijt, R. M., Dicinoski, G. W., Haddad, P. R., *Anal . Chem.* 2007, *79*, 7005–7013.

[11] Kennedy, S., Caddy, C., Douse, J. M. F., *J. Cromatogr. A* 1996, *745*, 211–222.

[12] Bailey, C. G., Wallenborg, S. N. *Electrophoresis* 2000, *21*, 3081–3087.

[13] Pumera, M., Wang, J., Grushka, E., Lev, O., *Talanta* 2007, *72*, 711–715.

[14] Francisco, K. J., do Lago, C. L., *Electrophoresis* 2009, *30*, 3458–3464.

[15] Zemann, A. J., *Electrophoresis* 2003, *24*, 2125–2137.

[16] Blanco, G. A., Nai, Y. H., Hilder, E. F., Shellie, R. A., Dicinoski, G. W., Haddad, P. R., Breadmore, M. C., *Anal. Chem.* 2011, *83*, 9068–9075.

[17] Sarazin, C. Delaunay, N., Varenne, A., Costanza, C., Eudes, V., *Separ. Purif. Rev.* 2010, *39*, 63–94.

[18] Hutchinson, J. P., Johns, C., Breadmore, M. C., Hilder, E. F., Guijt, R. M., Lennard, C., Dicinoski, G., Haddad, P. R., *Electrophoresis* 2008, *29*, 4593–4602.

[19] Hopper, K. G., LeClair, H., McCord, B. R., *Talanta* 2005, *67*, 304–312.

[20] Kubáň, P., Karlberg, B., *Anal. Chem.* 1998, *70*, 360–365.

[21] Padarauskas, A., Olšauskaite, V., Schwedt, G., *J. Chromatogr. A* 1998, *800*, 369–375.

[22] Kubáň, P., Seiman, A., Makarõtševa, N., Vaher, M., Kaljurand, M., *J. Chromatogr. A* 2011, *1218*, 2618–2625.

[23] Seiman, A., Jaanus, M., Vaher, M., Kaljurand, M. *Electrophoresis* 2009, *30*, 507–514.

[24] Makarotseva, N., Seiman, A., Vaher, M., Kaljurand, M., in: Kaljurand, M., (Ed.), *5th symposium by nordic separation science society*, Procedia Chemistry, Estonia, 2010, pp. 20–25.

[25] Kubáň, P., Seiman, A., Kaljurand, M., *J. Chromatogr. A* 2011, *1218*, 1273–1280.

[26] Unterholzner, V., Macka, M., Haddad, P. R., Zemann, A., *Analyst.*, 2002, *127*, 715–718

[27] Kubáň, P., Kobrin, E.-G., Kaljurand, M., *J. Chromatogr. A.*, 2012, *1267*, 239–245.

[28] Brereton, R. G., *Chemometrics: Data Analysis for the Laboratory and Chemical Plant*, John Wiley & Sons Ltd. Chichester 2003.

Publication IV

H. Lees, F. Zapata, M. Vaher, C. García-Ruiz, Simple multispectral imaging approach for determining the transfer of explosive residues in consecutive fingerprints, Talanta. 184 (2018) 437–445.

Simple multispectral imaging approach for determining the transfer of explosive residues in consecutive fingerprints

Heidi Lees[a], Félix Zapata[b], Merike Vaher[a], Carmen García-Ruiz[b],*

[a] Department of Chemistry, Institute of Chemistry and Biotechnology, Tallinn University of Technology, Akadeemia tee 15, 12618 Tallinn, Estonia
[b] Inquifor Research Group, Department of Analytical Chemistry, Physical Chemistry and Chemical Engineering and University Institute of Research in Police Sciences (IUICP), University of Alcalá, Ctra. Madrid-Barcelona km 33.600, 28871 Alcalá de Henares, Madrid, Spain

ABSTRACT

This novel investigation focused on studying the transfer of explosive residues (TNT, HMTD, PETN, ANFO, dynamite, black powder, NH_4NO_3, KNO_3, $NaClO_3$) in ten consecutive fingerprints to two different surfaces – cotton fabric and polycarbonate plastic – by using multispectral imaging (MSI). Imaging was performed employing a reflex camera in a purpose-built photo studio. Images were processed in MATLAB to select the most discriminating frame – the one that provided the sharpest contrast between the explosive and the material in the red-green-blue (RGB) visible region. The amount of explosive residues transferred in each fingerprint was determined as the number of pixels containing explosive particles. First, the pattern of PETN transfer by ten different persons in successive fingerprints was studied. No significant differences in the pattern of transfer of PETN between subjects were observed, which was also confirmed by multivariate analysis of variance (MANOVA). Then, the transfer of traces of the nine above explosives in ten consecutive fingerprints to cotton fabric and polycarbonate plastic was investigated. The obtained results demonstrated that the amount of explosive residues deposited on successive fingerprints tended to undergo a power or exponential decrease, with the exception of inorganic salts (NH_4NO_3, KNO_3, $NaClO_3$) and ANFO (consists of 90% NH_4NO_3).

1. Introduction

In recent years, numerous terrorist attacks have taken place globally, representing a constant threat to citizens in many countries. It is very probable that when a terrorist handles an explosive, there will remain a certain amount of explosive residues on his/her hands and clothes. Therefore, the detection of explosive traces directly from the hands and cloths of suspects [1–3] or through the collection of the explosive traces by swabbing [4–8] has been the subject of many studies. In this regard, Perret et al. [4] demonstrated that handling of different explosives resulted in significant transfer of explosives to the hands and traces were still detectable even after washing hands with soap. Furthermore, explosive residues may be transferred from contaminated hands and clothes to other items, such as laptops, luggage, etc. The search for and detection of trace amounts of explosives on people and objects at airports and other high-risk venues is a major challenge in counterterrorism activities [9,10]. The transfer of explosive residues through a person's fingerprints enables the detection of concealed explosives through surface sampling [11]. As a matter of fact, fingerprints are one of the main means for transferring trace amounts of

explosives during handling and preparation of improvised explosive devices [12]. To date, significant progress has been made in the detection of explosive traces in fingerprints [12–21]. Lately, there has been keen interest in developing methods for the rapid detection of explosive residues in fingerprints by using various spectroscopic, imaging and microscopic techniques, including laser-induced breakdown spectroscopy [12,22,23], X-ray fluorescence [24], vibrational spectroscopy (infrared [1,2,17,25–27] and Raman [14,28–32]) and visible spectroscopy [33]. Most studies are focused on detecting and identifying the explosive residues from fingerprints placed on different surfaces, which is the most important goal for counterterrorism purposes. However, the transfer of explosives in consecutive fingerprints to those materials on which they are detected has been scarcely studied. In this respect, Turano [34] quantified the amount of NH_4NO_3 and $KClO_3$ deposited by successive fingerprints on three different surfaces (filter paper, polypropylene, and polyurethane) by using ion chromatography. Verkouteren et al. [10] analyzed and characterized fifty composition-4 (C-4) fingerprints by using polarized light microscopy and image analysis. Gresham et al. [35] determined the mass of 1,3,5-trinitroperhydro-1,3,5-triazine (RDX) and the particle size distribution of

the C-4 residues deposited on polyethylene films by fingerprint transfer. Mass of RDX was determined by gas chromatography and the particle size distribution of residues was determined by microscopic examination. Choi and Son [36] used ion mobility spectrometry to detect traces of RDX and TNT transferred to three smear matrices – stainless steel mesh, cellulose paper and cotton fabric – by using a stainless steel roller.

Spectral imaging is a well-known non-destructive, fast and inexpensive technique with high potential for studying the transfer of explosive residues since it combines the spectral and spatial information about the imaged sample [17]. Although, selective spectral ranges using infrared or Raman vibrational spectroscopy are needed for explosives identification, the identification of explosives was not the objective of this study. This work aims to study the transfer of known explosives through successive fingerprints to different materials. For this purpose, the simplest visible multispectral imaging (MSI) system consisting of red-green-blue (RGB) wavelengths that operate in professional and non-professional cameras as well as mobile phones was applied. The goal of the study was to develop a simple approach for acquiring fundamental knowledge about the transfer of explosive residues in ten consecutive fingerprints to two different surfaces, cotton fabric and polycarbonate plastic.

2. Material and methods

2.1. Explosives and inorganic salts

In this research, the transfer of nine different explosive residues –TNT, HMTD, PETN, dynamite, ANFO, black powder, NH_4NO_3, KNO_3, $NaClO_3$ – was examined. Organic explosives and explosive mixtures were obtained from TEDAX, Spanish Explosive Ordnance Disposal (EOD). Inorganic salts (NH_4NO_3, KNO_3, $NaClO_3$) were purchased from Sigma-Aldrich (St. Louis, MO, USA) and were of ACS reagent grade (purity > 98%). The composition and average particle diameter of the studied explosive residues are given in Table 1. However, during the experiments it was observed that, in some cases, the particles of explosives became aggregated because of the pressing/transfer procedure.

2.2. Sample preparation and fingerprint collection

HMTD, PETN, ANFO, black powder, NH_4NO_3, KNO_3 and $NaClO_3$ were obtained already in powdered form and were used without any pretreatment before experiments. Initial experiments showed that big and heavy particles of non-treated TNT ($\approx 5\,mm$ particles and 12–13 mg) and dynamite (2 cm cylindrical cartridge) did not adhere to

Table 1
Composition and average particle diameter of the studied explosive residues.

Explosive residues	Composition[a]	Average particle diameter[b] (µm)
NH_4NO_3	Ammonium nitrate (100%)	≈ 300
KNO_3	Potassium nitrate (100%)	≈ 400
$NaClO_3$	Sodium chlorate (100%)	≈ 500
ANFO	Ammonium nitrate (90%) + diesel (10%)	≈ 500
Dynamite[c]	Ammonium nitrate (66%) + ethylene glycol dinitrate (29%) + nitrocellulose (1%) + dibutyl phthalate (2.5%) + sawdust (1.2%) + calcium carbonate (0.3%)	≈ 300
Black powder	Potassium nitrate (75%) + charcoal (15%) + sulfur (10%)	≈ 400 (KNO_3) ≈ 50 (charcoal)
TNT[c]	2,4,6-Trinitrotoluene (100%)	≈ 75
HMTD	Hexamethylene triperoxide diamine (100%)	≈ 20
PETN	Pentaerythritol tetranitrate (100%)	≈ 40

[a] Information provided by the manufacturer or by TEDAX (Spanish EOD).
[b] Experimentally determined by averaging the diameter of 30-50 particles by using a Raman microscope (Thermo Scientific, Waltham, MA, USA).
[c] Particle diameter after sample preparation (Section 2.2).

the finger and therefore transfer did not occur. Due to this, it was decided to prepare powdered dynamite and TNT in order to study the transfer of explosives with a similar weight (10 mg) and range of particle sizes (< 1 mm). For this, TNT was dissolved in acetonitrile. The solution was left to dry overnight to enable evaporation of acetonitrile. As a result, the powdered TNT remained on Petri dish. Dynamite was mechanically powdered in the mortar. The particle sizes after these pretreatments are indicated in Table 1.

Cotton fabric and polycarbonate plastic as the two most common clothing and luggage materials, respectively, were chosen to study the transfer of explosive residues through fingerprints. For experiments, a cotton T-shirt bought from a local supermarket was cut into $3 \times 3\,cm$ pieces. A 5-gallon (ca 19 L) polycarbonate plastic water bottle was also cut into $3 \times 3\,cm$ pieces, instead of using a real polycarbonate luggage.

The amount of explosive residues remaining in fingerprints depends on the initial amount present on a person's hands, the number of successive impressions made after contamination and the force applied by the contaminated finger [10,11]. Therefore, to take repeatable fingerprints, the applied force (1 kg) and time (3 s), were fixed to standardize the transfer procedure. The controlled force was applied by placing a 1-kg cuboid bottle on the index finger while taking the fingerprints. The time was fixed with a stopper. Additionally, the printing surfaces were all prepared in the same manner and the fingerprints were taken by ensuring the contact of the whole index finger area with the surface. To ensure the presence of the same amount of natural oils and sweat in the finger, a subject's hands were always washed 15 min before each experiment. During these 15 min the normal routine work was allowed to continue. The initial amount of explosive was always balanced at around 10.00 mg on a weighing pan using an Ohaus DV215CD analytical balance with a precision of 5 decimal places (0.00001 g). As previously evidenced in Table 1, the average particle size was different for each explosive, and consequently the number of particles contained in 10 mg of substance was different for each explosive. For instance, 10 mg meant 5–40 particles for inorganic salts (KNO_3, NH_4NO_3 and $NaClO_3$), while hundreds/thousands of particles for organic explosives (PETN, HMTD, powdered TNT) and black powder (due to fine particles of charcoal). The number of particles for 10 mg of ANFO and dynamite was intermediate.

2.3. Instrumentation

Fingerprints of explosive residues on the two studied surfaces were photographed using the Nikon D5000 Digital SLR Camera equipped with a 12.9 megapixel DX-format CMOS sensor and AF-S DX Zoom-Nikkor 18–55 mm f/3.5–5.6G ED II lens. A purpose-built photo studio having controlled light, tripod (a fixed height and perpendicular angle) and remote control was used to minimize the error of imaging. Pictures of samples were taken together with that of a clean blank sample (cotton or polycarbonate) to check the correct intensity value for the background of each picture. Three replicates per explosive and material were prepared. Using the remote control three consecutive photographs of each replicate were taken.

2.4. Image processing

Image processing was performed in MATLAB R2017a (MathWorks, USA) using a self-written code. The used image processing was similar to the previous study performed by this research group [37]. Three pictures of each replicate were processed as follows. The region of interest (ROI) was selected by removing the unnecessary edges of the image. Raw images contained 2848×4288 pixels $\times$ 3 wavelengths, the spatial resolution of each pixel was $19.2 \times 19.2\,µm$. ROI involved a square selection of 1000×1000 pixels in the correct frame. In order to select the correct frame, the three RGB frames of each image were compared. The frame that provided the sharpest contrast between the explosive and the background material was chosen. This contrast was

Table 2
Selected frames and optimized intensity threshold values for counting the explosive particles on each surface.

	RGB frame selected	Intensity threshold value (0-1)
		0 = completely black, 1 = completely white
White explosives on red cotton	Green	> 0.39
Black powder on red cotton	Red	< 0.30 (black charcoal particles)
	Green	> 0.34 (white-grayish KNO_3 particles)[a]
White explosives on polycarbonate (dark background behind polycarbonate)	Red	> 0.39
Black powder on polycarbonate (light background behind polycarbonate)	Blue	< 0.59 (black charcoal + white-grayish KNO_3 particles)[a]

[a] KNO_3 particles were covered with charcoal and were therefore not completely white.

evaluated by both the visual inspection of the image and the numerical examination of the values in the matrix. For instance, in case of red cotton fabric and white explosive, the green frame was selected, while for polycarbonate plastic and white explosive, the red frame was selected, as summarized in Table 2. In fact, the selection of materials of the above colors was not random. Bearing in mind the aim of maximizing the contrast, materials of different colors (*i.e.* green, blue, red, gray, white and black cotton fabrics or paper sheets placed behind the transparent polycarbonate plastic) were initially examined. Of the tested materials, red cotton fabric provided the highest contrast for both white and dark explosives. Regarding the colored paper sheet placed behind polycarbonate, black paper for white explosives, and light gray paper for black powder were selected.

After selecting the proper frame, the amount of pixels containing explosive residues was quantified. To this end, pixels whose values of intensity in the specific frame exceeded a specific value were summed up. Different intensity thresholds were tested by controlling the maximum intensity present in the blank sample and assuring visually that the program would not count any pixels from the background. Then, the quantification of pixels in each image was performed through automatically counting the pixels whose intensity values were higher (in case of white explosives) or lower (in case of black powder) than the threshold value. For black powder on cotton fabric, the combination of two frames was employed and the number of grayish and black pixels were finally summed up. Table 2 summarizes the threshold values optimized for each surface and explosive to count the explosive particles on that surface.

After counting the pixels, the image was binarized, *i.e.* converted only to black and white (values 0 and 1 only) for better visualization. A simplified scheme of image processing in MATLAB for ANFO on cotton fabric is displayed in Fig. 1.

It is important to point out that the number of pixels containing explosive residues in the image does not exactly respond to the number of explosive particles itself. The two reasons for this are that (a) the size of the particles is different even within the same explosive and (b) the particles may become aggregated during the pressing/transferring procedure, but only pixels in the upper layer of fingerprints are counted. Nevertheless, despite the above-mentioned shortcomings, some fundamental insights can be established about the transfer of explosive residues.

2.5. Data treatment

The numbers of pixels obtained by MATLAB were imported as a matrix to Excel (Microsoft Office 2016) and STATGRAPHICS Centurion XVI.I (Statpoint Technologies, Inc., USA). Different fitting trendlines using Excel were tested by evaluating the R^2 coefficient. Multivariate Analysis of Variance (MANOVA) was performed in STATGRAPHICS to analyze the variance in the amount of pixels containing explosives among samples and replicates. Before performing MANOVA it was verified that data distribution was normal and linear, there was homogeneity of variances and no outliers were present. The number of

dependent variables was 10 (ten fingerprints) to 1 predictive factor (subjects). In brief, an analysis of variance (ANOVA) was conducted for each variable separately, evaluating its performance at an alpha level of 0.05. The multiple comparison procedure to discriminate among the means of transferred explosive residues between subjects was based on Fisher's least significant difference (LSD).

3. Results and discussion

3.1. Transfer of explosive residues in ten consecutive fingerprints by ten persons

The transfer of PETN in ten consecutive fingerprints to cotton fabric was investigated. Ten consecutive fingerprints were taken of ten persons in triplicate. The test group consisted of five females and five males at the age between 22 and 29 years. A standardized procedure (as described in Section 2.2) for taking fingerprints was followed by all participants. To this end, the index finger of each person's right hand was exposed for 3 s to 10 mg of the explosive powder on a weighing pan. After that, the fingertip with the explosive particles adhered to was pressed consecutively on ten pieces of cotton fabric. The amount of explosive particles remaining on the weighing pan was re-weighed after pressing the finger on the pan to determine the initial amount of explosive adhered to the subject's fingertip. This was done by subtracting the two weight values of the weighing pan (initial and after).

The amount of PETN adhered to the bare finger after pressing varied from 3.7 to 7.5 mg between the subjects. Interestingly, the pattern of transfer of PETN through successive impressions to cotton fabric was similar in all subjects – the amount of explosive residues in the fingerprints decreased with the increasing number of fingerprintings.

The graph showing the average number of pixels containing PETN residues (with standard deviation) in each fingerprint taken of the ten subjects is depicted in Fig. 2. As an example, the pictures of ten consecutive fingerprints of PETN on cotton fabric taken of one person are also given in the figure.

According to the standard deviation bars seen on Fig. 2, it is evident that there were differences in the amounts of PETN (amount of pixels) transferred by the subjects despite employing the standardized fingerprinting procedure. However, even with those differences, the general results were the same – a similar decrease in the transferred amounts of PETN through successive fingerprints was observed for every person. In fact, this decrease of the transferred PETN amount in consecutive fingerprints may be explained using the power function $y = 42556x^{-1.844}$ with an acceptable coefficient of determination ($R^2 = 0.99$).

In order to check whether the slight differences visually observed among the subjects were statistically significant, MANOVA was performed. Since the p-value for the first variable (the first fingerprint) was less than 0.05 (p-value was 0.0132), there was a statistically significant difference between the subjects considering the first fingerprint at a 95.0% confidence level (*i.e.* rejection of the null hypothesis). ANOVA results for all the other variables gave p-values higher than 0.05, which meant that the differences in the amount of transferred explosive
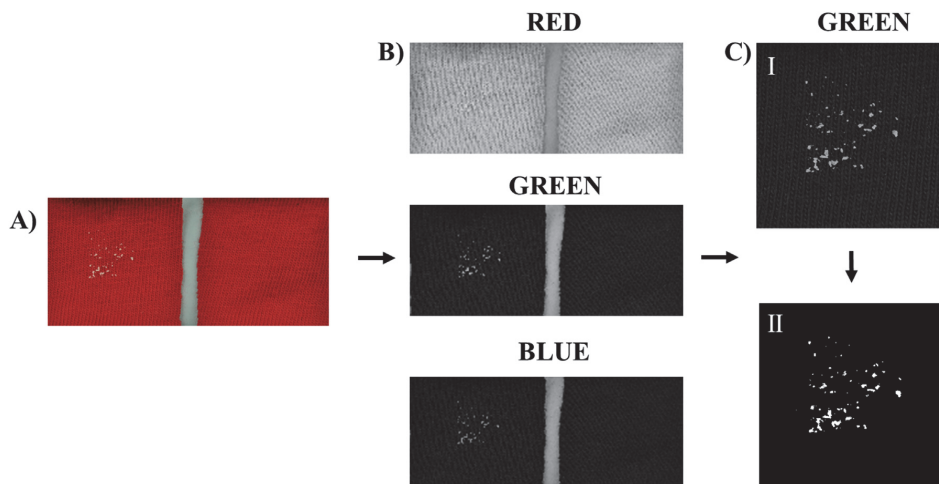
Fig. 1. Simplified scheme of image processing in MATLAB: A) explosive residues (ANFO) on cotton fabric (left) compared to a blank sample (right), B) RGB frames for evaluation and selection, C) selection of ROI in the correct frame (I) and binarization of the image (II).
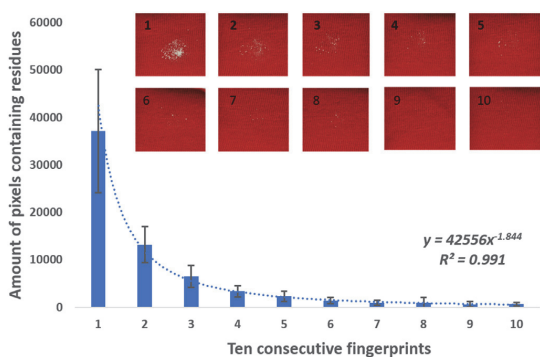

Fig. 2. Graph showing the variation of the amount of PETN (amount of pixels) transferred through ten successive fingerprints of ten persons. As an example, images of ten consecutive fingerprints of one person are shown (red squares 1–10).

Table 3
Multiple comparison procedure of the ANOVA results of the first fingerprint for the ten subjects.

	Groups in which transfer is not significantly different			
Subject 1	X			
Subject 2	X	X		
Subject 3	X	X	X	
Subject 4	X	X	X	X
Subject 5		X	X	X	X
Subject 6			X	X	X
Subject 7			X	X	X
Subject 8			X	X	X
Subject 9				X	X
Subject 10					X

residues between subjects from their second to tenth fingerprint were not statistically significant.

A popular way to investigate the cause of rejection of the null hypothesis is the multiple comparison procedure. Therefore, this procedure was applied to the ANOVA of the first variable (the first fingerprint) to determine which means were significantly different from which others. The Fisher's LSD estimated difference between each pair of means showed that out of 45 pairs (all possible combinations among the ten persons), 14 pairs of means showed statistically significant differences at a 95.0% confidence level. From Table 3 it can be seen that five groups were created using columns of X's. Within each column, the levels containing X's form a group of means within which there were no statistically significant differences.

Surprisingly, even though there were significant differences in the explosive amount present in the first fingerprint between some specific subjects, Table 3 reveals that none of the subjects differed markedly from the others. The amount of transferred explosive residues in consecutive fingerprints remained in a definite similar range for all subjects. For example, even though there were statistically significant differences (considering the first fingerprint) between subjects 1 and

10, no statistical differences between subjects 1 and 4, neither between subjects 4 and 9 or between subjects 9 and 10 were observed.

Despite the statistically significant differences that may occur between some persons in the explosive amount in their first fingerprint, there are no differences that perfectly distinguish people's transfer behavior. In conclusion, there is not a significant influence from the person when transferring the explosives while following a standardized procedure.

3.2. Transfer of residues of nine explosives in ten consecutive fingerprints to cotton fabric or polycarbonate plastic

The transfer of residues of nine different explosives (HMTD, TNT, PETN, black powder, dynamite, ANFO, NH_4NO_3, KNO_3 and $NaClO_3$) in ten fingerprints to two surfaces, cotton fabric and polycarbonate plastic, was investigated. It was evidenced in the preceding experiment that the
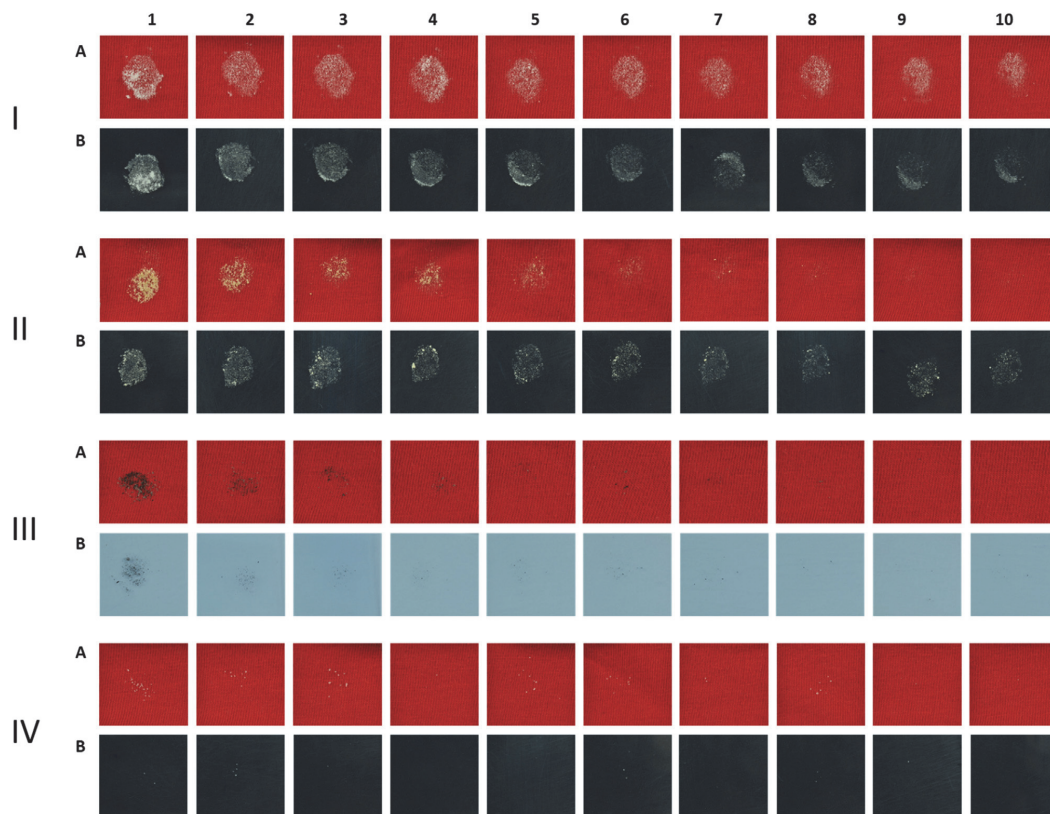
Fig. 3. Transfer of explosive residues in ten successive fingerprints to cotton fabric (A) and polycarbonate plastic (B). I – HMTD, II – TNT, III – black powder, IV – KNO$_3$.

transfer of explosive residues was not strongly influenced by the person doing it when following a standardized procedure. Therefore, only one person (doing three replicates per explosive residue and surface) participated in all the experiments.

As in the preceding experiment, the weighing pan with the explosive residues was balanced before and after pressing the finger on it to determine the amount of explosive which had adhered to the subjects' fingertips. Interestingly, residues of NH$_4$NO$_3$, KNO$_3$, NaClO$_3$, ANFO, dynamite, TNT and HMTD adhered to fingertips almost entirely from the weighing pan – the adherence of residues to the fingertip after one touch was 93 ± 4% (n = 42). However, the amount of black powder and PETN adhered to the person's fingertip after the first pressing was lower and more variable compared to the other explosives, being 62 ± 11% (n = 6) and 72 ± 8% (n = 6), respectively.

Fig. 3 displays, as an example, one replicate of ten successive fingerprints containing HMTD, TNT, black powder and KNO$_3$ on cotton fabric and polycarbonate plastic. As can be visually observed from the figure, the amount of residues of explosives transferred through fingerprints significantly varies for every explosive. In addition, there seems to be differences in the transferred explosive amount between consecutive impressions. In fact, there are several studies that demonstrated some variability in the amount of transferred explosive from one fingerprint to the next [10,34,35]. However, no far-reaching conclusions can be drawn on the basis of visual examination only. Therefore, in this study information contained in the multispectral image was maximized by quantifying the pixels containing explosive residues.

According to the obtained results, two entirely different tendencies

could be observed in the transfer of explosive residues through consecutive fingerprints when using a standardized procedure. On the one hand, organic explosives (HMTD, TNT, PETN), black powder and dynamite evidenced a particular decrease in the amount of transferred residues through consecutive fingerprints. On the other hand, no clear decrease in the amount of transferred residues of oxidizing inorganic salts (NH$_4$NO$_3$, KNO$_3$, NaClO$_3$) and ANFO (composed of 90% NH$_4$NO$_3$) through consecutive fingerprints was noticed. Instead, a random transfer of residues of these explosives was noticed.

The transferred amount of residues of HMTD, TNT, PETN, black powder and dynamite showed a clear decrease (either power or exponential) as illustrated in Fig. 4. Fig. 4 displays the quantification of pixels containing explosive residues (y-axis) on consecutive fingerprints (x-axis) together with the respective fitted functions for the transfer of each explosive, as well as their mathematical equations and coefficients of determination.

The amount of HTMD transferred to both surfaces under study was clearly the highest. Large number of residues of this explosive could be found in all fingerprints, including the tenth. It should be pointed out that HMTD represented the finest powder (average particle diameter 20 µm), which could explain the higher amounts of transferred residues of this explosive compared to the other explosives. However, the amounts of HMTD residues transferred to cotton fabric and polycarbonate plastic somewhat differed. Specifically, the amount of HMTD transferred to polycarbonate plastic fitted perfectly a power function (R^2 = 0.99), while the amount transferred to cotton fabric presented a slighter decrease (exponential) through consecutive fingerprints and
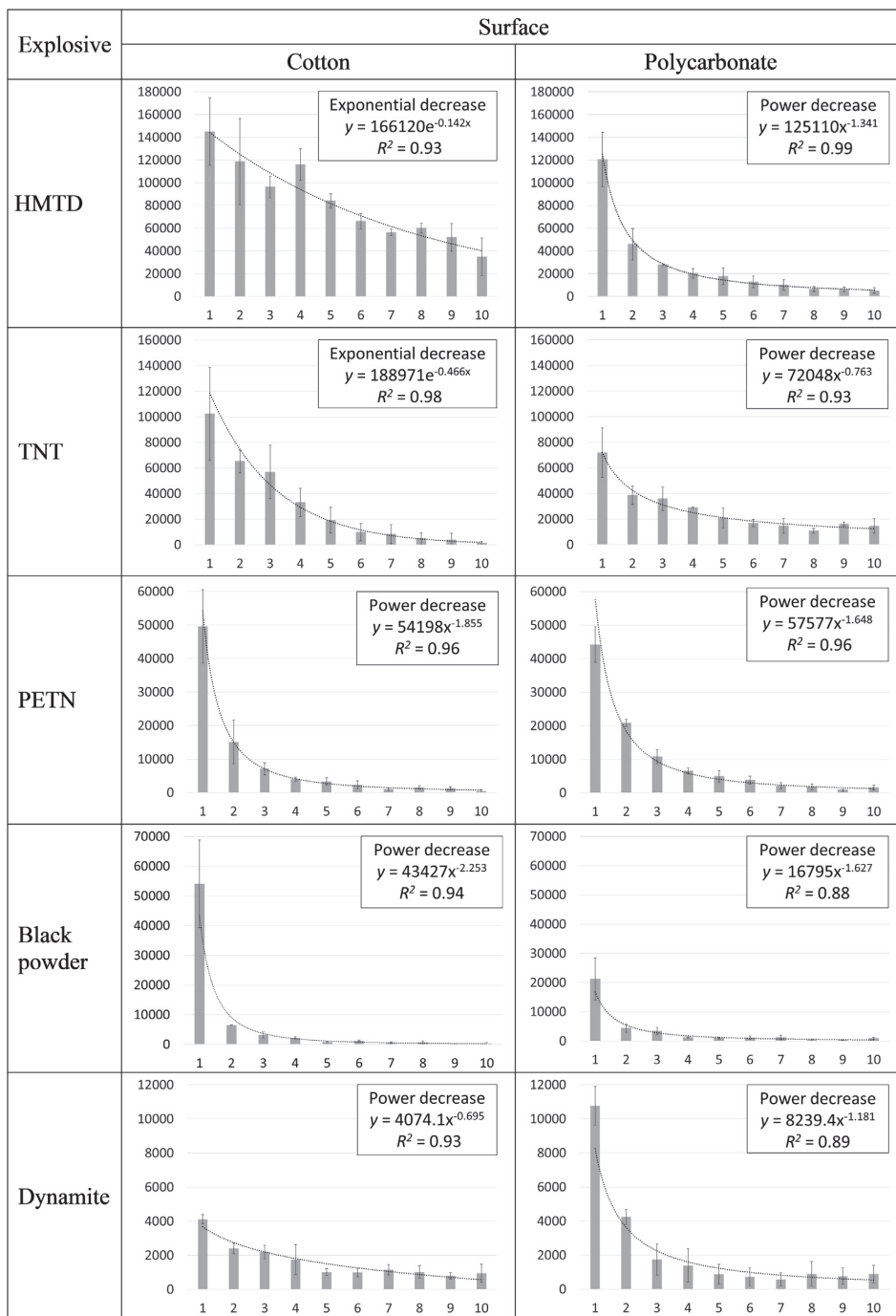
Fig. 4. Bar graphs, fitting trendlines, mathematical equations and coefficients of determination showing the amounts of transferred explosive residues undergoing a particular decrease along the ten consecutive fingerprints. X-axis: ten consecutive fingerprints, y-axis: amount of pixels containing explosive residues.

underwent some dispersion that accounted for the lower value of R^2.

The amount of TNT transferred to both surfaces was also higher compared to the other explosives. Based on the quantification of the pixels containing explosive residues (Fig. 4), the transfer of TNT in fingerprints also depended on the target surface. There was a clear decrease through ten fingerprints to cotton fabric – there were only a few particles left by the last fingerprints. This decrease could be explained by an exponential function with R^2 of 0.98. On the other hand, the transfer of TNT to polycarbonate plastic followed a tendency that fitted the power function ($R^2 = 0.93$).

The patterns of transfer of PETN to both materials were very similar and the amounts transferred showed a clear decrease in consecutive fingerprints. The transfer of PETN to cotton fabric and polycarbonate plastic was best described by power functions with R^2 being 0.96 for both surfaces.

The transfer of black powder was characterized by a huge amount of residues left in the first fingerprint on both surfaces (see Fig. 4), while the second fingerprint contained approximately five to eight times less residues than the first. One explanation to this may be related to the dryness of black powder (due to the charcoal present) and therefore it did not adhere very firmly to the finger, so after the first touch almost the whole amount of explosive fell off from the finger to the surface. Since there were a lot of particles in the first fingerprint and few particles by the last fingerprints, this decay was explained best by power functions, R^2 being 0.94 and 0.88 for cotton fabric and polycarbonate plastic, respectively.

Similarly to PETN and black powder, the transfer of dynamite fitted best power functions to both surfaces (R^2 was 0.93 and 0.89 for cotton fabric and polycarbonate plastic, respectively). However, the amounts of residues transferred to polycarbonate plastic (especially in the first fingerprints) were higher than those transferred to cotton fabric.

In general, it was noticed that the transfer of explosive residues was not only affected by the type of explosive, but also by the surface to which the residues were transferred. In fact, the amount of transferred organic explosives HMTD and TNT underwent an exponential decrease when transferred to cotton fabric, while a power decrease when transferred to polycarbonate plastic. The transfer of PETN, black powder and dynamite fitted best the power decrease in case of both surfaces, indicating that these explosives influenced their transfer more than the surface to which they were transferred.

The transfer of residues of NH_4NO_3, KNO_3, $NaClO_3$ and ANFO was quite chaotic with ten consecutive fingerprints to cotton fabric and polycarbonate plastic (see Fig. 5).

The pattern of transfer of inorganic salts NH_4NO_3, KNO_3 and $NaClO_3$ to both surfaces under study was rather random and unpredictable. However, as displayed in Fig. 5, the amount of residues transferred to polycarbonate plastic was very low, on several occasions the number of pixels containing residues was almost zero, as against cotton fabric. Among these three inorganic salts, $NaClO_3$ showed the lowest degree of transfer, while the amount of KNO_3 transferred was the highest. Overall, the transfer of inorganic salts by fingertip was poor (up to 24,000 explosive-pixels for salt explosive residues, while up to 167,000 pixels for organic explosive residues). Due to their high hygroscopicity the salt particles tended to adhere to the bare finger rather than to be transferred to another surface. What is more, the hygroscopic salts formed aggregates which occasionally dropped from the finger during the transfer procedure. This behavior explained the huge standard deviations obtained for these salts since already one large particle of KNO_3 or NH_4NO_3 could contain 1000 pixels. Therefore, the occasional transfer of a couple of explosive particles increased significantly the standard deviation value. Turano [34] also suggested that variations in his work were likely due to the salt aggregates formed.

The amount of ANFO transferred to cotton fabric showed a doubtful decrease not fitting well to either the power or exponential function. In fact, the pattern of transfer of ANFO to cotton fabric was similar to that of inorganic salts, which is well understood since ANFO consists of 90% NH_4NO_3. However, to both surfaces the amount of ANFO particles transferred was higher compared to those of NH_4NO_3. The particles of ANFO were oily (one component of which is fuel oil) and when pressuring on them with a warm fingertip, the particles became aggregated. This resulted in the adherence of the particles to the bare finger, making the transfer less controllable. For instance, one big aggregate may correspond to 3600 pixels in the image, while a smaller particle contained about 30 pixels. This explains the large error (standard deviation) in the transferred amounts when an aggregate is inevitably formed and dropped during the transfer procedure. The amount of ANFO particles transferred to polycarbonate plastic in each fingerprint was similar and no decrease in the transferred amount in consecutive fingerprints was observed.

4. Conclusions

A pioneering fundamental study evaluating the transfer of explosive residues through ten consecutive fingerprints to two different surfaces – cotton fabric and polycarbonate plastic – was carried out using a simple RGB-multispectral imaging approach. The contrast in images was maximized utilizing advantageous colored backgrounds and selecting the proper frame. This enabled us to estimate the amount of transferred explosive residues through the number of pixels in the image containing explosive residues. Despite the small inequality that may exist between the amount of explosive residues and number of pixels, on the basis of the results obtained, some general conclusions can be drawn.

First, it was shown using PETN as an example that a person does not seem to have a significant impact on the transfer of explosive residues when following a standardized procedure – similar transfer patterns of PETN residues were observed for all subjects. Nevertheless, for stating a general conclusion, further studies with involvement of more subjects and explosives would give more reliable results.

Regarding explosives, large amount of residues of organic explosives HMTD and TNT were transferred showing either an exponential or power decrease. The amount of residues of PETN, black powder and dynamite transferred throughout ten fingerprints was lower, but nonetheless displayed a power decrease on both surfaces, cotton fabric and polycarbonate plastic. On the other hand, no decrease of the transferred amounts of inorganic oxidizing salts (NH_4NO_3, KNO_3 and $NaClO_3$) and ANFO was observed – the transfer seemed to be mainly governed by random effects.

Regarding the surfaces under study, cotton fabric and polycarbonate plastic, in general, higher amounts of explosive residues were left on the former, which was probably due to the stronger adherence of explosive residues to its fibres than to the smooth surface of polycarbonate plastic. In addition, a sharper decrease in the amount of explosive residues transferred with ten fingerprints to polycarbonate plastic was observed (the transferred amounts of all the explosive residues that presented a decrease, exhibited a power decrease in polycarbonate plastic).

In general, the results obtained may contribute to the scarcely investigated, yet important field – the transfer of explosives through fingerprints to different materials. To date, most investigations have dealt with the trace detection of explosive residues but only few of them have focused on studying the explosives transfer. In fact, still a huge amount of work remains to be done in order to have a more accurate understanding about the transfer pattern of explosives. Further studies including other explosives and ammunitions should be carried out, involving more subjects and more replicates, as well as higher number of fingerprints, to have more representative results. These proposed studies would further increase the knowledge about the transfer pattern of different explosives in various circumstances.
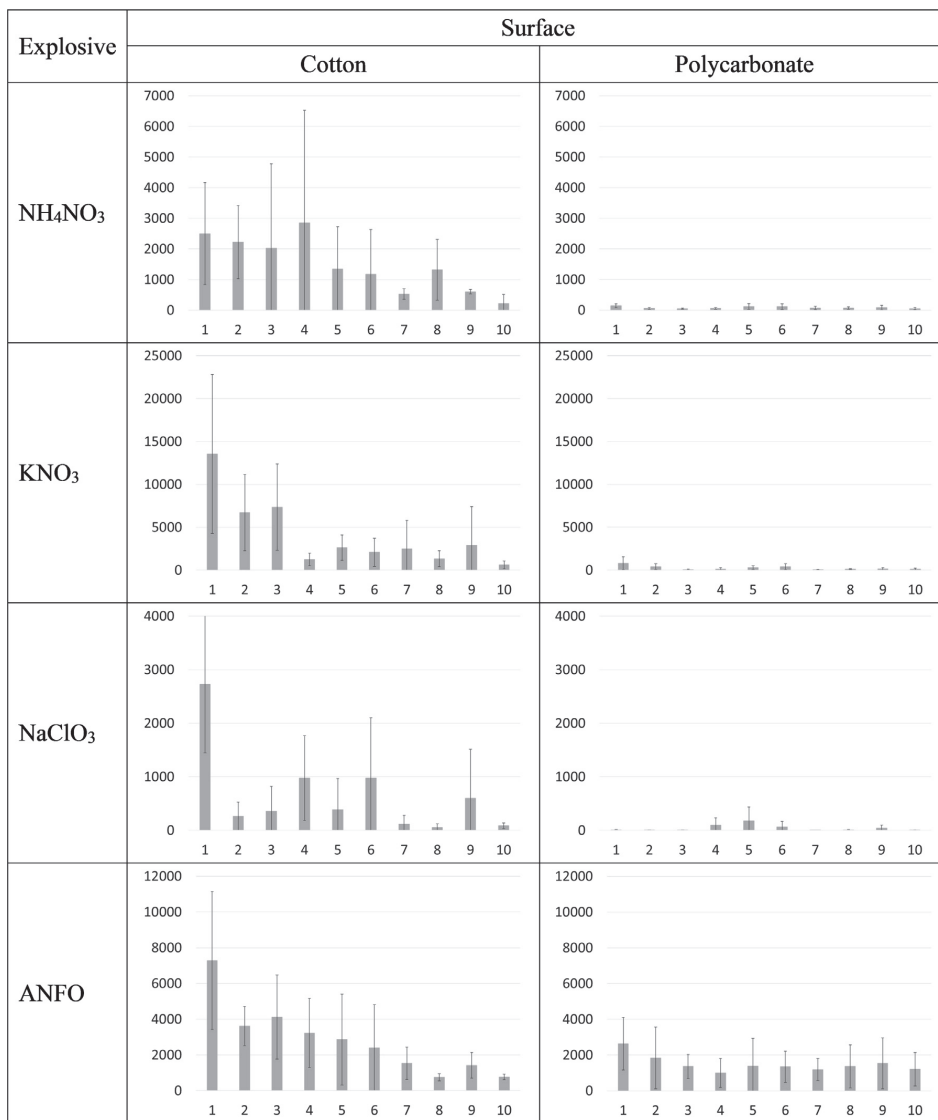
Fig. 5. Bar graphs and standard deviations showing the transfer of explosive residues of random nature through ten consecutive fingerprints. X-axis: ten consecutive fingerprints; y-axis: amount of pixels containing explosive residues.

Acknowledgements

Conflicts of interest

The authors have declared no conflicts of interest.

References

[1] M.Á. Fernández de la Ossa, J.M. Amigo, C. García-Ruiz, Detection of residues from explosive manipulation by near infrared hyperspectral imaging: a promising forensic tool, Forensic Sci. Int. 242 (2014) 228–235, http://dx.doi.org/10.1016/j.forsciint.2014.06.023.
[2] M.Á. Fernández de la Ossa, C. García-Ruiz, J.M. Amigo, Near infrared spectral imaging for the analysis of dynamite residues on human handprints, Talanta 130 (2014) 315–321, http://dx.doi.org/10.1016/j.talanta.2014.07.026.

[3] F. Zapata, M.Á. Fernández de la Ossa, E. Gilchrist, L. Barron, C. García-Ruiz, Progressing the analysis of improvised explosive devices: comparative study for trace detection of explosive residues in handprints by Raman spectroscopy and liquid chromatography, Talanta 161 (2016) 219–227, http://dx.doi.org/10.1016/j.talanta.2016.05.057.

[4] D. Perret, S. Marchese, A. Gentili, R. Curini, A. Terracciano, E. Bafile, F. Romolo, LC–MS–MS determination of stabilizers and explosives residues in hand-swabs, Chromatographia 68 (2008) 517–524, http://dx.doi.org/10.1365/s10337-008-0746-8.

[5] F.S. Romolo, L. Cassioli, S. Grossi, G. Cinelli, M.V. Russo, Surface-sampling and analysis of TATP by swabbing and gas chromatography/mass spectrometry, Forensic Sci. Int. 224 (2013) 96–100, http://dx.doi.org/10.1016/j.forsciint.2012.11.005.

[6] N. Song-im, S. Benson, C. Lennard, Establishing a universal swabbing and clean-up protocol for the combined recovery of organic and inorganic explosive residues, Forensic Sci. Int. 223 (2012) 136–147, http://dx.doi.org/10.1016/j.forsciint.2012.08.017.

[7] K. Szomborg, F. Jongekrijg, E. Gilchrist, T. Webb, D. Wood, L. Barron, Residues from low-order energetic materials: the comparative performance of a range of sampling approaches prior to analysis by ion chromatography, Forensic Sci. Int. 233 (2013) 55–62, http://dx.doi.org/10.1016/j.forsciint.2013.08.018.

[8] D.A. Detata, P.A. Collins, A.J. McKinley, A comparison of common swabbing materials for the recovery of organic and inorganic explosive residues, J. Forensic Sci. 58 (2013) 757–763, http://dx.doi.org/10.1111/1556-4029.12078.

[9] J.R. Verkouteren, Particle characteristics of trace high explosives: RDX and PETN, J. Forensic Sci. 52 (2007) 335–340, http://dx.doi.org/10.1111/j.1556-4029.2006.00354.x.

[10] J.R. Verkouteren, J.L. Coleman, I. Cho, Automated mapping of explosives particles in composition C-4 fingerprints, J. Forensic Sci. 55 (2010) 334–340, http://dx.doi.org/10.1111/j.1556-4029.2009.01272.x.

[11] D.J. Phares, J.K. Holt, G.T. Smedley, R.C. Flagan, Method for characterization of adhesion properties of trace explosives in fingerprints and fingerprint simulations, J. Forensic Sci. 45 (2000) 774–784, http://dx.doi.org/10.1520/JFS14770J.

[12] P. Lucena, I. Gaona, J. Moros, J.J. Laserna, Location and detection of explosive-contaminated human fingerprints on distant targets using standoff laser-induced breakdown spectroscopy, Spectrochim. Acta – Part B At. Spectrosc. 85 (2013) 71–77, http://dx.doi.org/10.1016/j.sab.2013.04.003.

[13] E.D. Emmons, A. Tripathi, J.A. Guicheteau, S.D. Christesen, A.W. Fountain III, Raman chemical imaging of explosive-contaminated fingerprints, Appl. Spectrosc. 63 (2009) 1197–1203, http://dx.doi.org/10.1366/000370209789806812.

[14] A. Tripathi, E.D. Emmons, P.G. Wilcox, J.A. Guicheteau, D.K. Emge, S.D. Christesen, A.W. Fountain, Semi-automated detection of trace explosives in fingerprints on strongly interfering surfaces with Raman chemical imaging, Appl. Spectrosc. 65 (2011) 611–619, http://dx.doi.org/10.1366/10-06214.

[15] Y. Mou, J.W. Rabalais, Detection and identification of explosive particles in fingerprints using attenuated total Reflection-Fourier transform infrared spectromicroscopy, J. Forensic Sci. 54 (2009) 846–850, http://dx.doi.org/10.1111/j.1556-4029.2009.01060.x.

[16] S. Almaviva, S. Botti, L. Cantarini, A. Palucci, A. Puiu, F. Schnuerer, W. Schweikert, F.S. Romolo, Raman spectroscopy for the detection of explosives and their precursors on clothing in fingerprint concentration: a reliable technique for security and counterterrorism issues, Proc. SPIE 8901 (2013) 890102/1–890102/9, http://dx.doi.org/10.1117/12.2028855.

[17] P.H.R. Ng, S. Walker, M. Tahtouh, B. Reedy, Detection of illicit substances in fingerprints by infrared spectral imaging, Anal. Bioanal. Chem. 394 (2009) 2039–2048, http://dx.doi.org/10.1007/s00216-009-2806-9.

[18] J.S. Caygill, F. Davis, S.P.J. Higson, Current trends in explosive detection techniques, Talanta 88 (2012) 14–29, http://dx.doi.org/10.1016/j.talanta.2011.11.043.

[19] T. Peng, W. Qin, K. Wang, J. Shi, C. Fan, D. Li, Nanoplasmonic imaging of latent fingerprints with explosive RDX residues, Anal. Chem. 87 (2015) 9403–9407, http://dx.doi.org/10.1021/acs.analchem.5b02248.

[20] Y. Ma, H. Li, S. Peng, L. Wang, Highly selective and sensitive fluorescent paper sensor for nitroaromatic explosive detection, Anal. Chem. 84 (2012) 8415–8421, http://dx.doi.org/10.1021/ac302138c.

[21] T.P. Forbes, E. Sisco, Mass spectrometry detection and imaging of inorganic and organic explosive device signatures using desorption electro-flow focusing ionization, Anal. Chem. 86 (2014) 7788–7797, http://dx.doi.org/10.1021/ac501718j.

[22] M. Abdelhamid, F.J. Fortes, M.A. Harith, J.J. Laserna, Analysis of explosive residues in human fingerprints using optical catapulting-laser-induced breakdown spectroscopy, J. Anal. At. Spectrom. 26 (2011) 1445–1450, http://dx.doi.org/10.1039/c0ja00188k.

[23] J. Moros, J. Serrano, F.J. Gallego, J. Macıas, J.J. Laserna, Recognition of explosives fingerprints on objects for courier services using machine learning methods and laser-induced breakdown spectroscopy, Talanta 110 (2013) 108–117, http://dx.doi.org/10.1016/j.talanta.2013.02.026.

[24] C.G. Worley, S.S. Wiltshire, T.C. Miller, G.J. Havrilla, V. Majidi, Detection of visible and latent fingerprints using micro-X-ray fluorescence elemental imaging, J. Forensic Sci. 51 (2006) 57–63, http://dx.doi.org/10.1111/j.1556-4029.2005.00006.x.

[25] A. Banas, K. Banas, M.B.H. Breese, J. Loke, B. Heng Teo, S.K. Lim, Detection of microscopic particles present as contaminants in latent fingerprints by means of synchrotron radiation-based Fourier transform infra-red micro-imaging, Analyst 137 (2012) 3459–3465, http://dx.doi.org/10.1039/c2an35355e.

[26] N.J. Crane, E.G. Bartick, R.S. Perlman, S. Huffman, Infrared spectroscopic imaging for noninvasive detection of latent fingerprints, J. Forensic Sci. 52 (2007) 48–53, http://dx.doi.org/10.1111/j.1556-4029.2006.00330.x.

[27] T. Chen, Z.D. Schultz, I.W. Levin, Infrared spectroscopic imaging of latent fingerprints and associated forensic evidence, Analyst 134 (2009) 1902–1904, http://dx.doi.org/10.1039/b908228j.

[28] E.D. Emmons, A. Tripathi, J.A. Guicheteau, S.D. Christesen, A.W. Fountain III, Raman chemical imaging of explosive-contaminated fingerprints, Appl. Spectrosc. 63 (2009) 1197–1203, http://dx.doi.org/10.1366/000370209789806812.

[29] A. Tripathi, E.D. Emmons, J.A. Guicheteau, S.D. Christesen, P.G. Wilcox, D.K. Emge, A.W. Fountain III, Trace explosive detection in fingerprints with Raman chemical imaging, Proc. SPIE 7665 (2010), http://dx.doi.org/10.1117/12.865769 76650N/1–76650N/6.

[30] H. Östmark, M. Nordberg, T.E. Carlsson, Stand-off detection of explosives particles by multispectral imaging Raman spectroscopy, Appl. Opt. 50 (2011) 5592–5599, http://dx.doi.org/10.1364/AO.50.005592.

[31] I. Malka, A. Petrushansky, S. Rosenwaks, I. Bar, Detection of explosives and latent fingerprint residues utilizing laser pointer-based Raman spectroscopy, Appl. Phys. B Lasers Opt. 113 (2013) 511–518, http://dx.doi.org/10.1007/s00340-013-5500-8.

[32] M.R. Almeida, L.P.L. Logrado, J.J. Zacca, D.N. Correa, R.J. Poppi, Raman hyperspectral imaging in conjunction with independent component analysis as a forensic tool for explosive analysis: the case of an ATM explosion, Talanta 174 (2017) 628–632, http://dx.doi.org/10.1016/j.talanta.2017.06.064.

[33] B.E. Bernacki, T.A. Blake, A. Mendoza, T.J. Johnson, Visible hyperspectral imaging for standoff detection of explosives on surfaces, Proc. SPIE 7838 (2010), http://dx.doi.org/10.1117/12.870739 78380C/1–78380C/7.

[34] M.A. Turano, Transfer of Residues in Fingerprints, University of Rhode Island, Kingston, Rhode Island, U.S.A., 2013⟨http://digitalcommons.uri.edu/theses/153⟩.

[35] G.L. Gresham, J.P. Davies, L.D. Goodrich, L.G. Blackwood, B.Y.H. Liu, D. Thimsem, S.H. Yoo, S.F. Hallowell, Development of particle standards for testing detection systems: mass of RDX and particle size distribution of composition 4 residues, Proc. SPIE 2276 (1994) 34–44, http://dx.doi.org/10.1117/12.189198.

[36] S.-S. Choi, C.E. Son, Analytical method for the estimation of transfer and detection efficiencies of solid state explosives using ion mobility spectrometry and smear matrix, Anal. Methods 9 (2017) 2505–2510, http://dx.doi.org/10.1039/C7AY00529F.

[37] F. Zapata, M. López-López, J.M. Amigo, C. García-Ruiz, Multi-spectral imaging for the estimation of shooting distances, Forensic Sci. Int. 282 (2018) 80–85, http://dx.doi.org/10.1016/j.forsciint.2017.11.025.

ACKNOWLEDGEMENTS

This thesis was performed at the Chair of Analytical Chemistry, Department of Chemistry and Biotechnology at Tallinn University of Technology. Part of this thesis was carried out at the Department of Analytical Chemistry at the University of Alcalá in Spain.

Firstly, I am indebted to my supervisor **Merike Vaher**, to whom I owe my deepest gratitude. Her warm-heartedness and extraordinary helpfulness has carried me through the entire period during which I worked on my thesis. Thank you for your guidance, valuable suggestions, and discussions. I also express my sincere gratitude to my second supervisor **Mihkel Kaljurand**, whose continuous encouragement and constructive comments have been a great motivation throughout my studies. Thank you for always believing in me. Your support and faith have meant a lot to me, even if I was not the most ordinary PhD student with my cheerleading hobby. I would also like to thank my supervisor at University of Alcalá, **Félix Zapata**, for his scientific enthusiasm and constant help during my stay in Spain.

This work would not have been possible without my dear colleagues at the Chair of Analytical Chemistry. Thank you all for your recommendations, support, and goodwill. In particular, I would like to thank **Piia Jõul** for her endless help and good advice on many issues raised during my studies. I would also like to express my gratitude to the always cheerful **Tiina Aid**, whose positivity affected everyone around her and made the journey through my PhD studies enjoyable. I cannot forget **Piret Saar-Reismaa** for her valuable recommendations, especially the very valuable IT assistance, and honest opinions. Likewise, I cannot overlook **Birgit Maaten** and **Sandra Kaabel**, with whom I have shared my joys and concerns during my study period. In addition, I would like to acknowledge my lovely students **Annela Avarlaid** and **Kristjan Siilak**, without whose help this work would not have been possible.

Most importantly, I want to express my sincere gratitude and appreciation to **my family** and **friends**. This thesis was made possible through their help and support. Thank you all for believing in me and always being delighted with my achievements. I would especially like to thank **my mother** for encouraging and motivating me throughout these years. In addition, I would like to thank my friends and teammates from **TTÜ Tantsutüdrukud ja Saltopoisid** – trainings with you helped to break up my daily routine and gave a much needed fresh perspective.

ABSTRACT

Development of Analysis Methods to Detect the Use of Explosives and Chemical Warfare Agents

After World War II, large quantities of produced chemical weapons (CWs), whose use in armed conflicts had already been prohibited in 1925 by the Geneva Protocol, required disposal. At that time, dumping at sea was considered the easiest and cheapest disposal method. Thus, approximately 50,000 tons of CWs containing 15,000 tons of toxic chemical warfare agents (CWAs) were dumped into the Baltic Sea. The most abundant CWA dumped was sulfur mustard (HD), which accounted for over 60% of the dumped munitions near Gotland and Bornholm. In an aqueous environment, HD hydrolyzes to form various degradation products. The half-life of HD in seawater is 175 min at 5 °C; therefore, the parent HD is not very often detected in samples collected from dumpsites, rather than its degradation products. The main degradation products of HD are thiodiglycol (TDG), thiodiglycol sulfoxide (TDGO), and thiodiglycol sulfone (TDGOO). In the present thesis, a methodology based on capillary electrophoresis (CE) with UV detection was developed for the detection of TDG, TDGO, and TDGOO. Pre-capillary derivatization enabled sensitive detection of these compounds. In addition to the open-chain compounds mentioned above, HD can also degrade to form various cyclic degradation products. Cyclic compounds, such as 1,4-thioxane, 1,3-dithiolane, 1,4-dithiane, 1,2,5-trithiepane, and 1,4,5-oxadithiepane, are the most commonly detected HD degradation products in samples collected close to CW dumpsites. Thus, these five cyclic degradation products were chosen as the target compounds in this thesis. Two methods were developed for their detection. The first method was based on CE and the other on HPLC; both methods employed UV detection. The HPLC method with an optimized solid phase extraction (SPE) step provided sensitive detection and was applicable to real samples, while the developed CE method is easily miniaturized and adapted to on-site analysis. The latter feature proved to be of high importance, since experiments revealed the instability of the cyclic compounds (degradation of up to 15% over a 5-hour period at room temperature). Although the detection limits of the CE method were relatively high compared to the concentrations detected in real samples, the corrosion of CWs is still an ongoing process and, unfortunately, in the future an increasing amount of toxic chemicals will leak into the sea environment. The positive detection of the aforementioned degradation products in samples from the marine environment indicates the presence and leakage of HD from corroded shells. This, in turn, is a sign of chemical pollution of the sea, which poses a threat to the marine ecosystem.

In addition to CWs, another concern is the malicious use of explosives in terrorist attacks. Additional attacks could be prevented by developing new, rapid, simple, and sensitive methods to detect the use of explosives. This involves methods for early pre-blast detection of explosives at airports, as well as the post-blast detection of explosive residues at crime scenes. The latter could help to track down the origin of the chemicals and lead to possible suspects, which, in turn, helps to prevent future terrorist attacks. The development of a portable on-site CE method for the detection of post-blast explosive residues was achieved in the present thesis. Dual-opposite end injection (DOEI) enabled simultaneous separation of anions and cations from post-blast residues in less than 4 min. The developed methodology, together with principal component analysis, allowed the partial identification of explosives.

Fingerprints are one of the main mechanisms for transferring trace amounts of explosives during the handling and preparation of explosives. Therefore, the detection of explosive traces in fingerprints has been the subject of many studies. However, the transfer of explosives to different materials via consecutive fingerprints has scarcely been studied, and therefore was of interest in this thesis. For this purpose, the amount of explosive residues, *i.e.*, the number of pixels, in ten successive fingerprints deposited on cotton fabric and polycarbonate plastic was counted using multispectral imaging (MSI) and image processing in MATLAB. These two materials were chosen as they are the two most common clothing and luggage materials. Different transfer patterns were observed for different explosives. The amount of explosive residues deposited via consecutive fingerprints tended to undergo a power or exponential decrease, with the exception of inorganic salts and ANFO (which consists of 90% NH_4NO_3), whose transfer seemed to be random.

Considering the above-mentioned concerns, development of new, rapid, simple, and trustworthy methods for the detection of CWAs and explosives is still essential and of high importance.

KOKKUVÕTE

Analüüsimetoodikate arendamine keemiarelva- ja lõhkeainete kasutamise tuvastamiseks

Pärast Teist maailmasõda tekkis vajadus kõrvaldada suur hulk keemiarelvi, mille kasutamine sõjalistes konfliktides oli tegelikult keelatud juba 1925. aastal allkirjastatud Genfi protokolliga. Leiti, et lihtsaim ja odavaim viis keemiarelvadest vabanemiseks on nende merepõhja uputamine. Selle tagajärjel uputati Läänemerre ligikaudu 50 000 tonni keemiarelvi (CW), millest umbes 15 000 tonni moodustasid keemiarelvades sisalduvad toksilised ained (CWA). Kõige enam uputati väävel-sinepigaasi (HD) mahuteid, mis moodustasid üle 60% kõikidest Gotlandi ja Bornholmi lähistele uputatud keemiarelvades sisalduvatest ainetest. Vesikeskkonnas hüdrolüüsub HD erinevateks laguproduktideks. HD poolestusaeg merevees 5 °C juures on 175 minutit, seega detekteeritakse reaalsetes proovides peamiselt tema laguprodukte. HD esmased laguproduktid on tiodiglükool (TDG), tiodiglükool-sulfoksiid (TDGO) ja tiodiglükool-sulfoon (TDGOO). Käesolevas doktoritöös töötati välja metoodika nende ühendite määramiseks kasutades UV-detekteerimisega kapillaarelektroforeesi (CE) meetodit. UV kiirgust hästi absorbeeriva funktsionaalrühma lisamine uuritavate ühendite struktuuri (derivatiseerimine) võimaldas tundlikku detekteerimist. Peale nimetatud atsükliliste ühendite võib HD laguneda ka mitmeteks tsüklilisteks ühenditeks, nagu 1,4-tioksaan, 1,3-ditiolaan, 1,4-ditiaan, 1,2,5-tritiepaan ja 1,4,5-oksaditiepaan. Üllatuslikult detekteeritakse just neid ühendeid kõige sagedamini uputuskohtade lähedalt kogutud proovidest. Seetõttu töötati käesolevas doktoritöös välja metoodikad ka nende ühendite detekteerimiseks. Esimene metoodika põhines CE-l ja teine HPLC-l, kuid detekteerimiseks kasutati mõlemal juhul UV detektorit. Arendatud HPLC metoodika koos tahke faasi ekstraktsiooniga (SPE) võimaldas tundlikku analüüsi ja oli hõlpsasti rakendatav reaalsetele keemiarelvade uputuskohtade lähedalt kogutud proovidele. Seejuures on arendatud CE metoodika tulevikus kergesti miniaturiseeritav ja kohandatav kohapealseks analüüsiks. Uuringu tulemusena selgus, et tsüklilised ühendid olid ebastabiilsed, kuna lagunesid 5-tunnise perioodi jooksul toatemperatuuril hoiustades kuni 15%. See tõestas, et kohapealne analüüs nende ühendite detekteerimiseks on eriti oluline, et säästa aega proovide hoiustamiselt ja transpordilt. Kuigi arendatud CE metoodika tundlikkus oli suhteliselt madal võrreldes reaalsetes proovides leitud sisaldustega, siis arvestades keemiarelva mahutite jätkuvat korrosiooni, võib tulevikus prognoosida ulatuslikumat keemiarelva ainete lekkimist merekeskkonda ja seega suuremaid detekteeritavaid sisaldusi. Eespool nimetatud laguproduktide positiivne detekteerimine merekeskkonnast kogutud proovides viitab HD olemasolule ja lekkele roostetanud kestadest. See omakorda viitab mere keemilisele reostusele, mis on potentsiaalseks ohuks mere ökosüsteemile.

Lisaks keemiarelvadele on murekohaks lõhkeainete kuritegelik kasutamine terrorirünnakutes. Uusi rünnakuid oleks võimalik ära hoida kiirete, lihtsate ja usaldusväärsete metoodikate arendamisega lõhkeainete detekteerimiseks. See hõlmab uusi metoodikaid lõhkeainete tuvastamiseks lennujaamades enne nende lõhkamist (plahvatuste ennetamine), kuid ka lõhkeaine plahvatusproduktide analüüsimist pärast plahvatust kuriteopaikades. Lõhkeaine plahvatusproduktide analüüs võimaldab kindlaks teha kasutatud lõhkeaine tüüpi ja juhatab uurijaid konkreetse kurjategijani, mis omakorda aitab ära hoida lisaplahvatusi. Käesolevas doktoritöös töötati välja

CE metoodika, kasutades portatiivset juhtivusdetektoriga seadet lõhkeainete plahvatusproduktide kohapealseks analüüsiks. Kahepoolne proovi sisestamise metoodika (DOEI) võimaldas vähem kui 4 minutiga plahvatusproduktidest pärit anioonide ja katioonide samaaegset analüüsi. Väljatöötatud metoodika koos peakomponentide analüüsiga võimaldas lõhkeainete osalist identifitseerimist.

On teada, et lõhkeainete käitlemisel ja ettevalmistamisel jäävad mikrokogused lõhkeaine osakesi sõrmedele ning hiljem kanduvad sealt edasi järgmistele esemetele. Seetõttu on lõhkeainete detekteerimine sõrmejälgedes olnud paljude teadustööde uurimisobjektiks. Seevastu lõhkeainete edasikandumist järjestikustes sõrmejälgedes erinevatele materjalidele on vähe uuritud ning antud teema oli seetõttu käesoleva väitekirja huviobjektiks. Lõhkeaine koguste määramiseks järjestikustes sõrmejälgedes kasutati multispektraalset pildistamist koos pilditöötlusega MATLABis, mis võimaldas loendada piltides lõhkeainejääkidele kuuluvaid piksleid. Kümme järjestikust sõrmejälge teostati kahel erineval materjalil, polükarbonaadil ja puuvillal, mis on lennujaamades kõige sagedamini esinevad riide- ja pagasimaterjalid. Täheldati erinevaid lõhkeainete edasikandumise mustreid. Üldiselt vähenes lõhkeaine jääkide kogus järjestikes sõlmejälgedes eksponentsiaalselt või astmeliselt, v.a. anorgaaniliste soolade ja ANFO (90% moodustab NH_4NO_3) korral, kus edasikandumine tundus olevat juhuslik.

Arvestades eespool nimetatud probleeme, on uute, kiirete, lihtsate ja usaldusväärsete metoodikate väljatöötamine keemiarelvade ainete ja lõhkeainete tuvastamiseks jätkuvalt vajalik ja oluline.

LIST OF ORIGINAL PUBLICATIONS

1.1 – 5 publications

H. Lees, F. Zapata, M. Vaher, C. García-Ruiz, Study of the adhesion of explosive residues to the finger and transfer to clothing and luggage, Science & Justice. (2018) *[In Press]*.

H. Lees, F. Zapata, M. Vaher, C. García-Ruiz, Simple multispectral imaging approach for determining the transfer of explosive residues in consecutive fingerprints, Talanta. 184 (2018) 437–445.

H. Lees, M. Vaher, M. Kaljurand, Development and comparison of HPLC and MEKC methods for the analysis of cyclic sulfur mustard degradation products, Electrophoresis. 38 (2017) 1075–1082.

P. Jõul, **H. Lees**, M. Vaher, E.-G. Kobrin, M. Kaljurand, M. Kuhtinskaja, Development of a capillary electrophoresis method with direct UV detection for the analysis of thiodiglycol and its oxidation products, Electrophoresis. 36 (2015) 1202–1207.

E.-G. Kobrin, **H. Lees**, M. Fomitšenko, P. Kubáň, M. Kaljurand, Fingerprinting postblast explosive residues by portable capillary electrophoresis with contactless conductivity detection, Electrophoresis. 35 (2014) 1165–1172.

3.1 – 1 publication

M. Söderström, A. Östin, J. Qvarnström, R. Magnusson, J. Rattfelt-Nyholm, M. Vaher, P. Jõul, **H. Lees,** M. Kaljurand, M. Szubska, P. Vanninen, J. Bełdowski. Chemical Analysis of Dumped Chemical Warfare Agents During the MODUM Project. In: J. Bełdowski, R. Been, E. Turmus (Ed.). Towards the Monitoring of Dumped Munitions Threat (MODUM). NATO Science for Peace and Security Series C: Environmental Security. (2018) 71–103. Dordrecht: Springer.

5.2 – 7 publications

H. Lees, K. Siilak, M. Vaher. Development of nonaqueous capillary electrophoresis method with conductivity detection for the analysis of perfluorinated compounds. *Abstract Book: 42nd ISCC and 15th GC×GC Symposium, Riva del Garda, Italy, 13-18 May, 2018.* Ed. L. Mondello, P. Dugo. Italy: Chromaleont S.r.L (2018) 263.

H. Lees, M. Vaher, M. Kaljurand. Investigation of the adsorption and desorption of sulfur mustard degradation products in sediments by capillary electrophoresis. *Conference Proceedings: CECE 2016, 13th International Interdisciplinary Meeting on Bioanalysis, Brno, Czech Republic, 17-19 October, 2016.* Ed. F. Foret, J. Křenková, I. Drobníková, K. Klepárník. Institute of Analytical Chemistry of the CAS. (2016) 182–185.

H. Lees, A. Avarlaid, M. Vaher, M. Kaljurand. Analysis of cyclic sulfur mustard degradation products in water samples by HPLC and CE. *Book of Abstracts: 20th International Scientific Conference: EcoBalt 2016, 9-12 October, Tartu, Estonia,* University of Tartu. (2016) P23.

H. Lees, M. Kaljurand, M. Vaher. Development of HPLC and MEKC methods for the analysis of sulfur mustard cyclic degradation products. *Abstract Book: 40th ISCC and 13th GC×GC Symposium, Riva del Garda, Italy, 29 May-3 June, 2016.* Ed. L. Mondello, P. Dugo. Italy: Chromaleont S.r.L. (2016) 255.

H. Lees, P. Jõul, M. Vaher, M. Kuhtinskaja, M. Kaljurand. Analysis of sulfur mustard hydrolysis and oxidation products in seawater and sediments by capillary electrophoresis. *Science for the Environment 2015, Aarhus, Denmark, 1-2 October (2015).*

H. Lees, M. Vaher, M. Kaljurand. Analysis of thiodiglycol and its oxidation products in sediments by capillary electrophoresis. *ITP2015/NoSSS2015 Final Program and Book of Abstracts. Helsinki, Finland, 30 August-3 September 2015.* Helsinki University Press. (2015) P-55.

M. Kaljurand, J. Mazina, P. Saar, P. Jõul, **H. Lees**, A. Špiljova, M. Kulp, M. Vaher. Detection of banned chemicals in various matrices (saliva, sediments) by capillary electrophoresis. *ITP2015/NoSSS2015 Final Program and Book of Abstracts. Helsinki, Finland, 30 August-3 September 2015*. Helsinki University Press. (2015) L-36.

CURRICULUM VITAE

Personal data

Name	Heidi Lees
Date of birth	03.02.1990
Place of birth	Kuressaare, Estonia
Citizenship	Estonian

Contact data

E-mail	heidi.lees@ttu.ee

Education

2014–…	Tallinn University of Technology, Chemistry and Gene Technology, PhD Student
2012–2014	Tallinn University of Technology, Applied Chemistry and Biotechnology, MSc, *cum laude*
2009–2012	Tallinn University of Technology, Applied Chemistry and Biotechnology, BSc, *cum laude*
1998–2009	Saaremaa Co-Educational Gymnasium, silver medalist

Language competence

Estonian	Native
English	Fluent
Russian	Beginner
Spanish	Beginner

Professional employment

2017–…	Tallinn University of Technology, Institute of Chemistry and Biotechnology, Early Stage Researcher
2012–2017	Tallinn University of Technology, Chair of Analytical Chemistry, supervisor, teacher, investigator in projects
2011 summer	AS Tallinna Vesi, trainee

Special courses

01.03.2017–30.07.2017	INQUIFOR Research Group, Department of Analytical Chemistry, University of Alcalá, Spain
27.06.2016–01.07.2016	Summer School in Underwater Munitions, Nova Scotia Community College, Halifax, Canada
28.03.2016–08.05.2016	Estimation of measurement uncertainty in chemical analysis
16.07.2012–24.08.2012	Department of Chemistry, Durham University, UK

Honors and awards

2018	Funding for short-term study mobility by the European Regional Development Fund (Dora Plus)
2017	Funding for a pre-doctoral stay by the European Regional Development Fund (Dora Plus)
2016	Tiina Mõis Scholarship
2015	Competition of three-minute popular science lectures, TTÜ representative in the finals

2014	Doctoral Scholarship of the Estonian Ministry of Defense
2014	Competition of scientific work sponsored by the Estonian Ministry of Defense, additional award
2014	Participation in the President's reception in honor of the best graduates
2013	The Scholarship of Saare Kalur
2012	Johann von Luce Scholarship

Teaching

Practice lessons of subjects: Fundamentals of Chemistry, Analytical Chemistry, Instrumental Analysis, and Separation Methods in Chemistry.

Theses supervised

Kristjan Siilak, MSc, 2018, Analysis of perfluorinated acids by using nonaqueous capillary electrophoresis, Department of Chemistry and Biotechnology, Tallinn University of Technology.

Annela Avarlaid, BSc, 2016, Analysis of cyclic sulfur mustard degradation products by using micellar electrokinetic chromatography, Department of Chemistry, Tallinn University of Technology.

ELULOOKIRJELDUS

Isikuandmed

Nimi	Heidi Lees
Sünniaeg	03.02.1990
Sünnikoht	Kuressaare, Eesti
Kodakondsus	Eesti

Kontaktandmed

E-post	heidi.lees@ttu.ee

Hariduskäik

2014–…	Tallinna Tehnikaülikool, keemia ja geenitehnoloogia, doktorant
2012–2014	Tallinna Tehnikaülikool, rakenduskeemia ja biotehnoloogia, MSc, *cum laude*
2009–2012	Tallinna Tehnikaülikool; rakenduskeemia ja biotehnoloogia, BSc, *cum laude*
1998–2009	Saaremaa Ühisgümnaasium, bioloogia- ja matemaatikaklass, hõbemedal

Keelteoskus

Eesti keel	emakeel
Inglise keel	kõrgtase
Vene keel	algtase
Hispaania keel	algtase

Teenistuskäik

2017–…	Tallinna Tehnikaülikool, keemia ja biotehnoloogia instituut, doktorant-nooremteadur
2012–2017	Tallinna Tehnikaülikool, analüütilise keemia õppetool, juhendamine, õppetöö läbiviimine, projektide täitja
2011 suvi	AS Tallinna Vesi, laborant

Täiendusõpe

01.03.2017–30.07.2017	INQUIFOR uurimisgrupp, Alcalá Ülikool, Hispaania
27.06.2016–01.07.2016	Suvekool uputatud lahingumoonadest, Nova Scotia Community College, Halifax, Kanada
28.03.2016–08.05.2016	Mõõtemääramatuse hindamine keemilises analüüsis
16.07.2012–24.08.2012	Keemiainstituut, Durhami Ülikool, Suurbritannia

Teaduspreemiad ja tunnustused

2018	Euroopa Regionaalarengu Fondi finantseering lühiajaliseks õpirändeks (Dora Pluss)
2017	Euroopa Regionaalarengu Fondi finantseering õpirändeks (Dora Pluss)
2016	Tiina Mõisa doktoriõppe stipendium
2015	Kolmeminutiliste populaarteaduslike loengute konkursi finaalis TTÜ esindaja
2014	Kaitseministeeriumi doktoriõppe stipendiumi avaliku konkursi stipendiaat

2014	Kaitseministeeriumi teadustööde konkursi lisapreemia
2014	Osalemine Vabariigi Presidendi vastuvõtul parimate koolilõpetajate auks
2013	Saare Kaluri stipendium
2012	Johann von Luce nimeline stipendium

Õpetamine

Õppeainete keemia alused, analüütiline keemia, instrumentaalanalüüs ja lahutusmeetodid keemias praktikumide läbiviimine.

Juhendatud väitekirjad

Kristjan Siilak, MSc, 2018, Perfluoreeritud hapete analüüs kasutades mittevesikeskkonna kapillaarelektroforeesi, Keemia ja biotehnoloogia instituut, Tallinna Tehnikaülikool.

Annela Avarlaid, BSc, 2016, Väävel-sinepigaasi tsükliliste laguproduktide analüüs kasutades mitsellaarset elektrokineetilist kromatograafiat, Keemiainstituut, Tallinna Tehnikaülikool.